Dissertation
submitted to the
Combined Faculties for the Natural Sciences and for Mathematics
of the Ruperto-Carola University of Heidelberg, Germany
for the degree of
Doctor of Natural Sciences

presented by

Diplom-Biotechnologe Stefan Mockenhaupt

born in: Koblenz am Rhein

Oral examination: 24.05.2012

Alleviation of shRNA off-target effects via rAAV vector-encoded sense strand decoys

Referees: Prof.Dr. Ralf Bartenschlager

Dr. Dirk Grimm

CONTENTS

ABBREVIATIONS

7SK	Human 7SK promoter
A	Adenine nucleotide
AAV	Adeno-associated virus
ATP	Adenosine triphosphate
bp	Base pair
bs	Binding site
C	Cytosine nucleotide
cDNA	Complementary deoxyribonucleic acid
CDS	Coding sequence
CMV	Cytomegalovirus
CNS	Central nervous system
d2eGFP	Destabilized eGFP
DF	Degrees of freedom
DMEM	Dulbecco's modified Eagle's medium
DNA	Deoxyribonucleic acid
dNTP	Deoxynucleotide triphosphate
dsRNA	Double-stranded RNA
DTT	Dithiothreitol
EDTA	Ethylendinitrilo-N, N, N', N'-tetraacetate
eGFP	Enhanced green fluorescent protein
EGTA	Ethylene glycol tetraacetic acid
EtOH	Ethanol
FACS	Fluorescence activated cell sorting
FCS	Fetal calf serum
Fluc	Firefly luciferase
FSC	Forward scatter
G	Guanine nucleotide
H1	Human H1 promoter
hAAT	Human alpha-1- antitrypsin
hAgo1-4	Human Argonaute 1-4 proteins
HBV	Hepatitis B virus
HCV	Hepatitis C virus
HEK293T	Human embryonic kidney 293T cells
HEPES	4-(2-hydroxyethyl)-1-piperazineethanesulfonic acid
HGNC	Hugo genome nomenclature committee
Huh7	Human hepatoma 7 cell line
ITR	Inverted terminal repeat
LB media	Lysogeny broth media
MEF	Mouse embryonic fibroblast
miRNA	microRNA
MOI	Multiplicity of infection
mRNA	messenger ribonucleic acid

MW	Molecular weight
ncRNA	Non-coding RNA
NEAA	Non-essential amino acids
NSC	Non-silencing control
nt	Nucleotide
NTR	Non-translated region
ORF	Open reading frame
P/S	Penicillin/streptomycin
PABPC4	Cytoplasmic poly(A) binding protein 4
PAGE	Polyacrylamide gel electrophoresis
PBS	Phosphate buffered saline
PBS-MK	PBS with magnesium and potassium
PCR	Polymerase chain reaction
PEG	Polyethylene glycol
PEI	Polyethyleneimine
PFA	Paraformaldehyde
pre-miRNA	precursor miRNA
pre-shRNA	precursor shRNA
pri-miRNA	primary miRNA
qPCR	quantitative PCR
rAAV	recombinant AAV
RISC	RNA-induced silencing complex
RLU	Relative light units
Rluc	Renilla luciferase
RNA	Ribonucleic acid
RNAi	RNA interference
RNA-pol II	RNA polymerase II
RNA-pol III	RNA polymerase III
rpm	Rounds per minute
RSA	Relative strand activity
RSV	Rous sarcoma virus
RT	Room temperature
RT-PCR	Reverse transcription-polymerase chain reaction
sAg	HBV surface antigen
scAAV	Self-complementary AAV
SDS	Sodium dodecyl sulfate
SEM	Standard error of the mean
shRNA	short hairpin RNA
siRNA	small interfering RNA
ssAAV	single-stranded AAV
SSC	Side scatter
ssRNA	single-stranded RNA
T	Thymidine nucleotide
T4-PNK	Polynucleotide kinase of the T4 bacteriophage
Tm	Melting temperature
TNRC6A-C	Trinucleotide repeat containing protein 6A-C

trs	Terminal resolution site
TuD	Tough decoy
U	Uridine nucleotide
U6	Human U6 promoter
UTR	Untranslated region
UV	Ultraviolet
VLS	Virus lysis solution
Whc	AAV Wilson helper construct
WT	Wild type

ABSTRACT

The use of exogenous triggers of RNAi such as short hairpin RNAs (shRNAs) in combination with viral vector-mediated gene delivery holds great potential for applications in gene therapy, in biotechnological processes as well as in basic research. Ideally, shRNAs only exert their activity via the antisense strand that binds and silences the designated target mRNA. However, the undesired sense strand can also be activated and hence holds a certain silencing potential. In principle, this may contribute to erratic off-targeting which typically occurs via imperfect binding and subsequent inhibition of untargeted cellular mRNAs. The aim of this study was to assess whether shRNA sense strand activity plays an important role in producing off-target effects and –if so- to find novel means of counteracting this activity.

Functional characterization of relative strand activities of different shRNAs indeed revealed high levels of undesired sense strands activity for most RNAi triggers. This effect was found both upon plasmid transfection and rAAV2-mediated transduction which represents a therapeutically relevant system for gene delivery. We therefore devised a novel strategy for sense strand counteraction in which an shRNA is co-expressed with an inhibitor RNA transcript designed to stably sequester and inactivate the sense but not the antisense strand. Proof-of-concept for our approach was obtained in transfected human cells with an shRNA against hepatitis C virus (HCV). By using RNA-polymerase III-transcribed inhibitors known as tough decoys (TuDs) we could efficiently and specifically counteract the sense strand of the HCV-shRNA in luciferase and eGFP-based reporter assays. We then tested the shRNA-TuD combination in the context of a single self-complementary rAAV2 vector. TuD co-expression led to impairment of sense strand activity upon transduction of HEK293T and Huh7 cells. Inhibition of HCV replication in Huh7 cells was not altered indicating that the desired antisense strand activity was unaffected. Our strategy is hence compatible with rAAV-mediated gene delivery. Furthermore, expression profiling in Huh7 cells revealed that TuD co-expression specifically de-repressed endogenous off-target transcripts that carried seed matches to the shRNA sense strand leading to lower levels of perturbation of global gene expression. As expected, repression of transcripts carrying antisense strand seed matches remained unaffected. These

results show that shRNA sense strands can indeed contribute to off-targeting and that TuD-mediated inhibition can be used to counteract this effect.
Besides our functional data, we also defined rules for TuD and shRNA design as well as promoter choice which allows implementation of the system for other shRNAs.
In this study, we provide new insights into the functionalities and relative activities of both strands of shRNAs. We furthermore present TuD-mediated selective counteraction of shRNA sense strands as a novel method to improve the functional strand bias and thus increase shRNA specificity. We are optimistic that our strategy will facilitate and further foster the clinical implementation of vector-based RNAi.

ZUSAMMENFASSUNG

Die Kombination aus exogenen RNAi auslösenden Molekülen wie z.B. *short hairpin* RNAs (shRNAs) und Gentransfer durch virale Vektoren hat ein enormes Potenzial für Anwendungen in der Gentherapie, in biotechnologischen Prozessen sowie in der Grundlagenforschung. Idealerweise sollte die Aktivität von shRNAs nur durch den *antisense* Strang ausgeführt werden, welcher das erwünschte zelluläre Ziel bindet und inhibiert. Prinzipiell kann jedoch auch dem unerwünschten *sense* Strang eine gewisse Inhibierungsaktivität innewohnen. Dies kann zu unerwünschten *off-target* Effekten von shRNAs beitragen, welche normalerweise durch imperfekte Bindung und anschließende Inhibierung von nicht anvisierten zellulären mRNAs auftreten. Die vorliegende Studie sollte zunächst herausfinden, ob shRNA *sense* Strang Aktivität zu nennenswerten *off-target* Effekten führen kann. Falls zutreffend, sollten desweiteren neue Ansätze entwickelt werden, um diese Aktivität zu verringern.

Die funktionale Charakterisierung der relativen Strangaktivität verschiedener shRNAs offenbarte, dass die *sense* Stränge in den meisten Fällen tatsächlich eine hohe Aktivität aufweisen. Dies wurde sowohl nach Plasmidtransfektion als auch nach Transduktion durch AAV Vektoren, welche ein relevantes System für den therapeutischen Gentransfer darstellen, beobachtet. Aus diesem Grund entwickelten wir eine neue Strategie, in der shRNAs gemeinsam mit einer Inhibitor-RNA exprimiert werden, welche den unerwünschten *sense*-Strang, nicht jedoch den erwünschten *antisense* Strand der shRNA dauerhaft bindet und inaktiviert. Unser Ansatz wurde in transfizierten humanen Zellen mit einer vorher beschriebenen shRNA gegen Hepatitis C Virus (HCV) getestet. Mit Hilfe von RNA-Polymerase III-transkribierten Inhibitor Molekülen, die als tough decoys (TuDs) bekannt sind, konnten der *sense* Strang Aktivität der HCV shRNA effizient entgegengewirkt werden. Als nächstes wurde die Kombination aus shRNA und TuD im Kontext von selbst-komplementären rAAV2 Vektoren getestet. Wir konnten beobachten, dass Ko-Expression des TuDs nach Transduktion von HEK293T und Huh7 Zellen zu einer starken Beeinträchtigung der *sense* Strang Aktivität führte. Die Inhibition der HCV Replikation in Huh7 Zellen war jedoch unverändert, was auf einer unveränderte Aktivität des erwünschten *antisense* Stranges schließen lässt. Dies bedeutet, dass unsere Strategie mit dem

Gentranfer durch AAV Vektoren kompatibel ist. Eine Analyse der Genexpression in Huh7 Zellen offenbarte desweiteren, dass durch die Ko-expression des TuD endogene *off-target* Transkripte, welche komplemetäre Sequenzen zur *seed* Sequenz des shRNA *sense* Stranges trugen, spezifisch de-reprimiert wurden. Dies hatte auch eine geringere globale Deregulierung der Genexpression durch die shRNA zur Folge. Wie erwartet war die Repression von Transkripten mit komplementären Sequenzen zur *seed* Sequenz des *antisense* Stranges unverändert. Diese Ergebnisse verdeutlichen, dass der *sense* Strang von shRNAs tatsächlich zu *off-target* Effekten beitragen und dass diesen durch Ko-Expression von TuDs entgegengewirkt werden kann.

Zusätzlich zu den funktionalen Daten wurden Richtlinien für das Design von shRNA und TuD sowie für die Wahl des Promotors bestimmt, wodurch eine Übertragung des Systems auf andere shRNAs ermöglicht wird.

Diese Studie liefert neue Einblicke in die Funktionalität und die relativen Aktivitäten beider Stränge von shRNAs. Desweiteren wird die selektive Inhibition von shRNA *sense* Strängen durch TuDs als neue Methode zur Erhöhung von shRNA Spezifitäten vorgestellt. Diese Methode könnte zur zukünftigen klinischen Einführung von vektorbasierten RNAi Therapien beitragen.

1 INTRODUCTION

RNA interference (RNAi) is a cellular mechanism for post-transcriptional silencing of specific genes that can be found in a wide variety of eukaryotic organisms. It requires an endogenous or exogenous double-stranded small RNA molecule that interacts with, and subsequently inhibits a target mRNA. On the one hand, the discovery of the endogenous RNAi machinery has vastly improved our knowledge about cellular regulation of gene expression with important implications for human disease phenotypes. On the other hand, the application of exogenous triggers of RNAi has proven to be a highly versatile, potent and, importantly, easy-to-use gene silencing tool and has already started to revolutionize basic science as well as biomedical research and biotechnological applications. Another molecular state-of-the-art technology is the use of viral vectors for highly potent and to some degree specific delivery of genetic material to target cells. This approach exploits the natural ability of different viruses to infect cells and then unpack their genetic material for potent expression, and has been successfully applied in a wide variety of settings ranging from basic tissue culture experiments to more elaborate applications like gene therapy. Although first used in the early 70s, viral vector technology has only revealed its true potential within the past ten years culminating in its recent use in a range of clinical trials in different gene therapeutic applications. The combination of viral vectors and RNAi is thus a highly promising approach for the treatment of different human pathologies ranging from central nervous system (CNS) disorders over cancer to infectious diseases. While it has already shown a number of exciting results in the past years its use in gene therapy still requires further characterization and optimization. In this study, we aimed at improving current approaches for specific gene silencing in potentially gene therapeutic settings using viral vectors and RNAi.

1.1 RNA interference

1.1.1 History of RNA interference

The first report on what later would be identified as a completely novel class of conserved regulatory RNA molecules was published by the Ambros lab in 1993 (Lee *et al.*, 1993). The group described the gene product of the *lin-4* gene in

Caenorhabditis elegans (*C.elegans*) as two non-protein-coding RNAs of 22 nucleotides (nt) and 61nt in length that were able to negatively regulate expression of the *lin-14* gene which carried sequence similarities to *lin-4*. After this initial discovery it was not until 1998 that a major breakthrough would lead to a huge leap forward in the field. A groundbreaking publication by Andrew Fire and Craig Mello described for the first time the targeted inhibition of expression of specific genes by exogenous double-stranded RNA (dsRNA) molecules with perfect complementarity to a target mRNA (Fire *et al.*, 1998). The phenomenon was termed RNA interference (RNAi). Later a link between the previous findings of the Ambros lab and RNAi was discovered as it turned out that the *lin-4* gene products were in fact endogenous counterparts to the exogenous dsRNAs used by Fire and Mello (Ambros, 2001). Curiously, the description of exogenous RNAi preceded the discovery of the endogenous machinery turning the classical scenario where a biological discovery leads to a technological breakthrough upside down. When a second non-coding RNA molecule was discovered in the year 2000 that had characteristics similar to *lin-4* and that was widely conserved across species the term microRNA (miRNA) was coined for such small regulatory RNA molecules (Reinhart *et al*., 2000; Pasquellini *et al*., 2000; Lee and Ambros, 2001). While investigations on miRNAs soon became a discipline in molecular biology in its own right the more technological finding of exogenously induced RNAi started a revolution in modern molecular biology. After the initial discovery in *C.elegans* by Fire and Mello the same principles were found to be active in *Drosophila melanogaster* and shortly thereafter also in mammalian and most importantly in human cells (Kennerdell and Carthew, 1998; Caplen *et al.*, 2001; Elbashir *et al.*, 2001a). Nowadays we know that the principle of RNAi is highly conserved across eukaryotes and is thus believed to have arisen early in evolution (Cerutti and Casas-Mollano, 2006). The possibility to adapt the system to virtually any RNA sequence rapidly led to novel concepts in functional genomics and new strategies for the treatment of a wide range of both genetic and infectious diseases (Grimm and Kay, 2007a; Tiemann and Rossi, 2009).

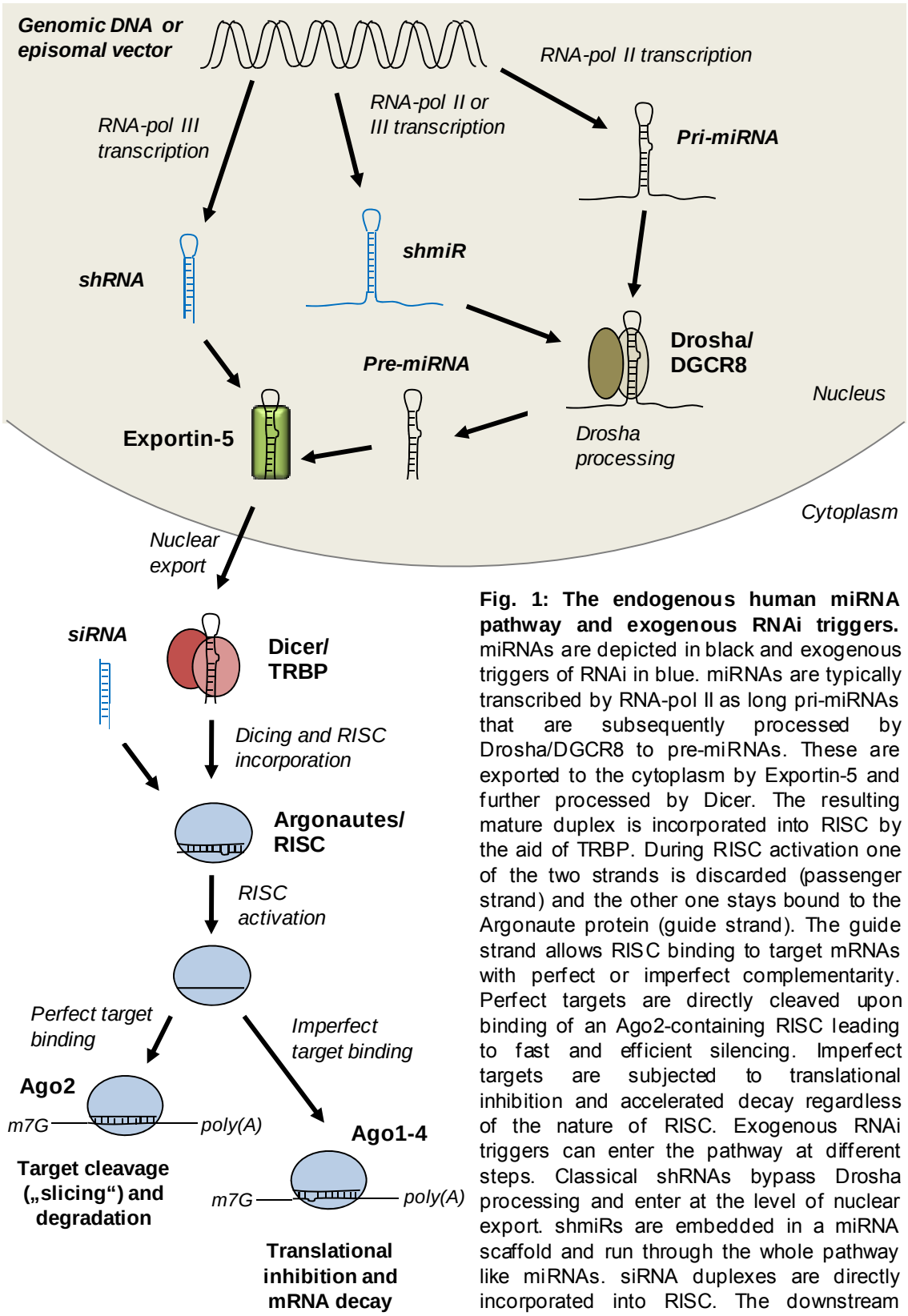

Fig. 1: The endogenous human miRNA pathway and exogenous RNAi triggers. miRNAs are depicted in black and exogenous triggers of RNAi in blue. miRNAs are typically transcribed by RNA-pol II as long pri-miRNAs that are subsequently processed by Drosha/DGCR8 to pre-miRNAs. These are exported to the cytoplasm by Exportin-5 and further processed by Dicer. The resulting mature duplex is incorporated into RISC by the aid of TRBP. During RISC activation one of the two strands is discarded (passenger strand) and the other one stays bound to the Argonaute protein (guide strand). The guide strand allows RISC binding to target mRNAs with perfect or imperfect complementarity. Perfect targets are directly cleaved upon binding of an Ago2-containing RISC leading to fast and efficient silencing. Imperfect targets are subjected to translational inhibition and accelerated decay regardless of the nature of RISC. Exogenous RNAi triggers can enter the pathway at different steps. Classical shRNAs bypass Drosha processing and enter at the level of nuclear export. shmiRs are embedded in a miRNA scaffold and run through the whole pathway like miRNAs. siRNA duplexes are directly incorporated into RISC. The downstream silencing mechanisms are similar for all triggers of RNAi. RISC = RNA-induced silencing complex.

1.1.2 Gene silencing by endogenous triggers of RNAi- the human miRNA pathway

The small RNA components of the RNAi machinery generally act as homing devices that sequence-specifically recruit effector proteins to cellular target RNAs which leads to their translational inhibition and/or degradation (for review see Fabian *et al.*, 2010). The major class of such homing RNAs in humans as well as in other species are miRNAs that are single-stranded 21-24nt long RNAs in their mature form. The canonical endogenous miRNA pathway starts with the nuclear synthesis of a primary transcript that is termed pri-miRNA mostly by RNA-polymerase II (RNA-pol II) (Lee *et al.*, 2002; Lee *et al.*, 2004; Fig. 1). A hairpin structure within these molecules is recognized by the endonuclease Drosha that in concert with DGCR8 is termed microprocessor and excises a hairpin-shaped precursor molecule named pre-miRNA (Lee *et al.*, 2003; Han *et al.*, 2004). These small hairpin precursors are subsequently bound by Exportin-5 and transported into the cytoplasm (Yi *et al.*, 2003; Zeng and Cullen, 2004). The preceding Drosha processing leaves a short overhang at the 3' end of the pre-miRNA which is recognized by another cytoplasmic endonuclease called Dicer that cuts 22nt upstream of the 3' end in an asymmetric fashion. This leads to the removal of the hairpin loop and a duplex RNA molecule with 3' overhangs at either end (Bernstein *et al.*, 2001; Provost *et al.*, 2002). Dicer and its co-factor TRBP then transfer the duplex into the RNA-induced silencing complex (RISC) whose main components are Argonaute (Ago) RNA binding proteins and associated TNRC6 proteins along with other factors required for downstream gene silencing processes (Chendrimada *et al.*, 2005; Landthaler *et al.*, 2008). In humans there exist four different Ago proteins (Ago1-4) and three different TNRC6 proteins (TNRC6A-C) whose functions seem largely redundant (Su *et al.*, 2009; Lazzaretti *et al.*, 2009; Zipprich *et al.*, 2009). After loading of the RNA duplex, one of the two strands is removed leaving the activated RISC which is ready to bind and silence RNAs that carry sequences partially or fully complementary to the loaded strand (Matranga *et al.*, 2005; Rand *et al.*, 2005). The strand that is finally guiding RISC to its targets is called "guide strand" and the discarded strand "passenger strand". RISC binding to target RNAs leads to two different outcomes depending on the nature of the miRNA binding site. In case of perfect complementarity to the guide strand the target may be directly cleaved and thus inactivated in a fast and

efficient way (Martinez *et al.*, 2002; see next section). Imperfect complementarity leads to translational inhibition as well as accelerated decay without direct cleavage (Valencia-Sanchez *et al.*, 2006). In case of such target RNAs that are not cleaved RISC recruits downstream factors such as the Ccr4-Not1 deadenylase complex and decapping factors like Dcp1 and Dcp2 that are part of the 5'→3' RNA degradation machinery (Behm-Ansmant *et al.*, 2006). The target RNAs are subsequently concentrated in cytoplasmic foci called processing bodies (P-bodies) which appear to be the sites of degradation (Parker and Sheth, 2007).

1.1.3 Perfect and imperfect targets and hAgo2 slicing activity

The exact sequence features that render a specific RNA susceptible to miRNA binding and subsequent silencing are still not fully understood (Bartel, 2009). This is because basically all identified endogenous targets for miRNAs do not show perfect complementarity to the respective miRNA (Lai, 2002). Instead, partial complementarity was found to be sufficient. Due to the low stringency of target recognition one single miRNA can potentially have hundreds of different targets (Lim *et al.*, 2005). A key finding in the search for parameters that are important for miRNA-target binding was the notion that sequence stretches with perfect complementarity to the first eight 5' nucleotides -with particular importance of nucleotide 2-8- of the miRNA are sufficient for mRNA binding and repression (Doench and Sharp, 2004). This suggests that the binding reaction between miRNA and target commences at the miRNA 5' end where the complementarity hence has to be rather optimal and then proceeds with less stringent requirements towards the 3' end. These essential 5' nucleotides within the miRNA strand were therefore termed "seed" region (Lewis *et al.*, 2005). However, it is important to note that i) the seed match rule is not exclusive as other binding modes have been proposed that, for example, require nucleotides matching the center of the miRNA or imperfect seed matches (Shin *et al.*, 2010; Chi *et al.*, 2012) and ii) the mere presence of a seed match does not guarantee that the corresponding mRNA is a real target (Didiano and Hobert, 2006). The latter is linked to the fact that unrelated sequence features flanking the seed match may dramatically alter the likelihood of the sequence to be bound (Kertesz *et al.*, 2007). Since these flanking features are difficult to take into account miRNA

target prediction is still far from being perfect. Nevertheless, seed matching is currently the best described binding mode and holds true for the majority of validated miRNA targets. It is also noteworthy that most miRNA binding sites have been found in the 3' UTRs of their target genes (Lai, 2002; Bartel, 2009). The biological reason for this appears to be that when RISC binds to targets in the 5' UTR or the open reading frame (ORF) it can be stripped off the transcript by polysomes (Gu *et al.*, 2009). In addition, 5' UTRs are also usually much shorter than 3' UTRs and therefore have a lower capacity for regulatory sequences (Mazumder *et al.*, 2003). However, it has been shown that binding sites in the 5' UTR and the coding sequence can also be functional (Lytle *et al.*, 2007; Hafner *et al.*, 2010; Reczko *et al.*, 2012).

Although imperfect binding sites represent the vast majority of known endogenous miRNA targets, the effect on perfect target sites as used initially by Mello and Fire in their application of exogenous triggers of RNAi is dramatically more potent. This phenomenon could be linked to a catalytic activity of some but not all members of the Ago family that cleave -or "slice"- target RNAs with perfect or nearly perfect complementarity to the bound guide strand, an attribute that is called "slicer activity" (Liu *et al.*, 2004; Meister *et al.*, 2004). In humans, only hAgo2 is able to slice whereas hAgo1, 3 and 4 exclusively act via accelerated decay and translational inhibition, regardless of the nature of the binding site (Su *et al.*, 2009). In addition to target slicing, the catalytic activity of hAgo2 has recently been linked to RISC activation with perfectly complementary RNA duplexes (Matranga *et al.*, 2005; Diederichs and Haber, 2007; Gu *et al.*, 2011). By slicing the passenger strand hAgo2 is able to destabilize the duplex so that the passenger strand can be efficiently removed. In contrast, the other human Agos remain bound to the duplex and are unable to direct target silencing if the thermodynamic stability of the molecule is too high. This effect is most pronounced with hairpin-derived RNAi triggers but not with siRNAs that mimic the Dicer processing product (Gu *et al.*, 2011). However, most but not all endogenous miRNAs do not have perfectly complementary stems and are thus readily activated in all four hAgos. One example for a particular miRNA with perfect stem is miR-451 whose final maturation and activation are uncoupled from the canonical miRNA pathway and depend solely on hAgo2 slicing activity

(Cheloufi *et al.*, 2010; Cifuentes *et al.*, 2010; Yang *et al.*, 2010a). Dicer which usually trims the miRNA precursor is not required in this process.

1.1.4 Gene silencing by exogenous triggers of RNAi – siRNAs and shRNAs

Aside from endogenous triggers of RNAi there are also different classes of exogenous counterparts that make use of the underlying molecular mechanisms for targeted silencing of specific genes (Fig. 1). All of these classes have in common that they are typically designed to have perfect complementarity to the designated target RNA in order to allow slicing to occur and thereby maximize the silencing effect. The first and still most famous molecules are exogenous small interfering RNAs (siRNAs) that were found to be potent inhibitors of gene expression in initial studies (Elbashir *et al.*, 2001b). siRNAs consist of two complementary 21nt long RNA strands that hybridize to form a 19-mer duplex with 2nt 3' overhangs at either side. They hence structurally resemble mature miRNA duplexes after Dicer processing and can be directly incorporated into RISC. While usually yielding potent silencing of target genes, siRNAs are expensive and only permit transient effects on gene expression as they are degraded in the cell with time (Czauderna *et al.*, 2003). However, for some applications -*e.g.* in gene therapy or long-term silencing experiments- it is necessary to generate more sustained RNAi responses. Thus, strategies were devised that did not require transfection of chemically synthesized siRNAs but, instead, were based on the production of the RNAi trigger within the target cell. To this end, RNA-polymerase III (RNA-pol III) promoters were used in an initial attempt to transcribe a defined DNA sequence from either side to obtain complementary RNAs that could form a duplex and provoke an RNAi response. However, although functional to a certain degree this strategy was rather inefficient (Miyagishi and Taira, 2002; Jin *et al.*, 2011). Hence, the stem-loop structure of miRNA precursors was copied so that instead of two separate strands one single precursor molecule was produced that carried the two complementary strands connected by a short loop sequence. Due to their structure these molecules were termed short hairpin RNAs (shRNAs). This approach yielded highly potent and sustained gene silencing and thus paved the way for a broad application in human functional genomics and potential gene therapeutic strategies (McManus *et al.*, 2002; Paddison *et al.*, 2002; Yu *et al.*,

2002; Zeng *et al.*, 2002). Ever since their initial description, shRNAs have been steadily modified and improved so that we now have a wide variety of different options at hand. Besides the “classical” RNA-pol III-driven shRNAs with perfectly complementary stems, shRNAs can also be designed to carry mismatches in their stems and to be transcribed by RNA-pol II promoters. Each of these strategies has advantages and drawbacks. RNA-pol III promoters, for instance, allow transcription of a precise precursor molecule that bypasses Drosha processing and yields high levels of mature shRNA strands but these promoters do not permit facile tissue-specific expression. The latter can only be envisioned with engineered inducible RNA-pol III promoter where a transcriptional activator is expressed from a tissue-specific RNA-pol II promoter (Gupta *et al.*, 2004). While tissue-specificity is much easier to obtain with RNA-pol II promoters regardless of inducibility, the resulting shRNAs have to be transcribed as primary transcripts that are Drosha substrates which might lead to potential interference with the endogenous miRNA pathway. In addition, the final intracellular levels of the mature shRNA are lower than with RNA-pol III counterparts. On the one hand, this leads to lower gene silencing efficiencies but may on the other hand decrease undesired side effects (Boudreau *et al.*, 2008; Li and Mahato, 2009 see also section 1.1.6.2).

Mismatches in the shRNA stem can be beneficial as they may positively influence the strand selection process and therefore increase the specificity of a given shRNA (see section 1.1.8). However, it is important to mention that shRNAs with bulged stems have also been found to be less potent gene suppressors than their perfect stem counterparts (Mcintyre *et al.*, 2006). Thus, given the number of different variables that have to be taken into account during shRNA design, it is still not clear which strategy is best suited for general use. Instead, the design has to be specifically adapted to the purpose of application.

1.1.5 Strand terminologies

The names used for the strands of different triggers of RNAi are sometimes ill-defined which may lead to confusion among readers unfamiliar with the topic but also people working in the field. The terminology used in this study is therefore briefly defined. As aforementioned, the strand that is finally incorporated into active RISC is called “guide strand” whereas the discarded strand is termed

"passenger strand". As this refers to single molecular events, in principle both physical strands of the small RNA duplex have the potential to become guide or passenger strand. However, in miRNA terminology the guide strand is classically the one that is mostly detected either by cloning or high-throughput analyses like miArray or deep sequencing with the other one being the star strand (*e.g.* miR-30 and miR-30*) (Tomari and Zamore, 2005). Yet, by classical definition the star strand can also act as guide strand although usually with lower frequency than the designated guide strand. In fact, a number of studies have recently cast doubt on the original model that proposed only one mature strand per miRNA precursor (Ro *et al.*, 2007; Kuchenbauer *et al.*, 2011; Zhou *et al.*, 2010; Yang *et al.*, 2011). A more appropriate way is thus to term the strands according to their position within the miRNA precursor, *i.e.* at the 5' or 3' end as it is nowadays done in the miRNA database miRBase 18 (*e.g.* miR-124-5p and -3p as proposed by Ro *et al.*, 2007). For miRNAs we will therefore stick to this strand definition.

Artificial molecules like shRNAs and siRNAs are designed to specifically silence a gene with a perfectly complementary sequence stretch so that the target mRNA is defined as "sense" and the complement as "antisense" (Fire *et al.*, 1998). The antisense strand of an si- or shRNA is thus the one that is supposed to be as active as possible whereas the sense strand that has exactly the same sequence as the mRNA target is supposed to be as inactive as possible. As in miRNAs, both strands have in principle equal opportunities to become either guide or passenger strand. A problem in terminology arises in the case of asymmetrical molecules like shRNAs where both sense and antisense strand can be located either at the 5' or 3' end of the molecule. The position of sense or antisense in the shRNAs used in this study will therefore be clearly indicated in each case.

1.1.6 Side effects of exogenous triggers of RNAi

1.1.6.1 Induction of the innate immune system

The initial enthusiasm about the potency and specificity of targeted RNAi was dampened by a number of studies that reported potentially adverse side effects. For instance, the double-stranded exogenous RNA can be recognized by pattern recognition receptors which may lead to an interferon response (Bridge *et al.*, 2003). Regardless of the RNA sequence, this effect can depend on the presence of blunt ends or on the length of the double-stranded molecule in a cell type-

dependent manner (Reynolds *et al.*, 2006; Marques *et al.*, 2006). Moreover, interferon induction can also be sequence-specific, *e.g.* GU-rich dsRNAs were found to be more likely to trigger a response (Judge *et al.*, 2005). Accordingly, the RNAi trigger should not exceed 29nt in length or contain blunt ends and certain immunostimulatory GU-rich sequences should be omitted when choosing the target site (Judge and Machlachlan, 2008). However, there may be more parameters that could influence stimulation of the innate immune system and that are currently unknown. In principle, the RNAi trigger of choice should therefore be carefully tested even when designed according to the abovementioned rules.

1.1.6.2 Interference with the endogenous miRNA pathway

In 2006, fatality in mice could be linked to high intracellular shRNA abundance after potent shRNA expression in mouse livers (Grimm *et al.*, 2006a). This dramatic phenotype was independent of the shRNA sequence and unrelated to any activation of the innate immune system. Instead, it could be linked to the degree of shRNA expression and a concomitant competition for miRNA pathway components resulting in perturbation of miRNA functionality. This could be deduced from the finding that the toxicity could be partially relieved by overexpression of Exportin-5. Later on, overexpression of Ago2 also proved to alleviate shRNA-mediated toxicity to a certain extent (Grimm *et al.*, 2010). Cytotoxicity from shRNA expression was also linked to tumor formation in mice (Beer *et al.*, 2010). The initial findings were confirmed in other tissues like brain and heart muscle meaning that the deleterious effects of shRNA expression *in vivo* are not restricted to the liver but may affect organs throughout the whole body (McBride *et al.*, 2008; Bish *et al.*, 2011). In addition, expression of exogenous triggers of RNAi can result in decreased miRNA functionality in tissue culture, too (Khan *et al.*, 2009). This may even lead to experimental failure and cytotoxicity in primary cells (Pan *et al.*, 2011; An *et al.*, 2006). As a result, the use of extremely strong promoters for shRNA expression -like the RNA-pol III U6 promoter- is not recommended. Instead, either weaker RNA-pol III promoters like H1 or 7SK or RNA-pol II promoters can be used for shRNA expression (Castanotto *et al.*, 2007; Giering *et al.*, 2008; Grimm *et al.*, 2010).

1.1.6.3 Off-targeting

Aside from their designated target with perfect complementarity to the antisense strand, exogenous RNAi triggers also sequence-specifically bind untargeted cellular transcripts -so-called off-targets- and lead to their silencing (Fig. 2; Doench *et al.*, 2003; Jackson *et al.*, 2003). This can be explained by the fact that shRNA or siRNA are functionally similar to miRNAs which may have hundreds of different cellular targets due to the relatively low stringency of their target selection mechanism. It therefore seems logical that the antisense strand of exogenous RNAi triggers could also silence targets with partial complementarity in a miRNA-like fashion (Zeng and Cullen, 2003a). Likewise, the sense strand is also able to exert silencing on both perfect and imperfect targets. This off-targeting was first experimentally addressed after transfection of siRNAs into mammalian cells (Jackson *et al.*, 2003). In a follow-up study Jackson and colleagues reported that the same effect was observed with shRNAs, too, which could be confirmed by independent studies (Jackson *et al.*, 2006a; Klinghoffer *et al.*, 2010). Subsequently, they and other groups also showed that off-target effects are linked to seed matching between si/shRNA and 3' UTR sequences of off-target genes proving that the underlying mechanism is indeed miRNA-like silencing (Birmingham *et al.*, 2006). This was further confirmed by a study showing that hAgo2 slicing activity is not required for siRNA-mediated off-target effects (Vickers *et al.*, 2009). Although the degree of silencing of untargeted genes is usually modest, off-targeting can still have deleterious side effects like experimental failure and toxic phenotypes (Fedorov *et al.*, 2006; Schultz *et al.*, 2011; Grimm, 2011)

1.1.7 Strategies to reduce off-targeting

Naturally, tremendous efforts have been put into making exogenous RNAi triggers more specific. However, one major obstacle lies within the low fidelity of off-target prediction methods due to the same problems that hamper miRNA target prediction. It is therefore not possible to rationally design the sequences of si- or shRNAs to guarantee prevention of off-target silencing of specific genes (such as proto-oncogenes). It was furthermore shown that the profile of off-target effects is species-specific, thus adding another layer of complexity to the issue (Burchard *et al.*, 2009). This means that potential therapeutic RNAi triggers

cannot be comprehensively tested in animal models to address possible off-targeting-related side effects before going into patients.

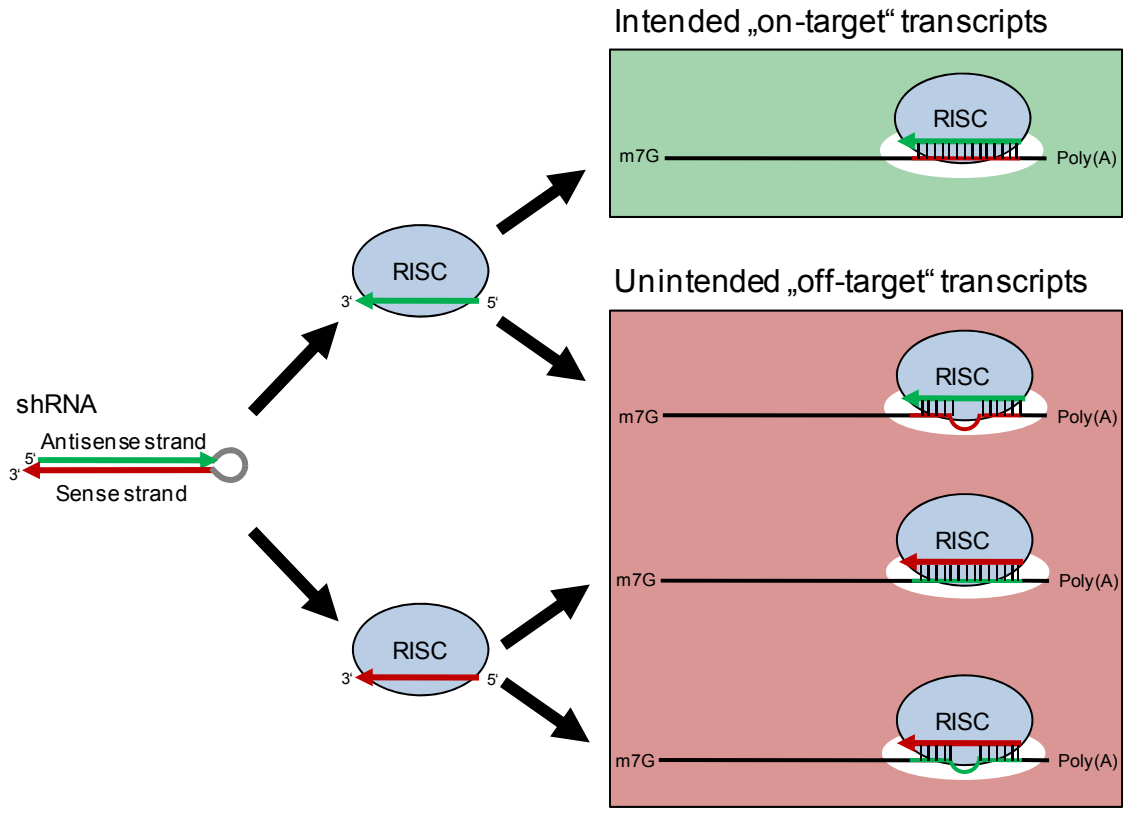

Fig. 2: **shRNA on- and off-target activities**. In principle, both strands of an shRNA can be active as RNAi trigger. The antisense strand mediates intended silencing of the designated cellular target RNA which is defined as „on-targeting“. However, both the antisense and the sense strand can produce silencing of untargeted transcripts by either imperfect (i.e. miRNA-like) or perfect binding sites. Ideally, an shRNA should produce maximal levels of intended target silencing and minimal levels of off-targeting. RISC = RNA-induced silencing complex.

1.1.7.1 Chemical modifications and rational choice of sequence

Certain chemical modifications at particular positions of siRNAs duplexes can beneficially influence target selectivity (Jackson *et al.*, 2006b). These modifications allow selective inactivation of the siRNA sense strand and exclusive silencing of perfect targets by the antisense strand (Jackson *et al.*, 2010). In addition, a plethora of different siRNA configurations and compositions has been proposed that all reduce off-target effects, for instance the incorporation of DNA or LNA nucleotides (Ui-Tei *et al.*, 2008; Elmen *et al.*, 2005). Yet, an ingenious study in 2008 also demonstrated the possibility to improve siRNA specificity by rational choice of the seed sequence (Anderson *et al.*, 2008). Upon analysis of

the frequencies of all 4096 possible hexamers in human 3' UTRs the authors found that some hexamers are present at much lower frequencies than others. By using such low frequency hexamers in siRNA seed regions they could considerably reduce the overall perturbation of gene expression produced by the siRNA. This design does not compromise activity of the respective strand *per se* but it reduces off-targeting simply by limiting the number of potential off-targets. In addition, using siRNA duplexes with high thermodynamic stability was reported to decrease off-target and increase on-target effects (Petri *et al.*, 2011). Taken together, it is evident that a lot of different methods exist to guarantee a high degree of target specificity with synthetic siRNAs.

However, most of these methods -*i.e.* any chemical modifications- are not applicable for shRNAs. A recent report therefore adopted the "safe seed" concept previously shown with siRNAs and proposed to design shRNAs in a way to contain seed regions with minimal frequencies of complementary sequences in 3' UTRs of cellular genes (Boudreau *et al.*, 2011). In addition, using seed regions with low melting temperatures in the seed-target duplex also reduce seed-mediated off-target effects of shRNAs (Naito *et al.*, 2009). While it is definitely advisable to take these strategies into account when designing new shRNAs, they are not always readily applicable. In the case of viral targets, for instance, the choice of the shRNA target site is often rather limited. This is due to the fact that many viruses present a high mutation rate during their replication cycle so that only those sequences that are highly conserved are suitable RNAi targets (Von Eije *et al.*, 2008).

1.1.7.2 Strand biasing mechanisms

While there are no other means of making shRNA antisense strands more specific apart from using "safe" and low melting temperature seed regions, additional strategies have been devised to reduce sense strand-derived off-targeting. These methods benefit from the fact that sense strand activity is not required for the desired silencing of the designated antisense target so that it can in principle be reduced to minimal levels without compromising shRNA potency.

A certain reduction of sense strand activity can be achieved by using naturally occurring strand biasing mechanisms (Boudreau *et al.*, 2008; Ding *et al.*, 2008; Boudreau *et al.*, 2011). The basis for this came from the notion that in most RNAi

triggers the two strands are not incorporated into RISC at equal frequencies. Mechanistic insights came from studies on siRNAs and miRNAs showing that the rate of incorporation of a given strand depends on the relative thermodynamic RNA duplex stability at its 5' end (Schwarz *et al.*, 2003; Khvorova *et al.*, 2003). This means that the strand with the lower thermodynamic stability at its 5' end has a higher likelihood of being used as guide strand. This may depend both on GC-content and existence of mismatches at either end of the duplex which is usually the case for miRNAs that rarely have perfectly matched stems. However, strand selection in miRNAs cannot be merely reduced to thermodynamic asymmetry of the duplex. Instead, the same pre-miRNA precursor can have a strong bias towards one strand in one tissue type but not in another indicating the involvement of additional, cell type-dependent factors (Ro *et al.*, 2007). In addition, in miRNAs with strong strand biasing a 5' cytosine was linked to the lower expressed strand while high purine content and a 5' uracil were shown to be characteristics of the higher expressed strand (Hu, 2009). The structural basis for the latter seems to lie in specific interactions between 5' uracil and a conserved loop within the hAgo2 Mid domain (Frank *et al.*, 2010). Implementation of these findings for optimal shRNA design is challenging as it is not always possible to find a suitable target site that is compatible with the abovementioned rules.

Besides via thermodynamic stability a certain strand bias may also be introduced by Dicer processing. The use of perfect RNA duplex molecules with DNA nucleotides at one end that only allowed Dicer processing from one side revealed a functional polarity towards the strand that carries a 2nt 3' overhang and that is thus bound by Dicer (Rose *et al.*, 2005). In shRNAs with perfect stems it is only the 3' strand that possesses a 3' overhang and, indeed, a general functional bias towards this strand has been shown (Boudreau *et al.*, 2008). However, a recent study reported that small RNA duplexes are first released from Dicer after cleavage and then rebound and repositioned according to their thermodynamic asymmetry (Noland *et al.*, 2011). This model suggests that there is no general mechanism that favors incorporation of the strand that is initially bound by Dicer but, instead, completely refers to thermodynamic asymmetry. Yet another study claims that Dicer does not contribute to asymmetric RISC loading at all (Betancur and Tomari, 2012). The mechanistic basis for the functional strand bias observed

by Rose and colleagues is thus not clear. Nevertheless, the standard design of RNA-pol III shRNA places the antisense strand at the 3' end of the hairpin molecule (Mcintyre *et al.*, 2011). To further increase the strand bias, strategies have been designed that introduce mismatches at the 5' end of the antisense strand, thus employing the thermodynamic stability rule (Ding *et al.*, 2008; Boudreau *et al.*, 2011). However, none of the studies convincingly showed reduction of shRNA sense strand activity to levels that do not contribute to off-targeting anymore under therapeutically relevant conditions, particularly upon expression from viral vectors.

1.2 Hepatitis C virus

Hepatitis C virus (HCV) is an enveloped, positive-sense single-stranded RNA virus of the family *Flaviviridae* and the causative agent of hepatitis C in humans. The viral core consists of the RNA genome surrounded by an icosahedral shell of core proteins (Bartenschlager *et al*., 2011). The core is enclosed by a lipid envelope. A transmembrane domain of the core proteins links the core to two viral glycoproteins E1 and E2 that are embedded in the envelope. Core and envelope form particles of around 60nm in size.

The HCV genome harbors a single open reading frame (ORF) of 9600 nucleotides (Bartenschlager and Lohmann, 2000). Translation of the ORF starts via an internal ribosomal entry site (IRES) producing a single protein product that is then proteolytically cleaved to yield smaller active proteins. The 5' and 3' ends of the RNA consist of non-translated regions (NTRs) that are important for translation and replication of the viral RNA (Friebe and Bartenschlager, 2009). Due to the high mutation rate during HCV replication a wide variety of different HCV genotypes exist (Kuiken and Simmons, 2009). The different genotypes result in different disease progressions and have different susceptibilities to antiviral treatments (see below).

1.2.1 HCV replication

HCV replicates mainly in hepatocytes but may also reside in peripheral blood mononuclear cells (Zignego *et al*., 1992). After viral entry and release of the RNA genome into the cytoplasm a first round of translation occurs that yields a polyprotein that is proteolytically cleaved into smaller active proteins

(Bartenschlager and Lohmann, 2000). One of the proteins is the viral RNA-dependent RNA polymerase NS5B that subsequently produces a negative strand template for further production of positive sense genomes. NS5B activity is highly error-prone leading to high mutation rates during HCV replication (Contreras *et al*., 2002). Replication of the viral genome occurs in a membranous web that is induced by another virally encoded protein, NS4B, and that is derived from the endoplasmic reticulum (ER) membrane (Alvisi *et al*., 2011). Genomes are then translated, further replicated or packaged into new virus particles that bud from the cells and spread the infection.

The human liver-specific miRNA miR-122-5p binds to a specific target sequence at the 5' end of the HCV genome (Jopling *et al*., 2005). However, miR-122-5p does not inhibit HCV as could be expected from the natural mode of action of miRNAs. Instead, miR-122-5p binding protects the HCV 5' end and leads to markedly increased viral replication and thus seems to act as an important co-factor for replication (Jopling *et al*., 2005; Shimakami *et al*., 2011). This is the only example of a miRNA positively influencing the translation and stability of a target RNA.

1.2.2 HCV therapies

There are an estimated 170 Mio HCV-infected individuals worldwide. Around 80% of infections lead to a chronic progression which is the primary cause of liver cirrhosis and hepatocellular carcinoma with 10-30% of infected subjects developing cirrhosis over 30 years (Rosen, 2011). The standard treatment for HCV genotypes 2 and 3 consists of pegylated interferon alpha (PEG-IFNa) and the antiviral drug ribavirin leading to viral eradication in around 85% of patients (Bühler and Bartenschlager, 2012). For HCV genotype 1 which is the most prevalent world-wide the probability of therapeutic success is lower with this therapy. A novel treatment has therefore recently been admitted for genotype 1 in the US that combines the standard treatment with the protease inhibitors boceprevir and telaprevir which improves the outcome of therapy (Bühler and Bartenschlager, 2012).

Current treatments have vastly icreased the survival rates of infected individuals but therapy is not always successful. Moreover, treatment of chronic infection with PEG-IFNa and ribavirin is expensive and can produce severe side effects.

Thus, alternative strategies are developed to effectively counteract or even cure chronic infection without the need of PEG-IFNa. In a recent clinical trial, a combination of a protease inhibitor, a NS5B polymerase inhibitor and ribavirin was shown to efficiently clear HCV after only 30 days of treatment without strong side effects (Zeuzem *et al*., 2011). In another clinical trial, HCV could be counteracted by miR-122 inhibition via locked nucleic acid (LNA) probes with a phosphothioesterate backbone (source: www.santaris.com). These approaches offer promising new treatment strategies but long-term patient progression has yet to be determined. Another approach that is not at the stage of clinical trials yet, but that also holds promise for the treatment of HCV infection is RNAi-based gene therapy (Grimm and Kay, 2006). In this strategy, a single gene therapeutic treatment could ideally lead to life-long resistance to the virus. A number of studies have shown the effectiveness of vector-encoded shRNAs against HCV (Kapadia et al., 2003; Wilson et al., 2003; Randall et al., 2003). To avoid viral escape from RNAi treatment due to mutations the shRNAs are commonly directed against conserved sequences within the HCV genome (Wilson and Richardson, 2005; Yang *et al*., 2010b). The suitability of conserved target sites within the HCV 5'NTR as RNAi targets was comprehensively shown by Krönke and colleagues in 2004 (Krönke *et al*., 2004). In addition, combinatorial RNAi strategies have been tested that express several shRNAs at the same time making viral escape less likely (Yang *et al*., 2010b).

1.3 Adeno-associated virus

1.3.1 Wildtype AAV

Adeno-associated virus (AAV) is a non-enveloped, helper-dependent virus that belongs to the family of *Parvoviridae* (Berns and Giraud, 1995). With a diameter of around 20nm it is among the smallest known viruses. The single-stranded DNA (ssDNA) genome of wildtype AAV (wtAAV) only encodes two genes that give rise to a total of 8 proteins (Sonntag *et al*., 2010). Two promoters p5 and p19 drive expression of two overlapping mRNAs that are both alternatively spliced resulting in 4 different gene products. As these products are implicated in AAV replication, the corresponding genes are called *rep* genes and the encoded proteins Rep78, Rep68, Rep52 and Rep40, according to their molecular weight.

Another promoter -p40- drives expression of the assembly factor AAP and the three structural AAV proteins VP1-3 that are produced in a ratio of 1:1:10 and together form the viral capsid (Sonntag *et al.*, 2010; Rose *et al.*, 1971). The corresponding gene was therefore termed *cap* gene.

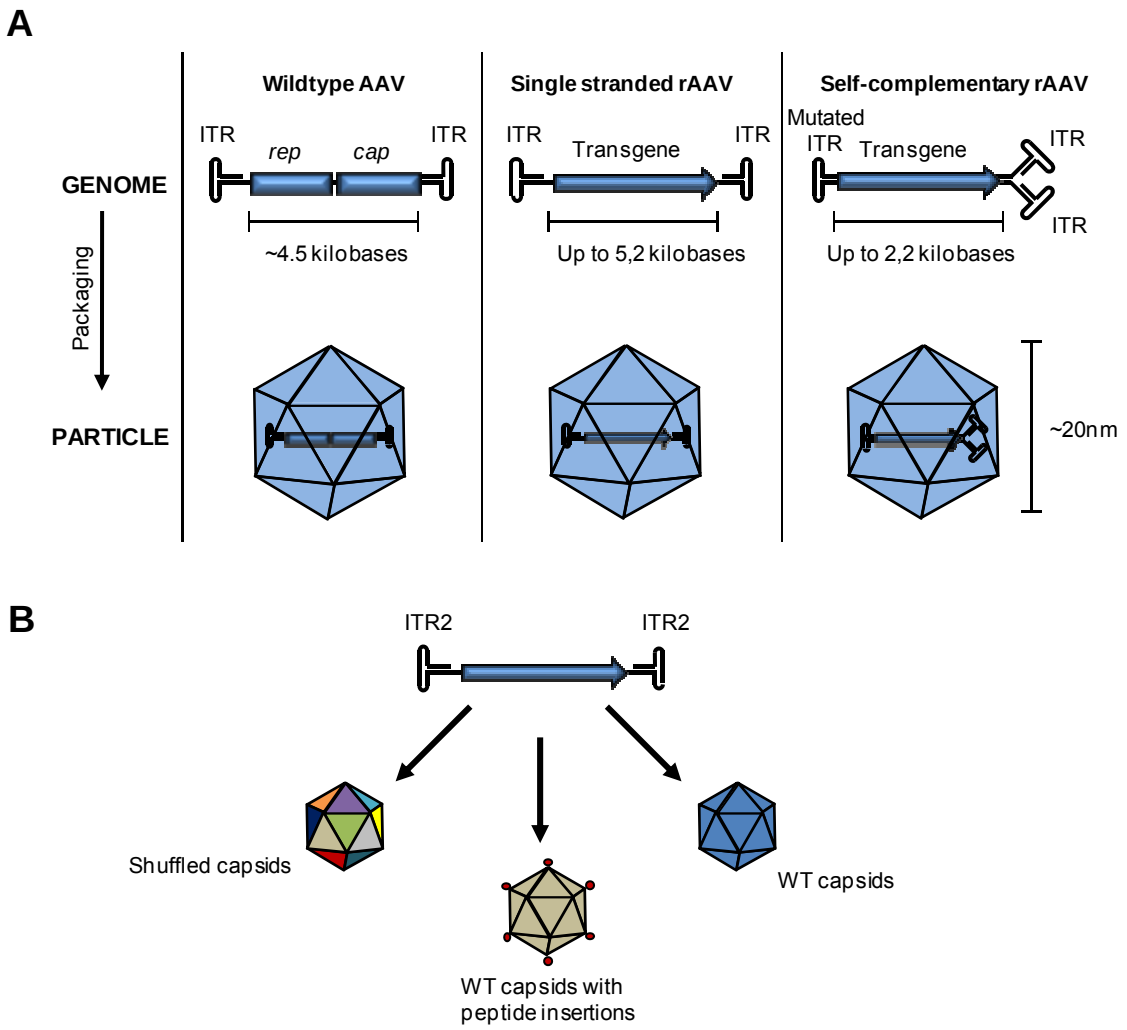

Fig. 3: Wildtype AAV and recombinant AAV technology. A: Wildtype AAV (wtAAV) carries two genes involved in replication (*rep*) or packaging (*cap*). The only sequence elements required for packaging *in cis* are the inverted terminal repeats (ITRs). Recombinant AAVs (rAAVs) can therefore be generated by packaging transgenes flanked by ITRs into AAV capsids. Single-stranded rAAVs replicate like wtAAV and carry a single stranded DNA copy of the transgene. Self-complementary vectors have one mutated ITR. This leads to the generation of inverted repeats during vector replication that can fold back and permit faster and enhanced transgene expression upon transduction. Adapted from Mockenhaupt and Grimm, 2011. **B:** Transgenes flanked by AAV ITRs can be pseudotyped with naturally occuring capsids from other WT serotypes or with synthetic capsids that carry peptide insertions or that are shuffled from different serotypes. This allows generation of particles with characteristics -especially tropisms- tailored to the application.

The *rep* and *cap* genes are flanked by inverted terminal repeats (ITRs) on either side. The ITRs have essential functions for AAV genome replication as their structure allows self-priming which subsequently permits the cellular replication machinery to initiate the replication reaction without the need for a primase (Xiao *et al.*, 1997). In addition, they also harbor the so-called terminal resolution site (trs). The trs is a particular DNA sequence targeted by the AAV replication protein Rep78 that generates a DNA single-strand break which then allows the double-stranded replication intermediate to be dissociated into two mature ssDNA AAV genomes that are ready for packaging (Snyder *et al.*, 1993). Unlike other parvoviruses, AAV packages both single-stranded versions of its genome so that particles with both genome polarities coexist (Berns and Adler, 1972). WtAAV site-specifically integrates with high frequency at a certain locus on human chromosome 19 which was termed AAVS1 (Kotin *et al.*, 1990). Integration into AAVS1 depends on Rep68 and 78 (Surosky *et al.*, 1997). Furthermore, AAV is able to infect both dividing and non-dividing cells (Flotte *et al.*, 1994; Podsakoff *et al.*, 1994). It produces only a mild innate immune response but robust humoral immunity (Zaiss *et al.*, 2002). The latter may pose potential problems for employing AAV as gene therapy vector. However, these issues can be largely circumvented by the use of engineered AAV serotypes (see below).

1.3.2 Recombinant AAV technology

The only wtAAV features required *in cis* for packaging into particles are the two ITRs (Xiao *et al.*, 1997). The *rep* and *cap* genes can be readily delivered *in trans* which makes it easy to package a totally unrelated sequence into AAV capsids (Fig. 3A). Such a particle that carries genetic material other than the WT genome is called recombinant AAV (rAAV).

1.3.2.1 Characteristics of rAAV

To date, there are at least 12 different wtAAV serotypes plus hundreds of isolates available whose most important difference lies within their *cap* sequences (Grimm and Kay, 2003). The resulting AAV particles vary considerably in their tropisms. For example, AAV8 has a strong but not exclusive liver tropism in mice whereas AAV1 is more efficient at infecting heart muscle cells (Gao *et al.*, 2002; Inagaki *et al.*, 2006). Besides the naturally occurring serotypes, an ever-expanding plethora of synthetic capsids further broadens the spectrum of cell

types that are susceptible to AAV infection. DNA family shuffling methods or peptide insertions into specific position within the capsid proteins followed by AAV library-based selections hold promise to target virtually any cell type of choice (Grimm *et al.*, 2008). Importantly, most ITRs are compatible with packaging into capsids from another serotype so that transgenes flanked by ITRs from the commonly used AAV2 serotype can be readily pseudotyped with different capsids (Fig. 3B; Rabinowitz *et al.*, 2002; Grimm *et al*., 2006b). This allows easy production of particles with tropisms matched to the experimental or therapeutic setup which greatly facilitates the use of rAAV as gene therapy vector and as an *in vitro* or *in vivo* transduction reagent.

Like wtAAV, rAAV can infect both dividing and non-dividing cells which is essential for using it as gene transfer vehicle *in vivo* as most cells in the body of mammals are quiescent in their normal state (Flotte *et al.*, 1994; Podsakoff *et al.*, 1994). However, there is no site-specific integration into AAVS1 as the vectors do not express the required Rep proteins. Instead, they circularize *in vivo* via their ITRs and can persist indefinitely as episomes thus allowing long-term transgene expression without vector integration (Yan *et al.*, 2005; Kaplitt *et al.*, 1994; Podsakoff *et al.*, 1994). One potential drawback of rAAVs is the low packaging capacity of up to 5.2kb (Dong *et al.*, 1996). While this does not allow delivery of large transgenes it is irrelevant for the transfer of short sequences such as shRNA expression cassettes that were used in this study.

1.3.2.2 Self-complementary AAV

Upon AAV infection, the particle trafficks to and into the nucleus where it is uncoated to release the ssDNA genome. For conventional rAAV vectors with ssDNA genomes (ssAAVs) the second DNA strand then has to be synthesized or complemented by a ssDNA genome of opposite polarity before any gene expression can occur; a step that rate-limits AAV-mediated transduction (Ferrari *et al.*, 1996; Fisher *et al.*, 1996; Nakai *et al.*, 2000). To overcome this issue, so-called self-complementary rAAV (scAAV) vectors were designed (McCarty *et al.*, 2003). For their generation, the trs of one of the two ITRs is mutated so that it cannot be nicked by Rep78 anymore. During replication of such structures the ensuing intermediates cannot be separated leading to a double-sized genome that forms a large inverted repeat. This inverted repeat genome is then packaged

as ssDNA into rAAVs. Upon infection, the genome rapidly folds into a dsDNA form and thus permits faster and enhanced gene expression both in tissue culture and *in vivo* as compared to ssAAVs. A drawback of scAAV vectors is the even smaller packaging capacity which is reduced to 2.2kb although this is no obstacle for shRNA delivery as mentioned before. All rAAVs used in this study were of the self-complementary type.

1.3.2.3 rAAV as gene therapy vectors

Until January 2012, rAAV vectors had been tested in 86 clinical trials with 12 of them being in phase II and 8 in phase III (source: The Journal of Gene Medicine, see section 6.2. for weblink). The range of diseases that are to be treated is extremely diverse and administration can be both local and systemic. Importantly, these trials show that rAAVs are versatile, potent and safe vectors for gene therapeutic applications.

1.4 shRNAs and rAAV vectors

1.4.1 Application in gene therapy

siRNAs are commonly used in tissue culture experiments. However, not all cell types are easy to transfect and, likewise, the main obstacle of using synthetic siRNAs *in vivo* is the difficulty of efficient systemic delivery rendering certain therapeutic applications impossible at this point. In addition, the effect of siRNAs is only transient which is not desirable in every application. Starting in the early 2000s, expressed shRNAs were tested as gene therapeutic silencing tool and combined with viral vectors -including rAAV- in the hope of finding ways of treating a wide range of different diseases that could not be treated otherwise. Highly promising results were obtained in proof-of-principle tissue culture studies for the treatment of diseases ranging from CNS disorders over viral infections to cancer (Grimm and Kay, 2007a). However, in pre-clinical *in vivo* studies expression of RNAi triggers was linked to cytotoxicity and fatality in mice (see section 1.1.6.2) which temporarily dampened the belief in the therapeutic potential of the technology. Fortunately, the use of weaker promoters and inducible expression strategies is starting to overcome this issue so that in the long run a therapeutic implementation seems possible. Given the flexibility in tropism and their high *in vivo* transduction efficiencies, rAAV vectors are

particularly interesting for the delivery of shRNA-based therapeutics to a variety of different tissues, especially liver, heart and brain (Danos, 2008).

1.4.2 Application in functional genomics

A second important application of RNAi triggers lies in functional genomics. Again, shRNAs expressed from viral vectors are able to overcome the abovementioned restrictions with siRNAs. On the one hand, this may facilitate studies that examine the function of particular genes. rAAV is an ideal candidate for such studies, especially if gene functions should be unraveled *in vivo*. On the other hand, virally-encoded shRNAs can increase the power of RNAi screens (Blakely *et al.*, 2011). This requires the generation of viral vector-based shRNA libraries which is much more challenging than producing siRNA libraries. However, once established these shRNA libraries offer a considerably higher versatility and thus applicability than siRNAs. While the most commonly used shRNA libraries are based on lentiviral vectors, rAAV could be an attractive alternative under certain experimental conditions (Danos, 2008).

1.5 Research questions and objectives

In this study, we aimed at improving current strategies for therapeutic shRNA expression. Specifically, we wanted to reduce off-target effects derived from shRNA sense strands to increase specificity and hence reliability of RNAi triggers for potential use in antiviral therapy. Our therapeutic target model system was hepatitis C virus.

We first focused on functionally characterizing previously published shRNAs with particular interest in the relative activities of sense and antisense strands. As we were aiming at maximal antisense strand potency we focused our work on RNA-pol III-transcribed “classical” shRNAs with perfectly matched stems that are more efficient in silencing their designated targets than other types of hairpins (see section 1.1.4). Our functional shRNA analysis allowed us to formulate some design rules that were next applied to generate an shRNA targeting a conserved sequence in the HCV 5’NTR. We subsequently further improved the anti-HCV shRNA expression vector by applying a novel strategy to reduce sense strand activity without altering antisense strand activity. Our method allowed us to decrease off-target effects without compromising HCV inhibition. The improved

system was tested in combination with rAAV-mediated gene delivery which represents a promising and powerful tool for *in vivo* application of RNAi therapeutics. Last but not least, we also examined the applicability of our strategy for reduction of sense strand activity with other shRNAs and tested the use of our expression vector design for purposes other than sense strand inhibition.

2 MATERIALS AND METHODS

2.1 Plasmid construction

For the construction of pBS-U6-CMV-empty, the CMV promoter was amplified from pDB2-EGFP-attB (Keravala *et al.*, 2006) by CMV F/CMV R, digested with XhoI/BamHI and inserted into SalI/BamHI-digested pBS-U6-GFP (Grimm *et al*., 2006a). Then, RSV-EGFP was amplified from pBS-U6-GFP with RSV F/EGFP R and BamHI/SpeI digested so that the EGFP cDNA could be inserted into the BamHI/NheI sites of the cloning intermediate. EGFP R introduces an AvrII/SalI cloning site in the EGFP 3' UTR for insertion of shRNA binding sites. pBS-H1-CMV-empty was generated by transferring the H1-empty cassette from pBS-H1-GFP (Grimm *et al.*, 2006a) into the same sites of pBS-U6-CMV-empty. shHCV318 annealed oligos were directly cloned into BbsI-digested pBS-H1-CMV-empty to yield pBS-H1-shHCV318-CMV-empty. This plasmid was further modified by insertion of a HCV318 target site into AvrII/SalI via annealed oligos HCV318-sponge F/R. pBS-U6-hAAT19-CMV-empty was generated by transfer of the AscI/NotI digested U6-hAAT19 cassette from pBS-U6-hAAT19-GFP (Grimm *et al.*, 2006a) into the same sites of pBS-U6-CMV-empty. For hAAT sponge construction, we concatemerized four hAAT binding sites by sequential cloning of hAAT sponge F/R first into AvrII/SalI and then into NheI/SalI.

To construct pBS-H1-TuD-empty-GFP and pBS-U6-TuD-empty-GFP, the annealed oligos TuD empty F/R were inserted into BbsI-digested pBS-H1-GFP or pBS-U6-GFP, respectively (Grimm *et al.* 2006a). Next, the entire H1-TuD-empty cassette was amplified with primers H1 F/TuD R and nt27-676 of the EGFP cDNA were amplified from pBS-H1-GFP with the primers EGFP stuffer F/R. The latter was supposed to function as stuffer and spacer sequence between the shRNA and the TuD cassette. Both fragments were joined by overlap extension PCR, digested with XbaI/SalI and inserted into NheI/SalI of pBS-H1-GFP to yield pBS-H1-H1-TuD-empty. Using the same strategy, we generated pBS-H1-U6-TuD-empty using primer U6 F and pBS-U6-TuD-GFP as template. As a results of this vector design the shRNA cassette remains excisable by unique AscI/NotI sites and the TuD cassette can be cut out via unique NheI/SalI sites. TuD target sites were inserted into the TuD-empty scaffold either by cloning of annealed oligos or PCR-amplified annealed oligos into BsmBI-digested pBS-H1-H1-TuD-

empty or pBS-H1-U6-TuD-empty. ShRNAs were generated either by insertion of annealed oligos into BbsI-digested pBS-H1-H1-TuD-empty or by cloning of an already existing shRNA cassette that was excised from either pBS-H1-GFP or pBS-U6-GFP by AscI/NotI and inserted into the same sites of pBS-H1-H1-TuD-empty. The entire sequence was flanked by two AAV ITRs which allows packaging of both shRNA and TuD into rAAVs. For a schematic representation of the shRNA-TuD vectors used in this study, please refer to Fig. 11A. The miR-122-5p TuD vector was cloned by insertion of annealed TuD-M122 F/R oligos into BsmBI-digested pBS-H1-TuD-empty-GFP.

Anti-hAAT, anti-sAg and anti-P53 shRNAs were available in the lab from previous studies (Grimm *et al.*, 2006a; Beer *et al.*, 2010).

Luciferase reporter constructs carrying single target sites were generated by insertion of annealed oligos carrying the respective binding site into XhoI/NotI in psiCheck-2 (Promega).

hAAT random target reporters were generated by annealing of 1µl each of hAAT randtarg F and hAAT randtarg R and subsequent elongation by Sequenase (usb) according to the manufacturers guidelines. The elongated dsDNA was digested with XhoI/NotI and inserted into the same sites of psiCheck-2 (Promega).

3' UTR reporters for shHCV318 off-target measurement were generated by PCR amplification of the respective 3' UTR or parts thereof using the primers indicated below, SalI/NotI digestion and insertion into XhoI/NotI of psiCheck-2 (Promega).

For generation of pSSV9-DualFluor-empty the bidirectional CMV promoter plus d2EGFP cDNA were amplified from pSMB-miMeasure (Heidelberg iGEM team 2010) with biCMV F and d2EGFP R. A minimal poly(A) was amplified from psiCheck-2 (Promega) with minimal p(A) F and R. biCMV-d2EGFP was digested with BglII/XhoI and the minimal poly(A) with SpeI/XhoI and both fragments were inserted into BglII/SpeI digested pSSV9-AAV2-SpeI in a single ligation reaction. The resulting pSSV9-biCMV-EGFP was digested with HindIII/BamHI and mCherry-SV40-poly(A) digested with the same enzymes from psiFluor-2* was inserted.

2.2 Oligonucleotides

2.2.1 General cloning

Primer name	**Sequence 5' → 3'** (restriction sites in bold)
CMV F	TGTAC **CTCGAG** GTTACATAACTTACGGTAAATGGCC
CMV R	TTAG **GGATCC** GGATCTGACGGTTCACTAAACCAG
RSV F	CAATTCTCATGTTTGACAGC
EGFP R	GT **ACTAGTCGAC** TATTG **CCTAGG** CTTTACTTGTACAGCTCGTCCATG
TuD empty F	CACC GACGGCGCTAGGATCATCCCA **GAGACG** AC **CGTCTC** ACCGATGATCCTAGCGCCGTC
TuD empty R	AAAA GACGGCGCTAGGATCATCGGT **GAGACG** GT **CGTCTC** TGGGATGATCCTAGCGCCGTC
H1 F	GGTCCTGCTGGAGTTCGTGA **GCTAGC** CATATTTGCATGTCGCTATGTGTTC
U6 F	GGTCCTGCTGGAGTTCGTGA **GCTAGC** CGAGTCCAACACCCGTGGGAATC
TuD R	TTAG **GTCGAC** CGGCCGCAAAAAAGACGGCGCTAG
EGFP stuffer F	TTAGT **ACTAGT** CACCGGGGTGGTGCCCATCCTG
EGFP stuffer R	TCACGAACTCCAGCAGGACCATG
GFP R	GT **ACTAGTCGAC** TATTG **CCTAGG** CTTTACTTGTACAGCTCGTCCATG
biCMV F	TCGA **AGATCT GGATCC** TAAGA **AAGCTT** GCGATCTGACGGTTCACTAAACG
d2EGFP R	TCGA **ACTAGT** TAGTC **CTCGAG** CGATCGCCTAGAA CTACACATTGATCCTAGCAGAAGC
minimal poly(A) F	GATCG**CTCGAG**CCCGGGAATTCG
minimal poly(A) R	TCGA **ACTAGT** CACACAAAAAACCAACACACAGATG

2.2.2 shRNA oligonucleotides

Oligo name	**Sequence 5' → 3'** (antisense sequence underlined, overhangs in lower case)
hAAT19 F	cacc GAAGCGTTTAGGCATGTTT TCAAGAG AAACATGCCTAAACGCTTC
hAAT19 R	aaaa GAAGCGTTTAGGCATGTTT CTCTTGA AAACATGCCTAAACGCTTC
hAAT25 F	cacc GAAGCGTTTAGGCATGTTTAACATC TCAAGAG GATGTTAAACATGCCTAAACGCTTC
hAAT25 R	aaaa GAAGCGTTTAGGCATGTTTAACATC CTCTTGA GATGTTAAACATGCCTAAACGCTTC
sAg21SA F	cacc GTTTACTAGTGCCATTTGTTC CTAAGAG GAACAAATGGCACTAGTAAAC
sAg21SA R	aaaa GTTTACTAGTGCCATTTGTTC CTCTTAG GAACAAATGGCACTAGTAAAC
shHCV318 F	cacc GGGAGGTCTCGTAGACCGTGCA CTAAGAG TGCACGGTCTACGAGACCTCCC
shHCV318 R	aaaa GGGAGGTCTCGTAGACCGTGCA CTCTTAG TGCACGGTCTACGAGACCTCCC
shHBVS1 F	cacc GGTATGTTGCCCGTTTGTCT TCAAGAG AGACAAACGGGCAACATACC
shHBVS1 R	aaaa GGTATGTTGCCCGTTTGTCT CTCTTGA AGACAAACGGGCAACATACC
shHBVS1-22nt F	cacc GGTATGTTGCCCGTTTGTCTTC TCAAGAG GAAGACAAACGGGCAACATACC
shHBVS1-22nt R	aaaa GGTATGTTGCCCGTTTGTCTTC TCAAGAG GAAGACAAACGGGCAACATACC

2.2.3 3' UTR targets

Oligo name	**Sequence** (5' → 3', overhangs in lower case)
sAg-S F	tcga CTCAGTTTACTAGTGCCATTTGTTC
sAg-S R	ggcc GAACAAATGGCACTAGTAAACTGAG
sAg-AS F	tcga GAACAAATGGCACTAGTAAACTGAG
sAg-AS R	ggcc CTCAGTTTACTAGTGCCATTTGTTC
hAAT-S F	tcga GAAGCGTTTAGGCATGTTTAACATC
hAAT-S R	ggcc GATGTTAAACATGCCTAAACGCTTC
hAAT-AS F	tcga GATGTTAAACATGCCTAAACGCTTC
hAAT-AS R	ggcc GAAGCGTTTAGGCATGTTTAACATC
hAAT-AS-b11CT F	tcga GATGTTAAACATGC**T**TAAACGCTTC
hAAT-AS-b11CT R	ggcc GAAGCGTTTA**A**GCATGTTTAACATC
HCV318-S F	tcga GGGAGGTCTCGTAGACCGTGCA
HCV318-S R	ggcc TGCACGGTCTACGAGACCTCCC
HCV318-AS F	tcga TGCACGGTCTACGAGACCTCCC
HCV318-AS R	ggcc GGGAGGTCTCGTAGACCGTGCA

HCV318-AS b11CT F	tcga TGCACGGTCTA**T**GAGACCTCCC
HCV318-AS b11CT R	ggcc GGGAGGTCTC**A**TAGACCGTGCA
HBVS1-S F	tcga GGTATGTTGCCCGTTTGTCT
HBVS1-S R	ggcc AGACAAACGGGCAACATACC
HBVS1-AS F	tcga AGACAAACGGGCAACATACC
HBVS1-AS R	ggcc GGTATGTTGCCCGTTTGTCT
HBVS1-AS-b11GC F	tcga AGACAAACG**C**GCAACATACC
HBVS1-AS-b11GC R	ggcc GGTATGTTGC**G**CGTTTGTCT
P53P7-S F	tcga GGAGCTGAATGAGGCCTTAGA
P53P7-S R	ggcc TCTAAGGCCTCATTCAGCTCC
P53P7-AS F	tcga TCTAAGGCCTCATTCAGCTCC
P53P7-AS R	ggcc GGAGCTGAATGAGGCCTTAGA
sh122-AS F	tcga TGGAGTGTGACAATGGTGTTTGT
sh122-AS R	ggcc ACAAACACCATTGTCACACTCCA
hAAT randtarg F	TGAC **CTCGAG** GATGTTAAACATG**NNN**AAACGCTTC **GCGGCCGC** TGACTT
hAAT randtarg R	AAGTCA **GCGGCCGC**GAAG
CLCN7 3'UTR F	GATA **GTCGAC** GGCCCAGCCCTGCCCATAATGG
CLCN7 3'UTR R	GATTA **GCGGCCGC** GCCCTGTGAGGGCTAAGCAGGG
BCL7B 3'UTR F	GATA **GTCGAC** CACCATCCCGGCCCTCCGCC
BCL7B 3'UTR R	GATTA **GCGGCCGC** TATGTCTTCACTCACTGTTGCCC
FRMD8 3'UTR F	GATA **GTCGAC** GGACGCTGCACCCGGCAGGAG
FRMD8 3'UTR F	GATTA **GCGGCCGC** GCAAGACCGAGCAACTCCAGGAC
CIRBP 3UTR F	AATA **GTCGAC** AAACCCTTCCTGCTCAAGATCG
CIRBP 3UTR R	AATTA **GCGGCCGC** GTGCACGTCCACTGTCCCTGC

2.2.4 Sponge target sites

Oligo name	**Sequence 5' → 3'** (restriction sites in bold, overhangs in lower case)
HCV318-sponge F	ctagg TAGA TGCACGGTCTATGAGACCTCCC **GCTAGC**TACTG g
HCV318-sponge R	tcgac CAGTA**GCTAGC** GGGAGGTCTCATAGACCGTGCA TCTA c
hAAT-sponge F	ctagg TTAAACATGCaTAAACGCTTC TGA TTAAACATGCCGAAACGCTTC **GCTAGC**TAC g
hAAT-sponge R	tcgac GTA**GCTAGC** GAAGCGTTTCGGCATGTTTAA TCA GAAGCGTTTATGCATGTTTAA c

2.2.5 TuD target sites

Oligo name	**Sequence 5' → 3'** (restriction sites in bold, overhangs in lower case)
For direct cloning	
TuD-hAAT F	tcccaTTAAACATGCATAAACGCTTCCAAGTATTCTGGTCACAGAATACAAC TTAAACATGCCGAAACGCTTC a
TuD-hAAT R	tcggt GAAGCGTTTCGGCATGTTTAA GTTGTATTCTGTGACCAGAATACTTG GAAGCGTTTATGCATGTTTAA t
TuD-HBVS1 F	tccca AGACAAACGTGCAACATACC CAAGTATTCTGGTCACAGAATACAAC AGACAAACGAGCAACATACC a
TuD-HBVS1 R	tcggt GGTATGTTGCTCGTTTGTCT GTTGTATTCTGTGACCAGAATACTTG GGTATGTTGCACGTTTGTCT t
TuD-M122 F	tccca CAAACACCATGCCAACACTCCA CAAGTATTCTGGTCACAGAATACAAC CAAACACCATGCCAACACTCCA a
TuD-M122 R	tcggt TGGAGTGTTGGCATGGTGTTTG GTTGTATTCTGTGACCAGAATACTTG TGGAGTGTTGGCATGGTGTTTG t
For overlap extension	
TuD-HCV318 F	AATA **GGTCTC** G TCCCA AGCACGATAAATGAGACCTCCC CAAGTATTCTGGTCACAGAATA,
TuD-hAATSp F	AATA **CGTCTC** G TCCCA AGCGTTTAGGCATGTTTAACAT CAAGTATTCTGGTCACAGAATA
TuD-hAATp F	AATA **CGTCTC** G TCCCA TTAAACATGCCTAAACGCTTC CAAGTATTCTGGTCACAGAATA
TuD- HCV318p R	AATA **CGTCTC** G TCGGT GGGAGGTCTCGTAGACCGTGCA GTTGTATTCTGTGACCAGAATA
TuD-HCV318 R	AATA **GGTCTC** G TCGGT GGGAGGTCTCATAGACCGTGCA GTTGTATTCTGTGACCAGAATA
TuD-hAATp R	AATA **CGTCTC** G TCGGT GAAGCGTTTAGGCATGTTTAAC GTTGTATTCTGTGACCAGAATA

2.3 PCR

In general, 50µl PCR reactions were set up as follows:

Component	Amount
5x Phusion® HF Buffer	10µl
FWD primer (100µM)	0.5µl (final conc.: 1µM)
REV primer (100µM)	0.5µl (final conc.: 1µM)
Plasmid template (1-10ng/µl)*	1µl
Phusion® Hot Start II DNA Polymerase (2U/µl)	0.5µl (final: 1U)
dH_2O	Ad 50µl

* for extension PCRs of two overlapping oligos, no template was added

Cycling was conducted in a FlexCycler (AnalytikJena) with the following cycling conditions:

30s, 98°C
35 cycles of
    10s, 98°C
    15s, variable temp; adjusted as Tm-3 of the lower Tm primer
    30s/kb of amplicon length, 72°C
1min, 72°C
Forever, 4°C

2.4 Molecular cloning

2.4.1 Preparative restriction digestion

For a standard cloning procedure, 2µg of both receiver and donor plasmid were digested for at least three hours with 0.5µl (2-10U, depending on the enzyme concentration) of each restriction enzyme in an appropriate restriction buffer (activities >75% according to manufacturer's information) at the recommended incubation temperature. For cloning of PCR products, the whole PCR reaction (typical yields are 1-2µg) was gel purified through a 1% agarose gel in 1xTAE buffer (QIAquick Gel extraction kit, QIAGEN), eluted in 30µl dH2O and digested in the same way as explained above. A standard restriction reaction looked as follows:

Component	Amount (plasmid / PCR)
10x restriction buffer	2µl / 3.5µl
Plasmid vector / PCR	2µg / 30µl
Restriction enzyme (4-20U/µl)	0.5µl
dH_2O	Ad 20µl / 35µl

Restriction digests were gel purified and eluted in 30µl dH2O.

2.4.2 Ligation and transformation

Ligation was conducted in 10µl reactions and incubated for 30-90min at room temperature:

Component	Amount
10x T4 ligation buffer (NEB)	1µl
Digested backbone	1.5µl
Digested insert / annealed oligos	7µl / 1µl
T4 DNA ligase (NEB)	0.5µl
dH_2O	Ad 10µl

After incubation, the ligation mix was incubated for 5min on ice. Per ligation reaction, 50µl of chemocompetent *E.coli* (DH5alpha) were thawed on ice in parallel. The bacteria were then mixed with the ligation mix and incubated on ice for 10-15min, followed by a heat shock at 42°C for 45-60s in a heating block (MB-102, BIOER) and subsequent incubation on ice for 5min. After that, the transformation mix was plated as a whole on LB-agar plates containing 50µl/ml ampicillin and incubated overnight at 37°C.

2.4.3 Identification of positive clones

For screening of correct clones, typically 2-3 colonies were picked per construct and incubated for 8h or overnight in 3ml LB media containing 50µg/ml ampicillin. 2ml of the culture were pelleted (2min@15000g@RT) for minipreparation of the plasmid DNA. The supernatant was removed with a vacuum pump and cells were resuspended in 300µl buffer P1 (50mM Tris-HCl, 10mM EDTA, 100µg/ml RNase A, pH8.0). 300µl buffer P2 (200mM NaOH, 1%SDS) were added and tubes were inverted 5x. After 1min incubation at RT 300µl buffer P3 (2.8M KAc, pH5.1) were added, and tubes were inverted 5x and incubated 1min at RT. Samples were then centrifuged for 10min at 15000g at RT. 800µl of the supernatant were mixed with 600µl isopropanol in a fresh tube and homogenized by shaking vigorously. Precipitated plasmid DNA was pelleted by centrifuging 15min at 15000g at RT. The supernatant was removed and the pellet washed once with 500µl 70% EtOH. After washing the plasmid DNA was dissolved in 50µl dH2O.

The miniprep DNA was then digested with appropriate restriction enzymes to identify positive clones:

Component	Amount
10x restriction buffer	1µl
Miniprep DNA	1µl
Restriction enzyme (4-20U/µl)	0.2µl
dH_2O	Ad 10µl

2.5 Tissue culture

HEK293T and MEF cells were cultured in DMEM supplemented with 10% FCS, 1% P/S and 1% L-Glu (PAA). Huh7 cells were cultured in DMEM supplemented with 10% FCS, 1% P/S, 1% L-Glu and 1% NEAA (PAA). All cells were cultured under standard growth conditions (5%CO_2, 37°C) and passaged upon confluency. For passaging, the growth media was removed, cells were washed once with sterile 1xPBS (PAA) and trypsinized by addition of 0.25% trypsin (PAA). After detachment of the cells (typically 2-5min depending on the cell type) an appropriate amount of growth media was added followed by thorough resuspension of the cells by pipetting up and down. A part of the suspension was then either discarded or used for subsequent plating and the remaining cells were provided with fresh media.

2.6 Transfection of mammalian cells

2.6.1 PEI

In this study, HEK293T cells were grown to 70-90% confluency and transfected using the PEI transfection method. The following table shows the transfection conditions for different plate formats:

Plate format	**96-well (/well)**	**24-well (/well)**	**6-well (/well)**	**144mm dish**
Cell density	$2x10^{4}$*	$1x10^{5}$*	$5x10^{5}$*	$5x10^{6}$**
DNA amount	50-200ng	400-800ng	3-3.6µg	44.1µg
DNA mix	3µl DNA 3µl NaCl, 300mM	12µl DNA 12µl NaCl, 300mM	50µl DNA 50µl NaCl, 300mM	790µl DNA 790µl NaCl, 300mM
PEI mix	3µl NaCl, 300mM 1.7µl dH_2O 1.3µl PEI***	12µl NaCl, 300mM 6.8µl dH_2O 5.2µl PEI***	50µl NaCl, 300mM 28µl dH_2O 22µl PEI***	790µl NaCl, 300mM 438µl dH_2O 352µl PEI***

*Seeded the day before transfection
**Seeded two days before transfection
***linear PEI (MW 25000, PolyScience Inc.) was subjected to 4 freeze-thaw cycles and stored at -80°C before use.

The DNA mix was combined with the PEI mix and incubated for 10min at RT. The entire solution was then added dropwise directly onto the cells.

2.6.2 Lipofectamine 2000

Huh7 cells and MEF cells were grown to 90-95% confluency and transfected using Lipofectamine 2000 (Invitrogen). 96-well transfections were done as follows:

Cell type	**Huh7**	**MEF 2G8 Dicer -/-**	**MEF IC1 WT**
Cell density	$1\text{-}1.2x10^{4}$*	$5x10^{3}$*	$6x10^{3}$*
DNA amount	50-200ng	200ng	200ng
DNA mix	<5µl DNA 25µl DMEM	<5µl DNA 25µl DMEM	<5µl DNA 25µl DMEM
Lipofectamine mix	0.5µl Lipofectamine 25µl DMEM	0.5µl Lipofectamine 25µl DMEM	0.5µl Lipofectamine 25µl DMEM

*Seeded the day before transfection

First, the Lipofectamine was mixed with DMEM and incubated for 5min at RT. Subsequently, the Lipofectamine mix was added to the DNA mix and incubated for 30min at RT. The entire solution was then added to the cells.

2.7 Dual luciferase knockdown assay

Cells were grown in transparent 96-well tissue culture plates (Greiner). In general, 2.5-5ng (HEK293T) or 50ng (Huh7, MEF) psiCheck-2 vector and 50-100ng shRNA or TuD vector were used if not stated otherwise. When the TuD was delivered *in trans* shRNA and TuD were transfected at a 1:1 ratio if not stated otherwise. Two days post-transfection, the media was removed from each well and cells were subsequently lysed in 25µl lysis buffer provided with the DualLuciferase assay kit (Promega) and incubated for 15min at RT. 5µl of the lysate were transferred into a white LIA plate. Renilla and Firefly luciferase activities were measured after consecutive injection of 25µl reconstituted luciferase assay buffer and Stop&Glow solution supplemented with Rluc substrate according to the DualLuciferase kit using a Glomax 96 microplate luminometer (Promega). All data analyses were performed with Microsoft Excel. In brief, for each well Rluc values were first normalized to the corresponding Fluc values. Subsequently shRNA containing samples were normalized to their respective non-silencing controls and plotted. All plots are mean values of several experiments (2-4 repetitions in duplicates or triplicates). Exceptions: Fig. 4B, 7B, 10B, 10C and 20C show representative examples of at least two experiments. The random target screen in Fig. 7A was only conducted once. Error bars represent the standard deviation.

2.8 GFP reporter assays

For GFP knockdown assays shown in Fig. 12, HEK293T cells were grown in 24-well plates (Greiner) and transfected with 500ng shRNA vector and 100ng pSSV9-DualFluor vector per well. Two days post-transfection cells were either analyzed by fluorescence microscopy or by FACS. For GFP target titration shown in Fig. 22, HEK293T cells were grown in a 96-well plate (Greiner) and transfected with 100ng of H1-shHCV318 plasmid and 2.5ng, 10ng, 40ng and 100ng of

pSSV9-DualFluor reporters carrying perfect binding sites for either the 5' (sense) or 3' (antisense) strand of shHCV318.

2.8.1 Fluorescence microscopy

Cells were not fixed with PFA and stained with DAPI as mCherry signals allowed visualization of all transfected cells and were strong enough to permit proper autofocusing. Fluorescence images were acquired with an Olympus IX61 microscope (10x objective; exposure times: 50ms for mCherry and 100ms for eGFP; 100% light intensity). Pictures were colored and merged using ImageJ.

2.8.2 Dual color FACS

For FACS, cells were trypsinized and washed once with 1xPBS and then kept in 1xPBS on ice. Analysis was done with a FACScalibur device (BD Bioscience). Instrument settings were as follows: Detector gain: FSC, E0 (lin); SSC, 454 (lin); GFP (FL-2), 425 (log); mCherry (FL-3), 535 (log). Compensation: FL-3 = 99% FL-2. Thresholds: primary parameter, FSC; secondary parameter, none. Per sample at least 10000 cells were analyzed. Live cells were selected via FSC/SSC. Of these, mCherry positive cells were gated such that no naïve HEK293T cells not expressing either mCherry or eGFP were detected. Mean values of eGFP signals and mCherry signals were quantified only for the mCherry positive cell populations. The gating strategy used is illustrated in Suppl.Fig.2. For the two perfect targets three and for the mismatch sense strand target two independent experiments were conducted. The plot in Fig. 12C represents the mean of the repetitions and standard deviation.

2.9 rAAV production

2.9.1 Iodixanol gradient

Two days prior to transfection, HEK293T cells were seeded in 144mm tissue culture dishes (Nunc) at a density of $5x10^6$ per dish and left to grow for two days. For rAAV preparations between 5 and 15 dishes were used per construct and purification was achieved by Iodixanol gradient ultracentrifugation. The cells were triple-transfected with 14.7µg each of pVAE2AE4-5 (Adeno helper plasmid, Matsushita *et al*., 1998), an AAV-helper plasmid (Whc2 for *in vitro* transduction assays) and the AAV genome plasmid (as indicated) using the PEI transfection

method. For a list of produced vectors please refer to Tab. 2. Three days post-transfection, cells were harvested using a cell scraper, washed once in PBS and resuspended in 0.5ml Virus lysis solution (VLS; 50mM Tris, pH8.5, 150mM NaCl). Cells were disrupted by three cycles of freezing at -80°C and thawing in a 37°C water bath. Samples were sonicated for 1min 20sec to further free the virus from the cellular debris. Free nucleic acids were removed by addition of 50U/ml Benzonase and incubation at 37°C for 30min while vortexing every 10min. The volume was subsequently adjusted to 7ml by addition of VLS. The samples were centrifuged for 15min at 5000g at 4°C, and the supernatant was transferred to a fresh tube and centrifuged again as before. For generation of the gradient, a clean Pasteur pipette was plugged into an ultracentrifuge tube (Re-seal, 16x76mm, Seton). The virus-containing solution was filled into the tube through the Pasteur pipette, followed by 1.5ml of 15% Iodixanole (Optiprep, 60% in PBS-MK, Sigma) in PBS-MK-NaCl (1xPBS, 1mM MgCl2, 2.5mM KCl, 1M NaCl), 1.5ml 25% Iodixanol in PBS-MK and 0.5% Phenolred, 1.5ml 40% Iodixanol in PBS-MK and finally 60% Iodixanol and 0.25% Phenolred. The Pasteur pipette was removed and the centrifuge tubes were filled with VLS until the neck and heat sealed using a Beckman tube sealer. Tubes were counterbalanced to a difference <0.01g and subjected to ultracentrifugation for 2h at 50000rpm at 4°C in a Beckman 70.1Ti rotor. After the run the virus-containing 40% Iodixanol phase was pulled from the gradient using a syringe and frozen at -80°C in aliquots the same day.

2.9.2 rAAV vector titration

10µl of each rAAV preparation were mixed with 10µl TE buffer (1mM Tris-HCl, 0.01mM EDTA pH8.0) and 20µl 2M NaOH prior to incubation for 30min at 56°C for lysis of the viral capsid. After neutralization with 39µl 1M HCl the volume was adjusted to 1ml with dH_2O. Genomic titers were subsequently determined by qPCR with the probes and primers as indicated in Tab. 1.

Component	**Per triplex**
2x Sensimix II Probe Mix (Bioline)	17.5µl
Forward primer (10µM)	1.4µl
Reverse primer (10µM)	1.4µl
Probe (10µM)	0.35µl
Nuclease-free water	9.35µl
Sample/standard	5µl
Total	**35µl**

Cycling conditions:
10min, 95°C
40 cycles of
10s, 95°C
20s, 60°C

The number of rAAV genome molecules was determined by a plasmid standard run in parallel.

Target	**Probe (5'→3')**	**5' primer (5'→3')**	**3' primer (5'→3')**
EGFP	FAM-ACGACGGCAACTACA-BHQ1	GAGCGCACCATCTTCTTCAAG	TGTCGCCCTCGAACTTCAC
CMV	FAM-AGTCATCGCTATTACCATGG-BHQ1	TGCCCAGTACATGACCTTATGG	GAAATCCCCGTGAGTCAAACC

Tab. 1: Real-time PCR primers and fluorescently labeled probes used for rAAV vector titrations.

#	Construct	Used for
1	H1-shHCV318-CMV-empty	- Reporter assays in HEK293T and Huh7 cells - HCV inhibition assays
2	H1-shHCV318-CMV-HCV318	- Reporter assays in HEK293T and Huh7 cells - HCV inhibition assays
3	H1-CMV-empty	- Reporter assays in HEK293T and Huh7 cells - HCV inhibition assays
4	H1-H1-TuD-empty	- Reporter assays in Huh7 cells - Expression profiling in Huh7
5	H1-shHCV318-H1-TuD-empty	- Reporter assays in HEK293T and Huh7 cells - HCV inhibition assays - Expression profiling in Huh7
6	H1-shHCV318-H1-TuD-HCV318	- Reporter assays in HEK293T and Huh7 cells - HCV inhibition assays - Expression profiling in Huh7
7	H1-H1-TuD-HCV318	- Reporter assays in HEK293T and Huh7 cells - HCV inhibition assays - Expression profiling in Huh7
8	H1-hAAT25-H1-TuD-empty	- Reporter assays in Huh7 cells
9	H1-hAAT25-H1-TuD-hAAT	- Reporter assays in Huh7 cells
10	H1-hAAT25-U6-TuD-empty	- Reporter assays in Huh7 cells
11	H1-hAAT25-U6-TuD-hAAT	- Reporter assays in Huh7 cells
12	H1-U6-TuD-hAAT	- Reporter assays in Huh7 cells
13	H1-shHBVS122nt-U6-TuD-empty	- Reporter assays in Huh7 cells
14	H1-shHBVS122nt-U6-TuD-HBVS1	- Reporter assays in Huh7 cells
15	H1-U6-TuD-HBVS1	- Reporter assays in Huh7 cells
16	H1-TuD-M122-GFP*	- HCV inhibition assay
17	H1-TuD-HCV318-GFP*	- HCV inhibition assay

Tab. 2: Vectors produced during the course of this study. All vector were packaged into AAV2 capsids and purified by Iodixanol gradient centrifugation. * produced by N. Schürmann.

2.10 HCV inhibition assay

Huh7.5-lucubineo-JFH1 or -ET replicon cell lines were cultured in DMEM supplemented with 10% FCS, 1% P/S, 1% L-Glu, 1% NEAA and 1mg/ml or 500µg/ml G418, respectively. On the day of infection, $1x10^6$ cells were seeded per 96-well plate and infected at an MOI of 10^3, 10^4 or 10^5 directly thereafter. Two days post-infection, the growth media was removed, cells were lysed in 30µl Fluc lysis buffer (0.1% Triton X-100, 25mM glycylglycin, pH7.8, 15mM $MgSO_4$, 4mM EGTA, pH7.8, 10% glycerol, 1mM DTT) per well and immediately frozen at -

20°C. After thawing, 20µl of lysate were transferred to white LIA plate, 50µl of Fluc assay buffer (25mM glycylglycin, 15mM KPO_4, pH7.8, 15mM $MgSO_4$, 4mM EGTA, 7µM D-luciferin, 2mM ATP, 1mM DTT) were added and incubated for 15min at room temperature in the dark. Fluc activity was measured using a Glomax 96 microplate luminometer (Promega). The HCV inhibition assay with TuD-miR-122-5p was conducted by N. Schürmann.

2.11 Expression profiling by microarray

$2x10^5$ Huh7 cells were seeded per well in a 6-well plate. The next day the cells were transduced at an MOI of 10^5 with the different shRNA/TuD rAAV2 vectors. Two days post-infection the cells were lysed and total RNA was prepared using Qiazol (QIAGEN) according to the manufacturer's instructions. Quality of the RNA was checked by Bioanalyzer (Agilent) using a RNA Nano Chip (Agilent). All RNA integrity numbers (RINs) were at least 8.7. The samples were then analyzed with a HumanHT-12 v4 Expression BeadChip (Illumina). Reverse transcription, hybridization and data normalization to reference transcripts were conducted by the DKFZ genomics core facility. For analysis of the results all transcripts whose expression was less than 3-fold higher than their standard deviation were excluded (background subtraction). Dysregulated transcripts were identified by comparison of either shRNA sample with the NSC (T-test, unpaired, two-sided, $p<0.01$, DF=14). Genes that were significantly less dysregulated in one shRNA sample than in the other were determined by comparing the two shRNA samples against each other (T-test, unpaired, two-sided, $p<0.01$). The respective genes were grouped as indicated in Fig. 15 and the 3' UTR sequences of each group were extracted from the Ensembl database using the HGNC gene symbols in the Biomart tool without any further specifications (see section 6.2 for weblink; sequence retrieval, 3' UTR). Not all genes on the chip had extractable 3' UTR sequences so that the number of genes used for seed match analysis was slightly lower than the total number of significant hits. For analysis of sequence enrichment in each gene group, the appearances of each of the indicated sequences in the 3' UTRs were counted and the frequency per gene was calculated by dividing the count by the number of genes in the respective group. All genes with extractable 3' UTR sequences present on the chip were used as

background set. Statistical significance of the counting results was determined by Fisher's exact test (in Group 1: one-sided test for sense strand seed matches; two-sided test for antisense strand seed matches; in Group 2: two-sided test for sense strand seed matches; one-sided test for antisense strand seed matches). Levels of significance are only given if $p<0.05$.

Experimentally validated target genes for miR-122-5p, miR-16-5p, miR-21-5p, miR-22-3p, miR-24-3p, miR-130a-3p and miR-192-5p were identified via the tarbase database (Vergoulis *et al.*, 2012; see section 6.2 for weblink). The genes selected for analysis are indicated in Tab. 3. The relative expression of these targets was plotted for each of the two shRNA samples.

miRNA	**HGNC symbols of analyzed target genes**
miR-122-5p	BCL2L2, CCNG1, IGF1R, CDK4, TRPV6, BCL2L1, HMOX1, BAX, NCAM1, G6PC3, GYS1, SRF, CALU, OSBP2, HSPA5, KRT18, C21orf34, BRI3BP, PSPH, EIF2S1, DDIT3, CHST12, C20orf3, ALDOA3, ALDOA2
miR-16-5p	BCL2a, BCL2b, ARL2, CCNT2, TPPP3, VEGFA, CCND1, RARS, PURA, PNPLA6, CA12, TMEM43, PISD, ZNF622, YIF1B, FNDC3B, ITGA2, FGF2, SHOC2, ATG9A
miR-21-5p	SERPINB1, PTEN, PDCD4, RECK, PPARA, TIMP3, TPM1, TGFBR2, CDK2AP1, VEGFA, BCL2a, BCL2b
miR-22-3p	ACVR1C, SP1, CCNT2, E2F2, BTF3, TBX3, TBC1D12, CDK6, SFRS7, LEMD3, FRAT2, FOXP1, C14ORF106, C20ORF117
miR-24-3p	FEN1, CDK4, CCNA2, CDC2, AURKB, HNF4A, MYC, PCNA, CHEK1, BRCA1, ACVR1B, MAPK14, CDKN2A, MLEC
miR-130a-3p	MEOX2, HOXA5, TAC1, ZFPM2, APP, ATXN1, MAFB, CSF1, HOXA10, KLF4
miR-192-5p	LMNB2, CUL5, CDC7, MAD2L1, PIM1, RACGAP1, SEPT10, DTL, ERCC3, BCL2a, BCL2b, DLG5, HRH1, SMARCB1, PRPF38A, MIS12

Tab. 3: List of miRNA target genes that were used for analysis of effects of shHCV318 expression on the miRNA pathway.

2.12 Reverse transcription quantitative PCR (RT-qPCR)

$2x10^5$ Huh7 cells were seeded per well in a 6-well plate. The next day the cells were transduced with an MOI of 10^5 with the different shRNA/TuD rAAV2 vectors or left naïve. Two days post-infection the cells were lysed and total RNA was prepared using Qiazol (QIAGEN) according to the manufacturer's instructions. DNA was removed from 2µg total RNA by treatment with TurboDNase (Ambion) in 20µl reaction volume according to the manufacturer's guidelines. 10µl (1µg) of DNA-free total RNA were carefully transferred to a fresh microfuge tube (DNase stop reagent interferes with a subsequent RT-qPCR reaction) and reverse transcribed using the Tetro cDNA kit (Bioline) according to the manufacturer's guidelines. The volume of the cDNA samples was brought to 50µl (final cDNA concentration was 20ng/µl). The respective genes were quantified using the Sensimix SYBR no-ROX kit (Bioline) in 10µl reactions according to the manufacturer's guidelines. Expression of each gene was first normalized to GAPDH by the deltaCt method and then further normalized to the NSC carrying the specific shHCV318 TuD. The primers were used for amplification are indicated in Tab. 4 (GAPDH primers were as previously published; all other primers obtained from PrimerBank database (see section 6.2 for weblink).

Gene name (HGNC symbol)	**FWD primer** (5'→3')	**REV primer** (5'→3')
GAPDH	GAAGGTGAAGGTCGGAGTC	GAAGATGGTGATGGGATTTC
CIRBP	AATGGGAAGTCTGTAGATGGACG	CGGGATCGGTTGTCTGACG
SEPT9	GTCCATCACGCACGATATTGA	TGCAGGTATTTCTCGTACTGGT
RAN	CTCTGGCTTGCTAGGAAGCTC	GCAACAAATTCCAAGTTAGGGTC

Tab. 4: List of primers used for RT-qPCR analysis.

2.13 Small RNA Northern blot

$2x10^5$ Huh7 or $5x10^5$ HEK293T cells were seeded per well in a 6-well plate. The next day the cells were transduced with an MOI of 10^5 with the different shRNA/TuD rAAV2 vectors (Huh7) or transfected with 3µg of shRNA expressing plasmids (HEK293T). Two days post-infection or -transfection the cells were lysed and total RNA was prepared using Qiazol (QIAGEN) according to the manufacturer's instructions. 6µg (for miR-122-5p detection in Huh7 cells), 10µg

(for shRNA and TuD detection in Huh7 cells) or 15µg (for shRNA detection in HEK293T cells) of total RNA were mixed with 3xRNA loading buffer (8M Urea, 1X TBE, 30 mM EDTA, 20% glycerol, dyes: BPB & XC), briefly denatured at 80°C and resolved in a 12% acrylamid / 8M urea gel in 1XTBE in a Protean running chamber (Biorad). In case the total volume of RNA and loading buffer exceeded 10µl, the RNA was first precipitated by addition of 1/10 volume of 3M NaAc, pH5.2, and 3 volumes of 100% EtOH and subsequently redissolved in 5µl nuclease-free dH_2O. The RNA was then electroblotted onto a Nylon membrane (Hybond N+, Amersham) and UV-crosslinked (time-program, CL-1000 UV crosslinker, UVP). For probe generation, 50pmol of an oligonucleotide were end-labeled by T4-PNK (NEB) for 30min at 37°C using 25µCi of [gamma-^{32}P]ATP under standard reaction conditions. The Nylon membrane was cut into the desired pieces, pre-hybridized in PerfectHyb hybridization buffer (Sigma) at 37°C for 30min and hybridized overnight with appropriate radioactively labeled probes at 37°C. Subsequently the membrane was washed with 2xSSPE/0.1%SDS (300mM NaCl, 25mM NaH_2PO_4, 2mM EDTA, 0.1% SDS, pH7.4) twice at 37°C (high stringency) and twice at room temp (low stringency) followed by exposure to phosphorimager screens for an appropriate period of time. A list of DNA probes used for small RNA Northern blot is given in Tab. 5.

Probe target	Probe sequence
U6 snRNA	TGTGCTGCCGAAGCGAGCAC
shHCV318 antisense strand	TCGAGGGAGGTCTCGTAGACCGTGCA
shHCV318 sense strand	TCGATGCACGGTCTACGAGACCTCCC
TuD-HCV318 perfect	GGCCGGGAGGTCTCATAGACCGTGCA
hAAT antisense strand	TCGAGAAGCGTTTAGGCATGTTTAACATC
hAAT sense strand	TCGAGATGTTAAACATGCCTAAACGCTTC
miR-122-5p	CAAACACCATTGTCACACTCCA

Tab. 5: List of DNA probes used for small RNA Northern blot.

2.14 mRNA Northern blot for GFP and mCherry

5x10^5 HEK293T cells were seeded per well in a 6-well plate. The next day the cells were transfected with 2µg shRNA/TuD expressing plasmids and 200ng DualFluor target plasmids. Two days post-transfection the cells were lysed and total RNA was prepared using Qiazol (QIAGEN) according to the manufacturer's

instructions. 2µg of total RNA were mixed with 1/3 loading buffer (Ambion), briefly denatured at 65°C and resolved in a 0.8% agarose/6.7% formaldehyde gel in 1XMOPS buffer (Northernmax, Ambion). The RNA was transferred onto a Nylon membrane (Hybond N+, Amersham) by passive diffusion overnight and UV crosslinked (time-program, CL-1000 UV crosslinker, UVP). For probe generation, the EYFP CDS was cut out of pIRESNeo-FLAG/HA-EYFP by BamHI or the mCherry CDS was cut out of pSSV9-DualFluor by HindIII/SalI and gel purified. 50ng template were then used for random priming probe generation using the Prime-it Rmt Random priming kit (Stratagene) according to the manufacturer's instructions. The Nylon membrane was pre-hybridized in pre-heated PerfectHyb hybridization buffer (Sigma) at 68°C for at least 15min followed by hybridization with the EGFP probe for at least 8h at 68°C. The membrane was washed twice in 2xSSC/0.1% SDS (300mM NaCl, 30mM sodium citrate, 0.1% SDS, pH7.0) at RT followed by two washings in 0.1xSSC/0.1% SDS (15mM NaCl, 1.5mM sodium citrate, 0.1%SDS, pH7.0) at 68°C. The membrane was subsequently exposed to phosphorimager screens for an appropriate period of time.

3 RESULTS

3.1 shRNA strand activities

3.1.1 Strand biasing

It has been reported previously that the sense strand of shRNAs with perfectly matched stems could be efficiently inactivated merely by placing it at the 5' end of the hairpin (Boudreau *et al.*, 2008). However, this effect was only shown for a limited number of shRNAs. In order to optimize the design of our own RNAi triggers we wanted to find out whether this rule could be readily applied to any shRNA. We hence measured the activities of both strands of various previously published shRNAs and compared them to the data of Boudreau and colleagues. Instead of directly comparing absolute silencing efficiencies of each strand we suggested that the relative strand activity (RSA) would be a better parameter for proper comparison. The RSA is a direct measure to evaluate the degree of strand biasing of shRNAs. It is calculated as activity of the antisense strand on a perfect match target divided by the activity of the sense strand on a perfect match target (Fig. 4A). Ideally, the RSA of an shRNA should be as high as possible meaning maximal activity of the antisense strand which is desired for silencing of the designated target of the shRNA and minimal activity of the sense strand.

We hence transfected HEK293T cells with a set of 11 shRNAs with varying stem lengths that were directed against 4 different targets along with luciferase reporters carrying perfect targets for either strand and measured relative luciferase activities 48h post-transfection. Sequences of all shRNAs and targets can be found in Suppl.Tab.1. As expected, we observed highly efficient silencing of the antisense strand target for all shRNAs (Fig. 4B). However, also the sense strands of all shRNAs yielded knockdown of their respective targets. Some of the shRNAs had their sense strand at the 5' and some at the 3' end (Suppl.Tab.1). For those shRNAs with stems ≥21nt we noticed a clear tendency towards higher activity of the 3' strand leading either to RSAs above or below 1 depending on the position of the sense strand. This correlates with the data of Boudreau and colleagues where all three shRNAs with strong strand bias had stems longer than 21nt. However, the RSAs measured here were highly variable (between 1.3 and 6.7 for those shRNAs with the sense strand at the 5' end) and for the majority of

our shRNAs lower than what had been reported previously (around 6-8 as estimated from Boudreau *et al.*, 2008).

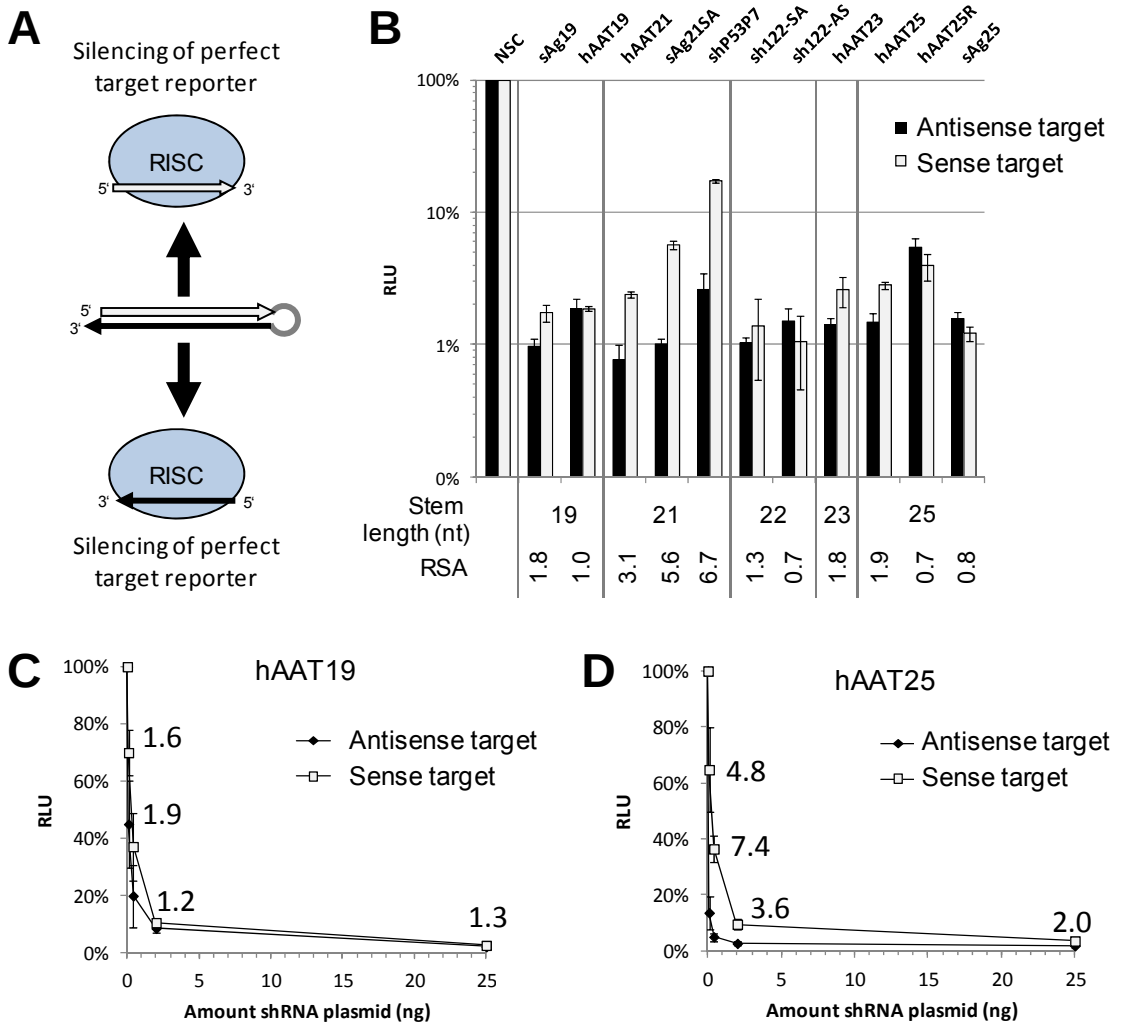

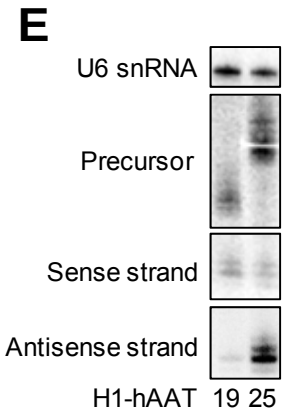

Fig. 4: Analysis of shRNA 3‘ and 5‘ strand activity. **A:** Schematic representation of experimental setup. Both 5‘ and 3‘ strand are incorporated into RISC and activity is measured by luciferase reporters carrying perfect target sites. **B:** 11 shRNAs against 4 different targets were transfected into HEK293T cells and activity of both strands was measured 48h post-transfection by dual luciferase assay. **C+D:** HEK293T cells were transfected with indicated amounts of U6-hAAT19 (C) or hAAT25 (D) and strand activities were determined 48h post-transfection. Numbers indicate the RSAs at the respective concentrations. **E:** HEK293T cells were transfected with hAAT19 or hAAT25. 48h post-transfection total RNA was extracted and shRNA expression determined by Northern blot. RLU=relative light units; RSA=relative strand activity; NSC=non-silencing control.

3.1.2 Concentration dependency of relative strand activities

To obtain further insights into the expression kinetics of both shRNA strands we next assessed the concentration dependency of the RSA. For this experiment, we selected two shRNAs targeting the same sequence in human-alpha-1-antitrypsin (hAAT) with either a 19-mer (hAAT19) or 25-mer (hAAT25) stem which allowed us to examine the influence of the stem length. These shRNAs have their antisense strand at the 3' end and sense strand at the 5' end. For hAAT19 both strands had shown equal activities in the previous assay (RSA=1) and hAAT25 had an intermediate bias towards the 3' strand (RSA=1.9). We transfected HEK293T cells with varying amounts of shRNA plasmids and measured activity of both strands by dual luciferase assay. We found that the RSA varied between the different plasmid doses for both shRNAs and was generally best at low amounts (Fig. 4C+D). The 3' strand hence appears to reach near-maximal levels of activity at lower concentrations than the 5' strand. The degree of strand biasing was considerably different between the short and the long version. At 0.4ng, the antisense strand was over 6-fold more active than the sense strand for hAAT25 but below 2-fold more active for hAAT19. We also observed that the absolute potency of the antisense strand was higher with the 25-mer than with the 19-mer shRNA which is in agreement with previous reports (Siolas *et al.*, 2005). It is important to note that for both shRNAs the activity ratio declined when the shRNA concentration was too low. Thus, there seems to be a certain window of shRNA concentration where the RSA is optimal. We next assessed the expression levels of the two strands after HEK293T transfection by Northern blot under conditions with optimal RSA. The sense strands of both shRNAs were expressed at comparable levels whereas the antisense strand of hAAT25 was much higher expressed than the hAAT19 antisense strand (Fig. 4E). This confirms that there is indeed a bias towards maturation of the 3' strand for hAAT25 but not hAAT19. We next conducted similar functional analyses with another shRNA pair of 19 or 25nt in length, *i.e.* sAg19 and sAg25, that have an inverted strand order as compared to the hAAT shRNAs. Their sense strand is therefore located at the 3' end and the antisense strand at the 5' end (Suppl.Fig. 1). Despite the structural similarity between the two shRNA pairs the results for sAg19 and -25 were fundamentally different to what had been measured for hAAT19 and -25. We found a bias towards the 5' antisense strand for sAg19

(RSA up to 1.6) and a slight preference for the 3' sense strand for sAg25 (RSA down to 0.8) and no clear concentration dependency. A similar finding for both shRNA pairs was a more pronounced bias towards the 3' strand for the 25-mer as compared to the 19-mer. The functional strand bias thus seems to depend both on shRNA sequence and stem length. From our data we conclude that shRNAs are best designed to have the sense strand at the 5' end and stems of 21 nucleotides or longer. However, this design does not appear to guarantee sense strand inactivation to negligible levels for all shRNAs.

3.1.3 3' but not 5' strand activity requires Dicer

Apart from functionally testing the two shRNA strands we also wanted to gain insight into the mechanism of the observed strand bias. It has been shown previously that in *in vitro* Dicer assays 25-mer shRNAs were readily processed by Dicer whereas a corresponding 19-mer shRNA was not (Siolas *et al.*, 2004). This finding seems logical in light of other studies reporting that the typical Dicer processing product is 22nt in length so that intuitively an shRNA with only 19nt stem length will be difficult to dice (Zhang *et al.*, 2002). It has also been demonstrated that Dicer substrate duplex RNAs have a significant bias towards the strand that is bound by Dicer which in case of shRNAs can only be the 3‘ strand via its 2nt 3‘ overhang (Rose *et al.*, 2005). The strong functional strand bias of hAAT25 that was not found with hAAT19 could thus be linked to Dicer. Consequently, we wanted to correlate our results on relative strand activities with Dicer processing. To this end, we conducted luciferase knockdown experiments in MEF WT and Dicer-/- cells and tested the activity of both strands with hAAT shRNAs of different stem lengths. Along with the aforementioned hAAT19 and -25 we also used hAAT21 and hAAT23 with respective stem lengths of 21 or 23nt. According to Siolas and colleagues we expected both strands to be Dicer-dependent for hAAT21-25 and both strands Dicer-independent for hAAT19 in this system (Siolas *et al.*, 2004). However, our results clearly show that the activity of the 3‘ but not the 5' strand depends on the presence of Dicer in the cells, regardless of shRNA stem length (Fig. 5A+B). We thus did not see any direct correlation between Dicer processing and the functional strand bias as we had previously expected. Thereby, these results show for the first time that the two

strands of both short and long shRNAs with perfect stems rely on different principles of maturation.

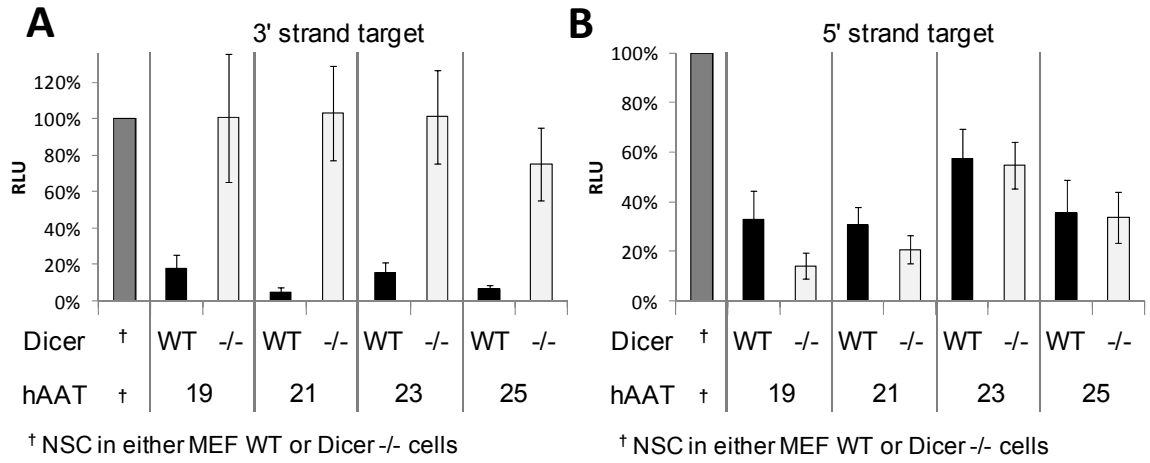

Fig. 5: 3‘ but not 5‘ strand activity depends on Dicer regardless of shRNA stem length. **A-B:** MEF WT or Dicer -/- cells were transfected with hAAT shRNAs with indicated stem lengths. 48h post-transfection, either 3‘ strand (A) or 5‘ strand (B) activity was determined by dual luciferase assay. RLU=relative light units; NSC=non-silencing control.

3.2 shRNA sense strand counteraction by RNA-pol II sponges

A previous study reported four different conserved sites in the HCV 5’NTR that were susceptible to shRNA-mediated silencing of HCV replication (Krönke et al., 2004). For our subsequent analyses we generated an shRNA against the target site that allowed the highest degree of HCV inhibition. The original shRNA described by Krönke and colleagues had a 19-mer stem. In order to apply the design that we had determined in section 3.1 we added 3nt to the 5’ end of the shRNA to increase the stem length above 20nt and termed it shHCV318. As previous reports showed deleterious side effects (see section 1.1.7.2) of U6-driven shRNAs we decided to use the weaker H1 promoter for shHCV318 expression. Due to the nature of this particular target site the antisense strand of the shRNA also has a seed that can be considered “safe” (see section 1.1.7.1). The number of hexamer matches to this seed in human 3’ UTRs is considerably lower than that of other hexamers (cf. Fig. 16B+C, note that the frequency of antisense seed matches in the background set are much lower those of the sense strand seed). This is presumably due to the presence of a CG dinucleotide

that has a relatively low frequency in the human genome (cf. Fig. 16A; Anderson *et al*., 2008).

To determine the relative strand activities of shHCV318 we measured sense and antisense activity by perfect match target reporters. Upon transfection of HEK293T cells shHCV318 produced potent knockdown from both strands with a minor bias towards the antisense strand located at the shRNA 3' end (Fig. 6A). This finding confirmed that the sense strand of shRNAs can be highly active even if the shRNA sequence is in agreement with state-of-the-art design methods.

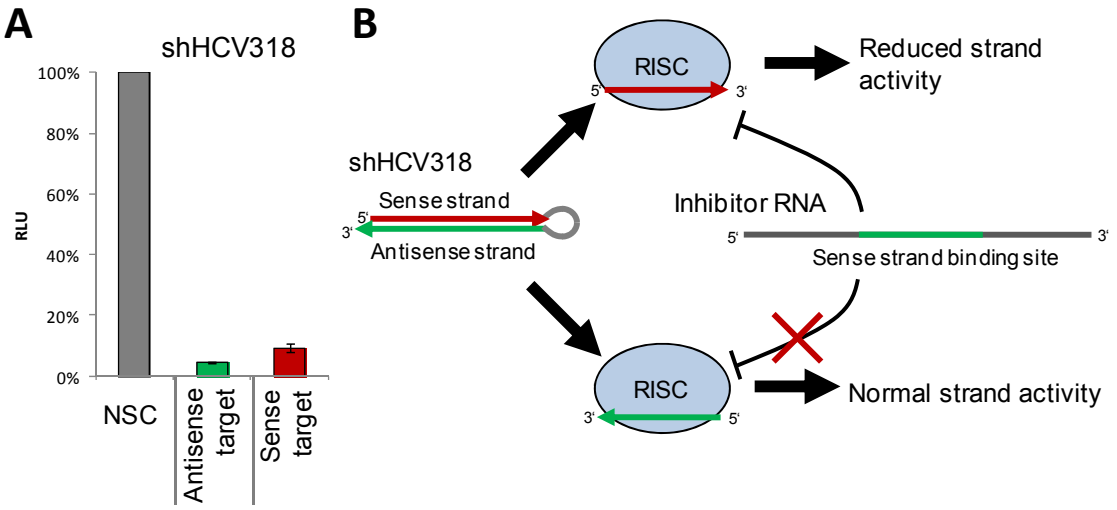

Fig. 6: shHCV318 strand activities and sense strand counteraction by inhibitor transcripts. **A:** HEK293T cells were transfected with shHCV318 and perfect target reporters for sense or antisense strands. 48h post-transfection strand activities were measured by dual luciferase assay. **B:** In principle, both strands of an shRNA can be active as RNAi trigger. By co-expressing an inhibitor RNA transcript carrying specific binding sites for the sense but not the antisense strand, activity of the sense strand could be selectively reduced without affecting the silencing potential of the antisense strand. RLU=relative light units; NSC=non-silencing control.

As shRNA sense strand activity appeared to play a more important role than initially expected, we decided to devise a novel strategy to improve the RSA of shRNAs by selectively decreasing sense strand activity with shHCV318 as example. Our approach is based on co-expression of an inhibitor RNA transcript that sequesters and selectively inactivates the sense strand without disturbing antisense-mediated silencing (Fig. 6B). In principle, the modular design of the proposed system should be advantageous as it should allow increasing specificity without the need to alter shRNA design algorithms and facile

implementation for already existing or new shRNAs. The same principle -*i.e.* quantitative sequestration- had already been reported for the inhibition of miRNAs where both RNA-pol II and RNA-pol III transcripts have been successfully used in different settings (Ebert and Sharp, 2010). In this context, RNA-pol II transcripts are called „sponges“, whereas RNA-pol III transcripts are termed „decoys“. Since we could not predict which transcript class would be best suited for our strategy, we commenced with RNA-pol II „sponge“ constructs that had been first described in 2007 (Ebert *et al.*, 2007). These sponges consist of an mRNA -in our case encoding eGFP- containing one or more binding sites for the respective RNAi trigger.

3.2.1 Binding sites with single central mismatches are high affinity shRNA targets

In the original publication Ebert and colleagues showed that imperfect target sites -*i.e.* non-slicer substrates- with triple central mismatches to the targeted miRNA yielded better sponge efficiencies than perfect target sites that are sliced upon RISC binding. Thus, to select an ideal binding site for sponge construction, we first tested a binding site with a triple mismatch to the sense strand of shHCV318. However, this binding site showed only little responsiveness when cloned into the 3’ UTR of a luciferase reporter so that it could not be used for shHCV318 sponge construction (Fig. 7B). Triple mismatch sites for the sense strands of hAAT and sAg shRNAs were found not to be functional, either (data not shown). As miRNAs can efficiently silence targets with triple central mismatches our results indicate that shRNAs seem to have somewhat different target sequence requirements. We therefore decided to conduct a random target screen to identify mismatched target sites that would allow shRNA sense strand binding with maximal potency and that could subsequently be used for sponge generation. To get a general idea about shRNA target requirements we first conducted the screen for hAAT and then applied the identified target design to shHCV318. To this end, we cloned luciferase constructs carrying target sites for the sense strand of hAAT19 and hAAT25 (the sense strands of which are similar) with randomized nucleotides at positions 10-12. By this means the majority of the resulting sequences had between 1 and 3 mismatches at these positions and could not be

sliced as the slicing reaction takes place between nt 10 and 11 (Martinez *et al.*, 2002).

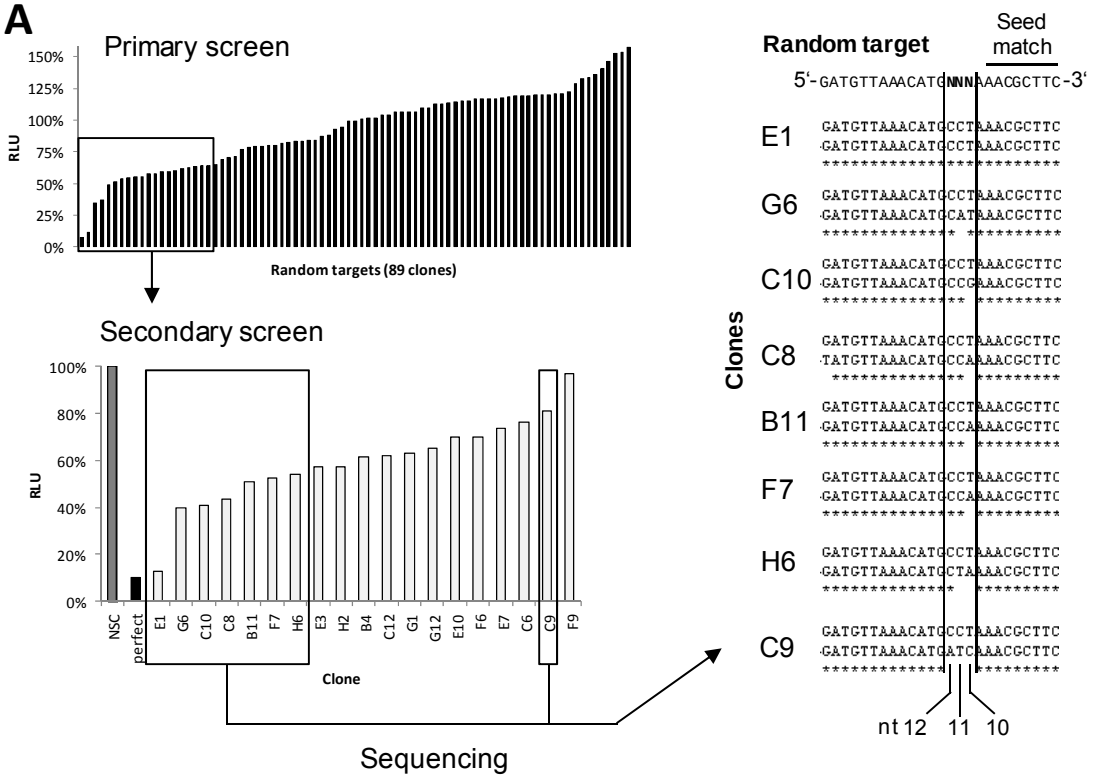

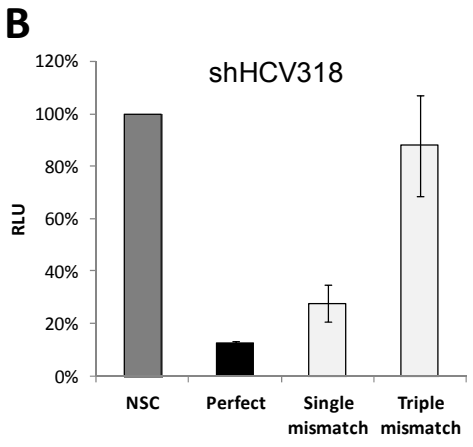

Fig. 7: Random target screen for identification of efficient shRNA target sites. A: Targets for the hAAT shRNA sense strand with randomized nucleotides at positions 10-12 were cloned into the Rluc 3' UTR. 89 clones were picked and co-expressed with hAAT19 or NSC in HEK293T cells and luciferase knockdown was measured 48h post-transfection. 20 clones that permitted best silencing including a perfect match control were tested in a second round of knockdown measurement. The target sites of the indicated clones were sequenced. Shown are the alignments to the perfect match target. **B:** shHCV318 was co-transfected with sense strand target reporters with either perfect complementarity or a single mismatch at position 11 or a triple mismatch at positions 10-12. Luciferase knockdown was measured 48h post-transfection. RLU=relative light units; NSC=non-silencing control.

We picked 89 different clones and tested them for susceptibility to silencing mediated by the hAAT19 sense strand (Fig. 7A). After a first round of luciferase expression screening we repeated the assay with 20 clones that permitted

strongest knockdown including a perfect match control. After the second round of measurement we sequenced the binding sites of 8 clones to determine the sequence requirements for efficient sense strand binding (Fig. 7A). We found that the most potent sites had single mismatches at either position 10 or 11 as counted from the 5' end of the shRNA sense strand with the exception of clone H6 that had a double mismatch. One clone -C8- had an additional mismatch at the 3' nucleotide which did not appear to influence its affinity to the shRNA sense strand. Clone C9 that was less susceptible to silencing carried a triple mismatch. Clone E1 that behaved like the perfect match control that we had included in the assay indeed carried a perfectly complementary target site, thus proving the validity of our results. Our data therefore suggested that binding sites with single mismatches at either position 10 or 11 are best suited for sponge construction.

We next determined whether this design could be applied to the sense strand of shHCV318. We cloned a target with a single mismatch at position 11 into the 3' UTR of Rluc and examined knockdown efficiencies in comparison to the perfect target and the triple mismatch target tested initially. The single mismatch target was efficiently silenced by the shHCV318 sense strand indicating that it should be well suited for subsequent construction of the sponge (Fig. 7B).

3.2.2 A sponge efficiently counteracts the shHCV318 sense strand upon transfection

In the next step, we used the single mismatch target site to generate a sponge for the sense strand of shHCV318. We constructed a bicistronic vector carrying both the H1-shRNA and a CMV-transcribed sponge (Fig. 8A). The whole insert is flanked by AAV ITRs that allow direct packaging into AAV particles. We first transfected HEK293T cells with shHCV318 and a control or a specific sense strand sponge and perfect target reporters for both shRNA strands. The sense strand sponge successfully counteracted shHCV318 sense strand activity ~3.5-fold (Fig. 8B). The desired antisense strand activity was not disturbed by the sponge proving that our concept of selective sense strand inhibition worked.

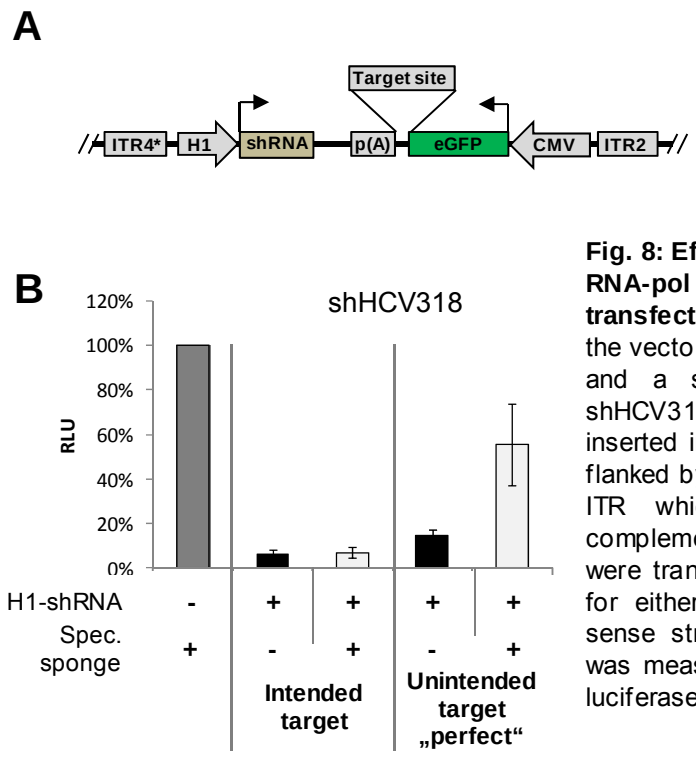

Fig. 8: Efficient sense strand inhibition via RNA-pol II sponges after plasmid transfection. A: Schematic representation of the vector constructs carrying both an shRNA and a sponge expression cassette. The shHCV318 sense strand target site was inserted in the 3' UTR of eGFP. The insert is flanked by an AAV2 ITR and a mutated AAV4 ITR which permits packaging as self-complementary rAAV. **B:** HEK293T cells were transfected with shHCV318, a reporter for either strand and a control or specific sense strand sponge. Reporter knockdown was measured 48h post-transfection by dual luciferase assay. RLU=relative light units.

3.2.3 Translation of the sponge into an rAAV context

To improve the applicability of the approach we next tested the compatibility with rAAV-mediated gene transfer. We hence packaged shHCV318 with either a control or a specific sponge into self-complementary rAAV2 particles and tested antisense strand activity in an HCV inhibition experiment and sense strand activity in a luciferase reporter experiment.

We used our vectors at different MOIs to transduce Huh7 cells carrying subgenomic RNA replicons of different HCV genotypes that encode Firefly luciferase (Fluc; Lohmann *et al.*, 1999). Fluc expression correlates with HCV replication and could thus be used as an easy means of measuring HCV inhibition by shHCV318. Indeed, we observed a strong dose-dependent reduction of HCV replication for both HCV genotypes 1b and 2a (Fig. 9A+B). At the highest MOI, both genotypes were silenced by around two orders of magnitude. As expected, we did not observe any effect of the sense strand sponge on the HCV silencing potential of the shRNA.

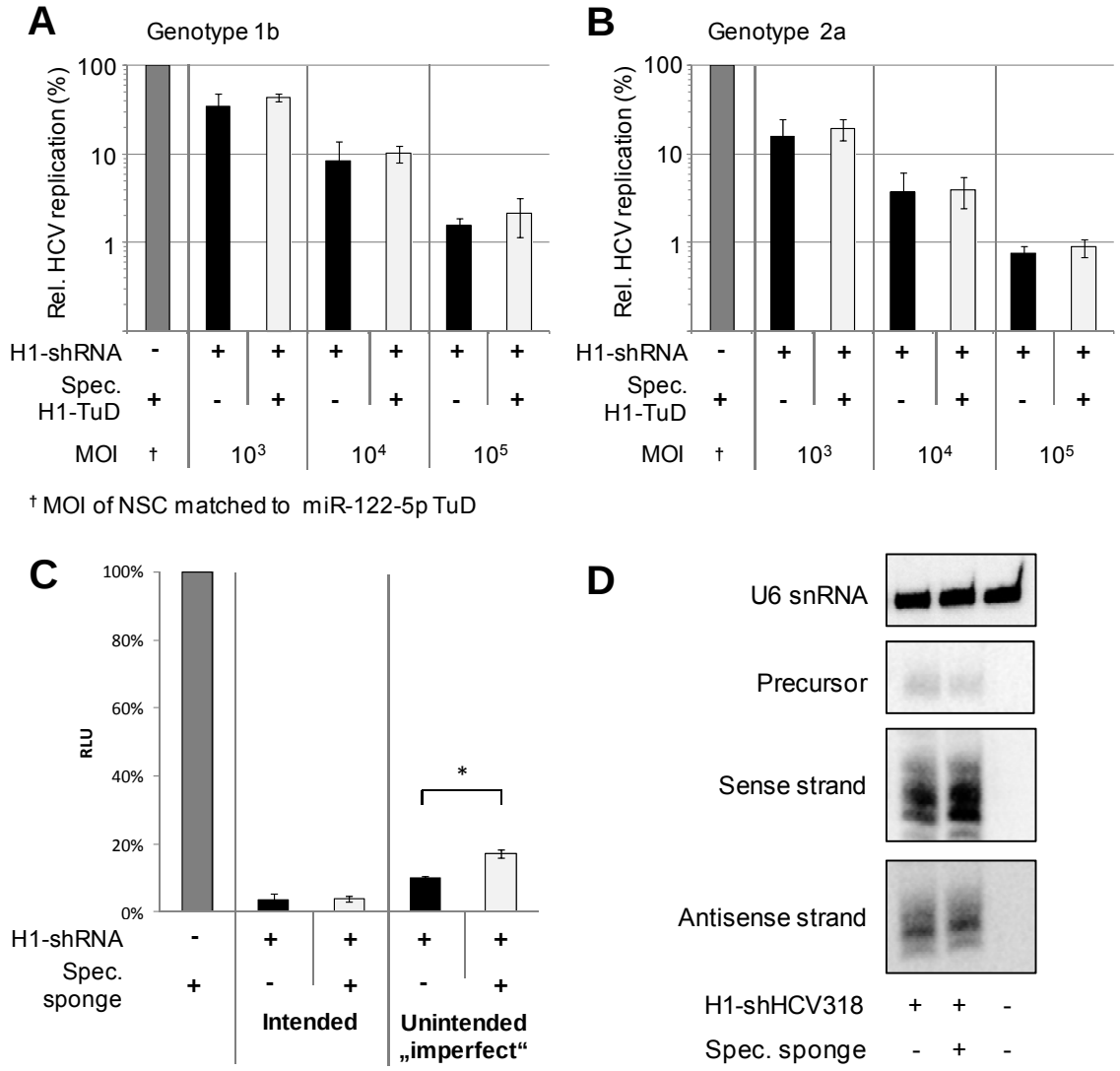

Fig. 9: Translation of RNA-pol II sponge strategy into rAAV2 context. A+B: HCV inhibition by shHCV318 after transduction of Huh7 cells carrying subgenomic replicons of HCV genotype 1b (A) or 2a (B) at indicated MOIs 48h post-infection. HCV replication was quantified by measurement of Fluc activity encoded by the HCV replicons. **C:** HEK293T cells were transduced with rAAV2 (MOI=10^5) encoding shHCV318 and control or specific sponge or a NSC and co-transfected with luciferase reporters for both strands. Strand activities were measured by dual luciferase assay after 48h. **D:** Huh7 cells were transduced with rAAV2 (MOI=10^5), total RNA was extracted 48h post-infection and sHCV318 expression was analyzed by small RNA Northern blot. Statistical analysis: unpaired, one-sided T-test, * $p<0.05$. RLU=relative light units; MOI=multiplicity of infection.

We next tested counteraction of the sense strand in the rAAV2 context in transduced HEK293T cells. Under these conditions, the sponge relieved repression of the unintended sense strand target by less than 2-fold with only weak statistical significance (Fig. 9C). The effect was hence more than 2-fold less pronounced than what we had observed upon HEK293T transfection (cf. Fig. 8B). To show that this was not due to differences in functionality of the two rAAV2

vectors encoding the shRNA plus control or specific sponge we visualized expression of the encoded shHCV318 by Northern blot. The signals of both shRNA strands did not differ between the samples meaning that expression from either vector was equally efficient (Fig. 9D). However, the functional discrepancy between transfection- and transduction-based gene delivery correlated with very high eGFP expression levels achieved in HEK293T cells upon transfection and considerably lower eGFP expression upon transduction as observed by fluorescence microscopy. While the shRNA was equally active upon transfection and transduction the sponge appeared to be higher expressed upon transfection which could explain the obtained results.

3.3 shRNA sense strand counteraction by RNA-pol III tough decoys

As a major goal of our study was to ultimately utilize rAAVs for delivery of RNAi-triggers the shHCV318 sponge did not appear to be the best option for our strategy for sense strand inhibition. We hence decided to test our approach with an RNA-pol III-transcribed decoy as an alternative. From all of the previously reported decoy constructs, “tough decoys” (TuDs) as first described by Haraguchi *et al.* in 2009 seemed to be best suited for our approach as they were shown to be highly active and yet easy to design (Fig. 10A) (Haraguchi *et al.*, 2009). In addition, they are very short and carry no single-stranded RNA stretches except for the miRNA -or in our case shRNA- binding sites thus minimizing the risk of unintended sequestration of miRNAs or other cellular RNA binding factors which is another advantage over the much longer sponge transcripts.

3.3.1 TuDs efficiently inhibit an shRNA sense strand upon transfection and rAAV-mediated transduction

We generated a TuD transcript against the sense strand of shHCV318 using the same imperfect binding site as previously for the sponge. For proof-of-principle, we expressed shHCV318 and TuD from separate plasmids and tested both the strong U6 and the weaker H1 promoter for TuD expression. We transfected HEK293T cells with shHCV318 or a non-silencing control (NSC) either with the control TuD without binding sites or the specific TuD carrying sense strand targets. With both promoters the specific TuD was able to efficiently counteract

the sense strand ~5-fold (Fig. 10B+C). As we did not find any significant difference in performance between the two promoters we decided to subsequently use the H1 promoter for TuD expression. In addition, the NSCs with control or specific TuD did not significantly differ in their behaviors in the reporter assays. This allowed us to use the NSC with specific TuD as unique control in subsequent experiments.

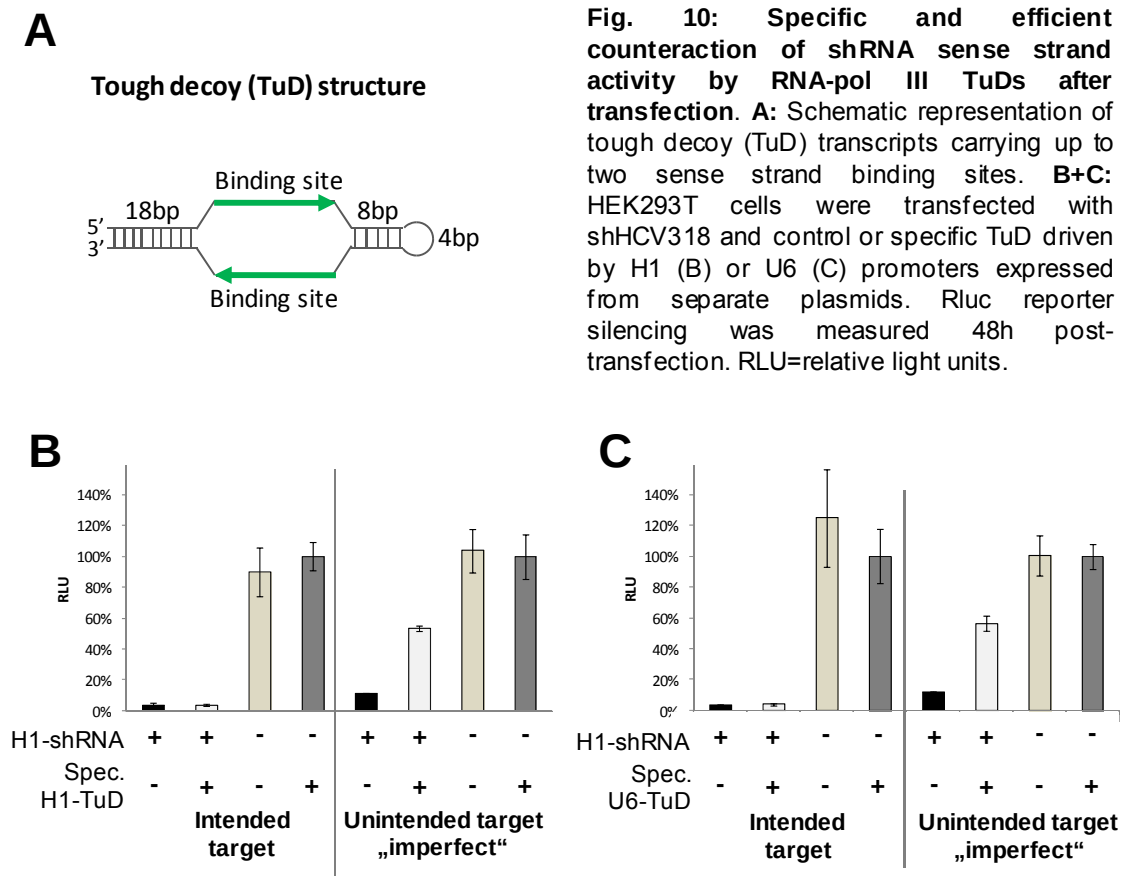

Fig. 10: Specific and efficient counteraction of shRNA sense strand activity by RNA-pol III TuDs after transfection. **A:** Schematic representation of tough decoy (TuD) transcripts carrying up to two sense strand binding sites. **B+C:** HEK293T cells were transfected with shHCV318 and control or specific TuD driven by H1 (B) or U6 (C) promoters expressed from separate plasmids. Rluc reporter silencing was measured 48h post-transfection. RLU=relative light units.

We next tested the functionality of the system with shRNA and TuD expressed from the same plasmid. We chose a vector design based on the shRNA vector described by Grimm *et al.* in 2006 (Grimm *et al.*, 2006a). Our final constructs allow easy *de novo* cloning of both shRNA and TuD binding sites as well as facile exchange of the whole expression cassettes (Fig. 11A). In addition, the whole insert is flanked by AAV ITRs that permit packaging into rAAV particles.

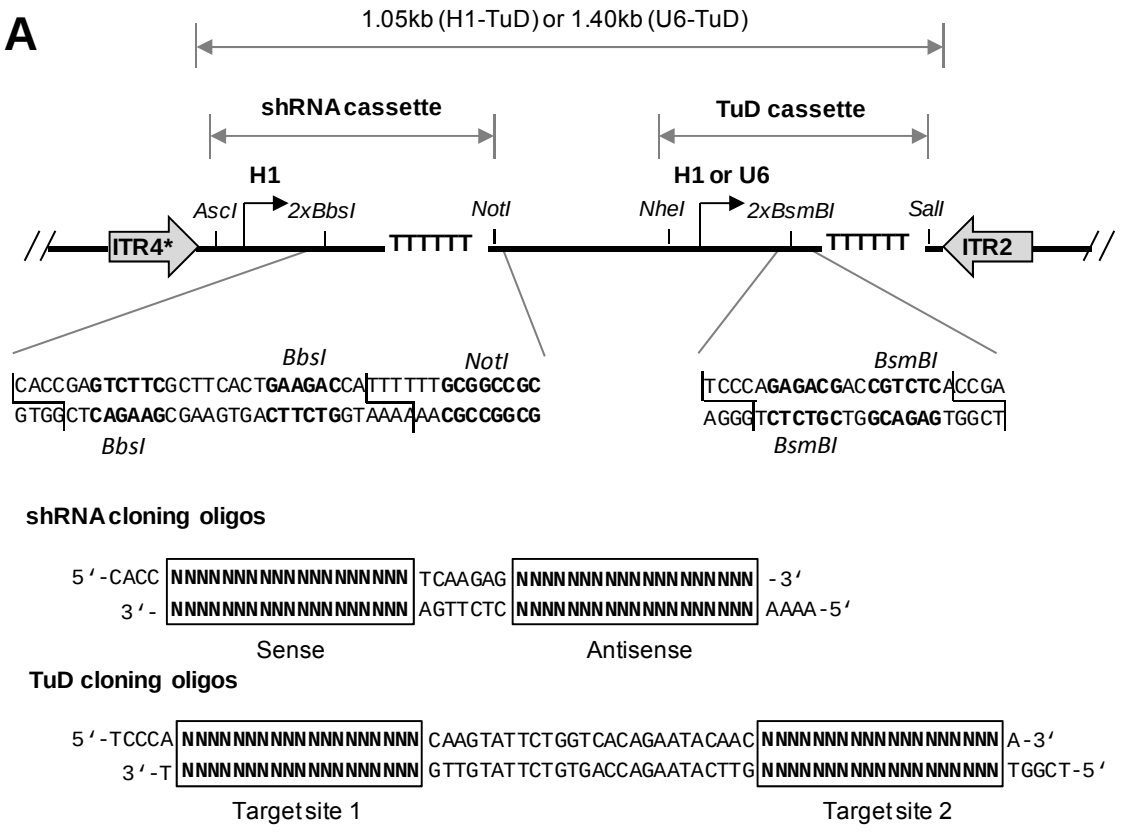

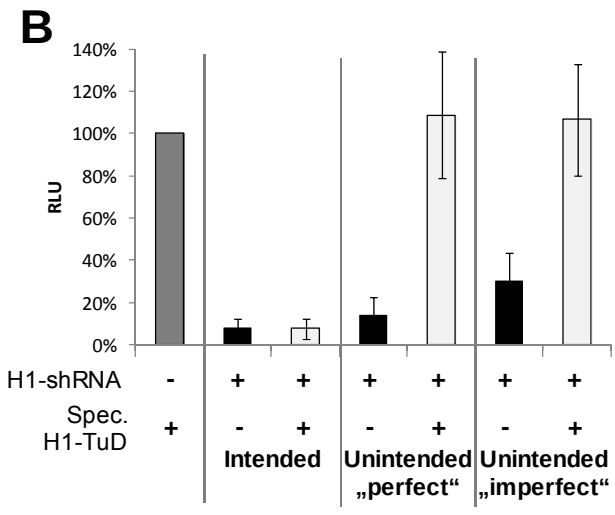

Fig. 11: shRNA and TuD can be expressed from a single vector. A: Schematic representation of the cloning strategy for TuD and shRNA cloning. The vector design allows rapid *de novo* cloning of shRNA or TuD binding sites via BbsI or BsmBI restriction sites, respectively. shRNA and TuD expression cassettes can be excised by AscI/NotI and NheI/SalI digestion, respectively, permitting easy transfer of whole cassettes between different vectors. **B:** HEK293T cells were transfected with a single construct carrying shHCV318 and H1-driven control or specific TuD. Rluc reporter silencing was measured 48h post-transfection. RLU=relative light units.

Along with the two perfect match reporters for antisense and sense strands we also included the imperfect target with single mismatch to the sense strand in this assay that better represented potential endogenous off-targets. We found that with our vector design we could achieve a complete relief of repression of both perfect and imperfect sense strand targets in HEK293T cells (Fig. 11B). Importantly, the antisense strand remained unaffected. In addition, the ~8-fold

attenuation of sense strand activity mediated by the TuD was superior to the degree of sense strand counteraction previously observed with the RNA-pol II sponges where the effect was less than 4-fold upon transfection into HEK293T cells (cf. Fig. 8B). These data suggest that the HCV318 TuD is more potent in inactivating the shHCV318 sense strand than the HCV318 sponge.

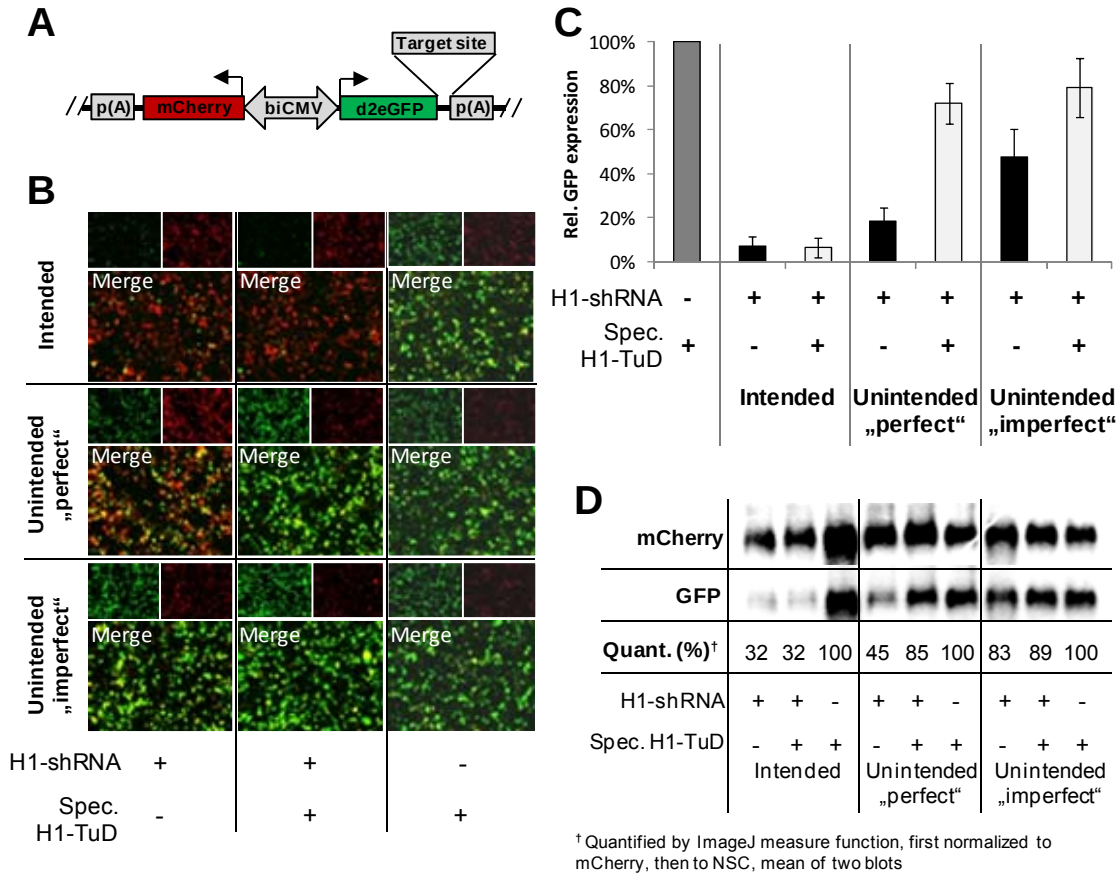

Fig. 12: **TuD acts both on protein and mRNA level of target reporters**. **A:** Schematic representation of the dual fluorescence reporter construct used. d2eGFP allows insertion of target sites in its 3' UTR and serves as knockdown reporter. mCherry serves as transfection control. Both proteins are expressed from the same bidirectional CMV promoter (biCMV). **B-D:** shHCV318 with control or specific TuD was transfected into HEK293T cells along with dual fluorescence reporter plasmids carrying the indicated target sites. 48h post-transfection, eGFP and mCherry were analyzed on the protein level by fluorescence microscopy (B) and FACS (C) or mRNA levels were visualized by Northern blot (D).

To confirm these results with another independent reporter system we cloned a dual fluorescence reporter plasmid carrying a bidirectional CMV promoter driving expression of both destabilized eGFP (d2eGFP) and mCherry (Fig. 12A). d2eGFP allows insertion of shRNA binding sites in its 3’ UTR and thus serves as

knockdown reporter, whereas mCherry acts as transfection control. Using this system, we could confirm the inhibitory effect of the specific TuD on the sense strand (Fig. 12B+C). For the unintended perfect target a clear derepression by the specific TuD could be observed in fluorescence microscope images while the intended target was equally repressed in the presence of either control or specific TuD (Fig. 12B). As the inhibitory effect for the imperfect target for the sense strand was not well visible in the pictures we also quantified relative eGFP expression by dual color FACS analysis (Fig. 12C; see Suppl.Fig. 2 for experimental details). The results matched our expectations from the luciferase assay. We noted, however, that in the GFP assays repression of the sense strand targets was somewhat less pronounced than observed before. This could be due to the high eGFP expression levels required for the assay which might have led to an unintended sponge effect mediated by the eGFP target transcript. We next visualized mCherry and d2eGFP mRNAs by Northern blotting to examine the effects of the specific TuD on target transcript levels. As expected, we found no change in mRNA levels of the intended target whereas repression of the perfect unintended target was relieved (Fig. 12D). The unintended imperfect target only exhibited a weak knockdown on the mRNA level which accordingly allowed merely a slight relief of repression by the specific TuD.

For reasons of applicability, we again tested whether this strategy would be compatible with rAAV-mediated gene transfer. We therefore packaged shHCV318 with either the specific or control TuD and the NSC into self-complementary rAAV2 vectors and transduced HEK293T cells with. We were able to successfully counteract the sense strand showing that the system is readily combinable with rAAV technology (Fig. 13A). Although the degree of de-repression of the unintended perfect target was lower than after HEK293T transfection the TuD effect was still ~4.5-fold. We also tested the efficacy of the TuD upon transduction of Huh7 hepatocytes which is a far more relevant setting in case of our anti-HCV shRNA which is supposed carry out its function in the liver. In this cell type, the overall knockdown of the three tested targets was more pronounced than in HEK293T cells (Fig. 13B). Nevertheless, we achieved a ~6-fold or ~3.5-fold de-repression of the unintended perfect or imperfect target, respectively, without affecting the antisense strand.

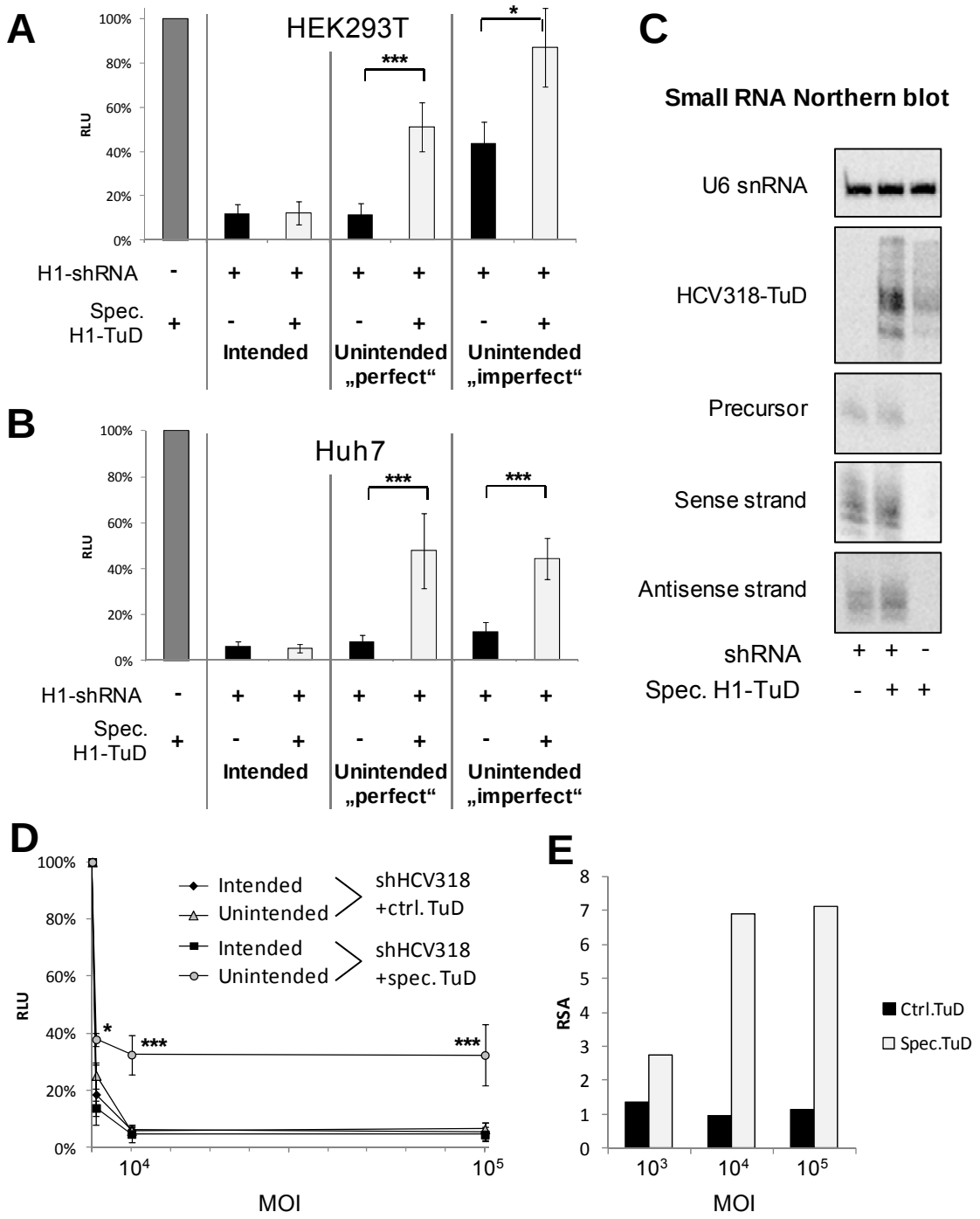

Fig. 13: **Translation of the plasmid-based transfection system into rAAVs**. **A-B**: Sense and antisense strand activity of H1-shHCV318 were measured by dual luciferase assay 48h after transduction of HEK293T (A, MOI=5x10^4) or Huh7 (B, MOI= 10^5) cells with rAAV2 vectors carrying shRNA and TuD as indicated. **C**: Huh7 cells were transduced (MOI=10^5) with rAAV2 encoding shHCV318 with control or specific TuD. 48h post-infection total RNA was purified, and shRNA and TuD were visualized by small RNA Northern blot. **D:** Huh7 cells were transduced with rAAV2 vectors encoding shHCV318 and control or specific TuD at indicated MOIs and transfected with perfect target reporters for both strands. Strand activities were determined by dual luciferase assay 48h post-infection. Asterisks indicate the level of significance for a difference between the control and specific TuD for the unintended target. **E:** Relative strand activities as calculated from D. Statistical analysis: unpaired, two-sided T-test, * $p<0.05$, *** $p<0.0005$. RLU=relative light units; MOI=multiplicity of infection.

We next tested whether TuD co-expression had any influence on the intracellular levels of the shHCV318 sense strand. In agreement with previously reported data we did not see any alterations in sense strand expression by small RNA Northern blotting, suggesting a mode of action that is solely based on competitive sequestration (Haraguchi *et al.*, 2009; Fig. 13C). In the shown blot the TuD was detected with the same probe as the antisense strand. Since this probe had a single mismatch towards the TuD binding site the signal intensities do not represent the relative levels of TuD and shRNA expression. To better estimate the relative expression levels of the two molecules we therefore also detected the TuD with a perfect match probe. Our results showed that TuD levels by far exceed shRNA levels (Suppl.Fig. 3).

We furthermore examined the concentration dependency of our strategy by infecting Huh7 cells at different MOIs. This titration experiment showed that the specific TuD is efficacious over a wide range of vector dose (Fig. 13D). Maximal effects were observed when sense strand activity was strong in the first place, *i.e.* at MOI 10^4 and 10^5 (Fig. 13E).

3.3.2 TuD co-expression does not interfere with intended target silencing

We next wanted to prove the utility of the approach by moving away from reporter assays towards real shRNA targets. Firstly, we thus had to show unaltered silencing efficiencies mediated by the antisense strand on the intended target -*i.e.* HCV virus RNA- with the specific TuD as compared to the control. Secondly, we needed to prove that under similar conditions sense strand-mediated silencing of endogenous off-target genes is indeed diminished by the specific TuD.

We therefore conducted the same HCV inhibition experiments as previously with the shRNA-sponge constructs. In agreement with the results obtained in the reporter assays we did not observe any differences in HCV silencing by shHCV318 with specific or control TuD (Fig. 14A+B). The degree of HCV inhibition was similar to what we had observed with the shHCV318-sponge vectors at MOI 10^5 (cf. Fig. 9A+B). Notably, at lower MOIs the shHCV318-TuD vectors outperformed the shHCV318-sponge vectors.

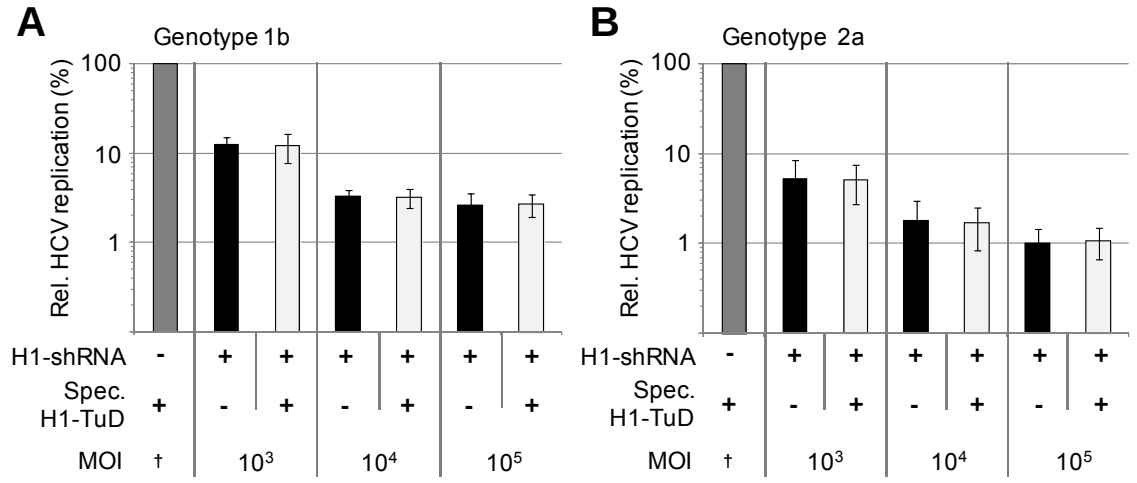

† MOI of NSC matched to miR-122-5p TuD

Fig. 14: **shHCV318 on-target silencing**. **A+B:** Inhibition of HCV replication by shHCV318 after transduction of Huh7 cells carrying subgenomic replicons of HCV genotype 1b (A) or 2a (B) at indicated MOIs 48h post-infection. HCV replication was quantified by measurement of Fluc activity encoded by the HCV replicons. MOI=multiplicity of infection.

3.3.3 TuD co-expression de-represses endogenous sense strand off-targets and reduces overall perturbance of gene expression

We considered it reasonable to use the highest vector dose for subsequent analysis of erroneous silencing of untargeted endogenous genes as in this particular application of HCV inhibition it is necessary to achieve maximal levels of RNAi potency. We therefore transduced Huh7 cells under similar conditions as previously the Huh7 replicon cells, extracted total RNA 48h post-transduction and analyzed the expression profiles by microarray covering the whole human transcriptome (Illumina HumanHT-12, conducted by DKFZ core facility).

After filtering out transcripts with too little difference to the background we found 1002 genes of a total of 17367 genes on the chip to be significantly different in at least one sample as compared to the NSC (T-test, unpaired, two-sided, $p<0.01$). Of these, 596 only differed mildly (less than $_2\log(0.5)$-fold difference) from the NSC and were thus not further analyzed (Fig. 15, grey square). 166 genes were considered down-regulated (relative expression $< {}_2\log(-0.5)$) upon expression of shHCV318 with the control TuD. Importantly, 111 of these were less down-regulated in the presence of the specific TuD with 38 reaching statistical significance (Fig. 15, left green square; T-test, unpaired, two-sided, $p<0.01$). In

contrast, of the 86 genes down-regulated upon co-expression of the specific TuD only 31 were concomitantly less down-regulated with the control TuD with only 3 being significantly different (Fig. 15, lower red square).

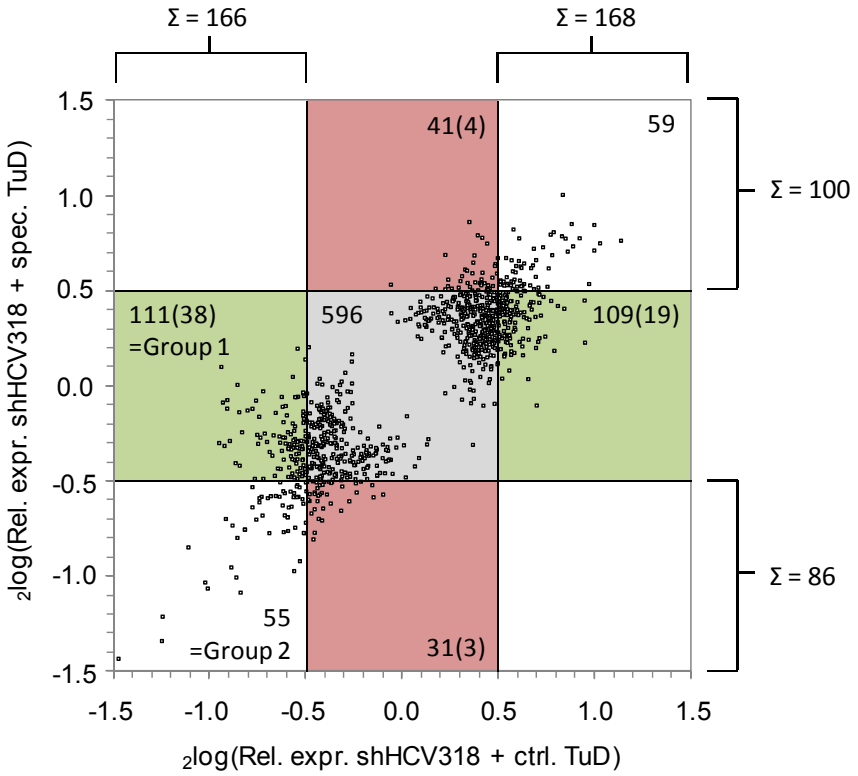

Fig. 15: Sense strand TuD reduces global perturbation of gene expression. Huh7 expression profiles after transduction with rAAV2 carrying either shHCV318 with control or specific TuD or a NSC (MOI=10^5). Dysregulated genes in one or both samples (T-test, unpaired, two-sided, $p<0.01$) were plotted. Numbers indicate gene counts in each area. Counts for genes that are statistically significantly different (T-test, unpaired, two-sided, $p<0.01$) in both samples are given in brackets. MOI=multiplicity of infection; NSC=non-silencing control.

Likewise, for the up-regulated genes (relative expression > $_2$log(0.5)) we observed a similar attenuating effect by the specific TuD. Of 168 genes that were up-regulated in the cells treated with shRNA and control TuD 109 were closer to the NSC in the cells treated with shRNA and specific TuD (19 significant, Fig. 15 right green square) while the other way around only 41 out of 100 were less up-regulated (4 significant, Fig. 15 upper red square).

These results show that the perturbation of the transcriptome produced by expression of shHCV318 is partly alleviated when the specific sense strand TuD is co-expressed. Generally, it is noteworthy that the overall levels of dysregulation after transduction with our shRNA-TuD-encoding rAAV2 vectors were modest

with the strongest response being less than 3-fold which is in the same range as previously reported shRNA off-target effects (Jackson *et al*., 2006a).

To prove that the observed attenuating effect by the specific TuD was indeed due to the inhibitory effects of the specific TuD on the shRNA sense strand, we analyzed the 3' UTRs of two different gene groups for the enrichment of specific sequences. The first gene group that was analyzed showed down-regulation by shHCV318 in the presence of the control TuD but not the specific TuD (Fig. 15, Group 1, only statistically significant genes were analyzed). If our system was working, this group should represent the endogenous off-targets of the shRNA sense strand that were rescued by the specific TuD. We therefore expected an enrichment of sense strand seed matches in the 3' UTRs of genes in Group 1. The second group of interest was down-regulated by shHCV318 regardless of whether we co-expressed control or specific TuD (Fig. 15, Group 2) and should contain targets of the antisense strand. Genes in Group 2 should thus be enriched in antisense strand seed matches in their 3' UTRs.

Frequencies of the indicated sequences in both groups were compared to the background frequencies in all transcripts analyzed on the microarray chip. Positions and sequence of the seed regions of both sense and antisense strand are given in Fig. 16A. We indeed observed a significant enrichment of sense strand seed matches in the 3' UTRs of Group 1 genes with a concomitant non-significant decrease in Group 2 (Fig. 16B). Although non-significant this latter effect may indicate that genes that were silenced by shHCV318 and carried a sense strand seed were more likely to fall into Group 1 so that there was a depletion of this motif in Group 2. The most significant and strongest enrichment of complementary seed sequences in Group 1 was found for a full match from nucleotide 1-8 where it was almost 5-fold (Fig. 16B).

When analyzing antisense strand seed matches we saw a significant enrichment in Group 2 but not in Group 1 (Fig. 16C). Again, the strongest enrichment was for the full octamer seed match (over 9-fold for nt 3-10). We also observed an apparent enrichment of antisense strand nt 3-9 matches in Group 1, yet the level of significance was very low ($p=0.04$) and neither of the other sequences was significantly enriched. As a whole, our results suggest that the specific TuD indeed counteracted endogenous off-target effects mediated by the sense strand and thereby alleviated dysregulation of gene expression.

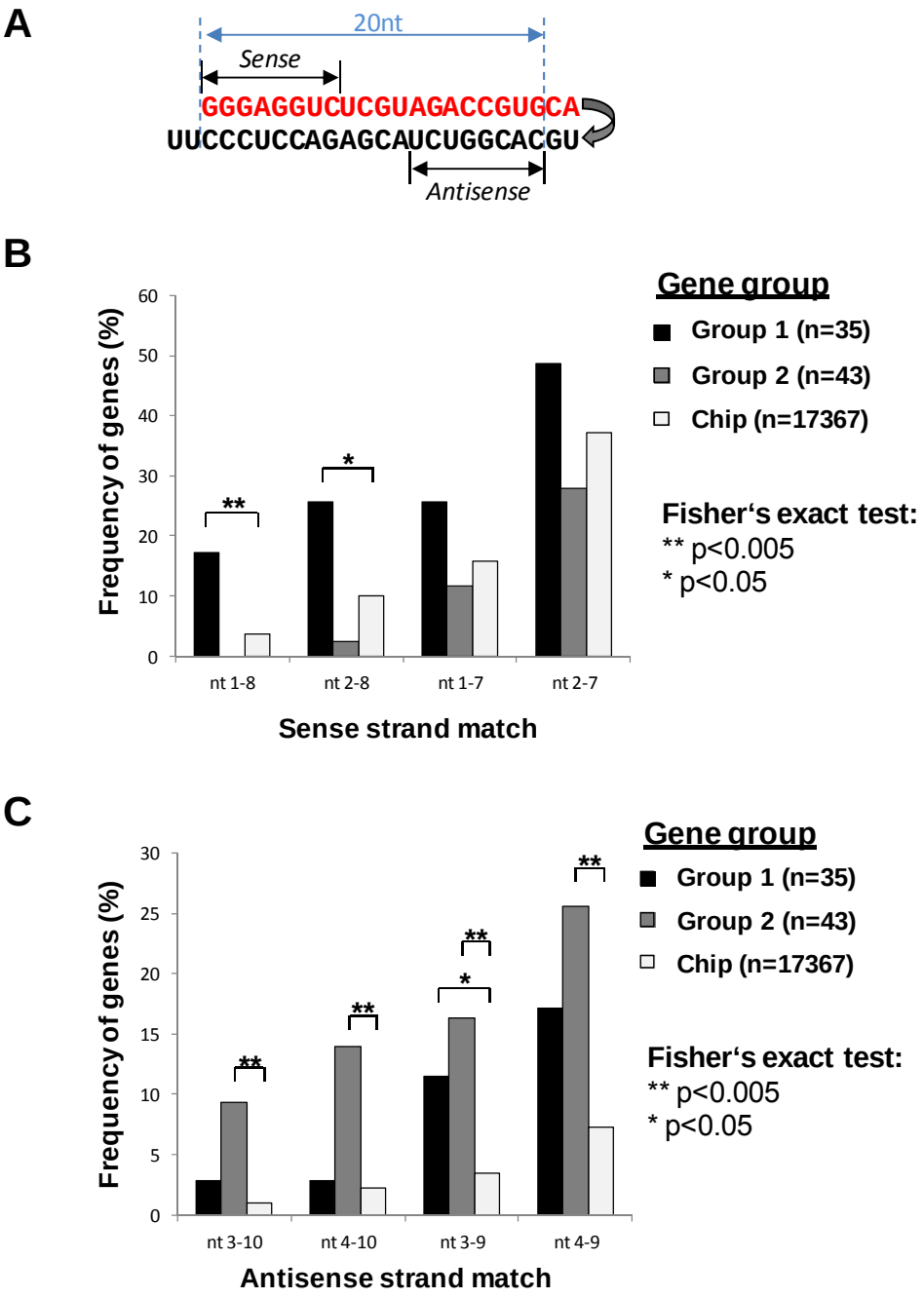

Fig. 16: Sense strand TuD relieves silencing of endogenous sense strand off-targets. 3' UTR sequences of genes in either Group 1 or 2 as defined in Fig.15 were extracted from the Refseq database and analyzed for the presence of either sense or antisense strand seed matches. **A:** Structure of shHCV318 with potential Dicer processing product (indicated by blue dotted lines) and respective octamer seed regions for the sense and antisense strand. **B-C:** Enrichment of sense strand seed matches (B) or antisense strand seed matches (C) in 3' UTRs of indicated gene groups. For Group 1 only statistically significant hits were analyzed. Chip=all genes on the miArray chip (=background set); n=number of genes with extractable sequences.

Expression profiling was conducted with only one NSC that carried the specific TuD. We hence wanted to rule out the possibility of unspecific effects by the specific TuD which would not be visible in the miArray data. We therefore extracted total RNA from Huh7 cells that had been treated as before and also included two more controls, *i.e.* a second NSC that carried the control TuD as well as naïve Huh7 cells. We then analyzed the most significant hits from Group 1 (SEPT9) and Group 2 (CIRBP) as well as an unregulated gene (RAN) by reverse transcription quantitative PCR (RT-qPCR). We found that although the degree of silencing of CIRBP was less pronounced and knockdown of SEPT9 was stronger all three genes behaved as in the miArray (Suppl.Fig. 4). Importantly, the two NSC controls did not differ for those two genes and only for RAN we observed a slight upregulation in the NSC with control TuD. SEPT9 was slightly lower expressed in naïve Huh7 cells than in the two NSCs with the NSC with specific TuD reaching statistical significance. In general we did not detect any aberrant behavior of the NSC with specific TuD.

In addition to RT-qPCR analysis, three 3' UTRs of genes from Group 1 (CLCN7, BCL7B and FRMD8) that contained sense seed matches and one 3' UTR of a gene from group 2 (CIRBP) that contained an antisense seed match were cloned into the 3' UTR of a Rluc reporter. SEPT9 was not used as it does not contain any sense strand seed match in its 3' UTR. It is thus likely an indirect target of shHCV318 so that 3' UTR cloning would not necessarily reflect the situation of the endogenous transcript. Huh7 cells were subsequently transduced with the same vectors and MOI as before and additionally transfected with the endogenous off-target reporters. The obtained luciferase data further confirmed the validity of the miArray results (Fig. 17A+B). Both CLCN7 and BCL7B 3' UTR reporters were highly significantly silenced by shHCV318 and this effect could be partially counteracted by the specific sense strand TuD which is in accordance with the data obtained from the miArray. For the FRMD8 3' UTR reporter, however, we only observed a weak knockdown effect. We did not see any ameliorating effect of the specific TuD, either. For technical reasons only a stretch of 1.4kb of the FRMD8 3' UTR containing the sense seed match was cloned. A possible reason for the discrepancy between the degree of silencing of the FRMD8 3' UTR reporter and the degree expected from our miArray data may therefore be that recognition of the sense binding site is influenced by

downstream sequences that were not cloned or also by upstream regions within the FRMD8 CDS.

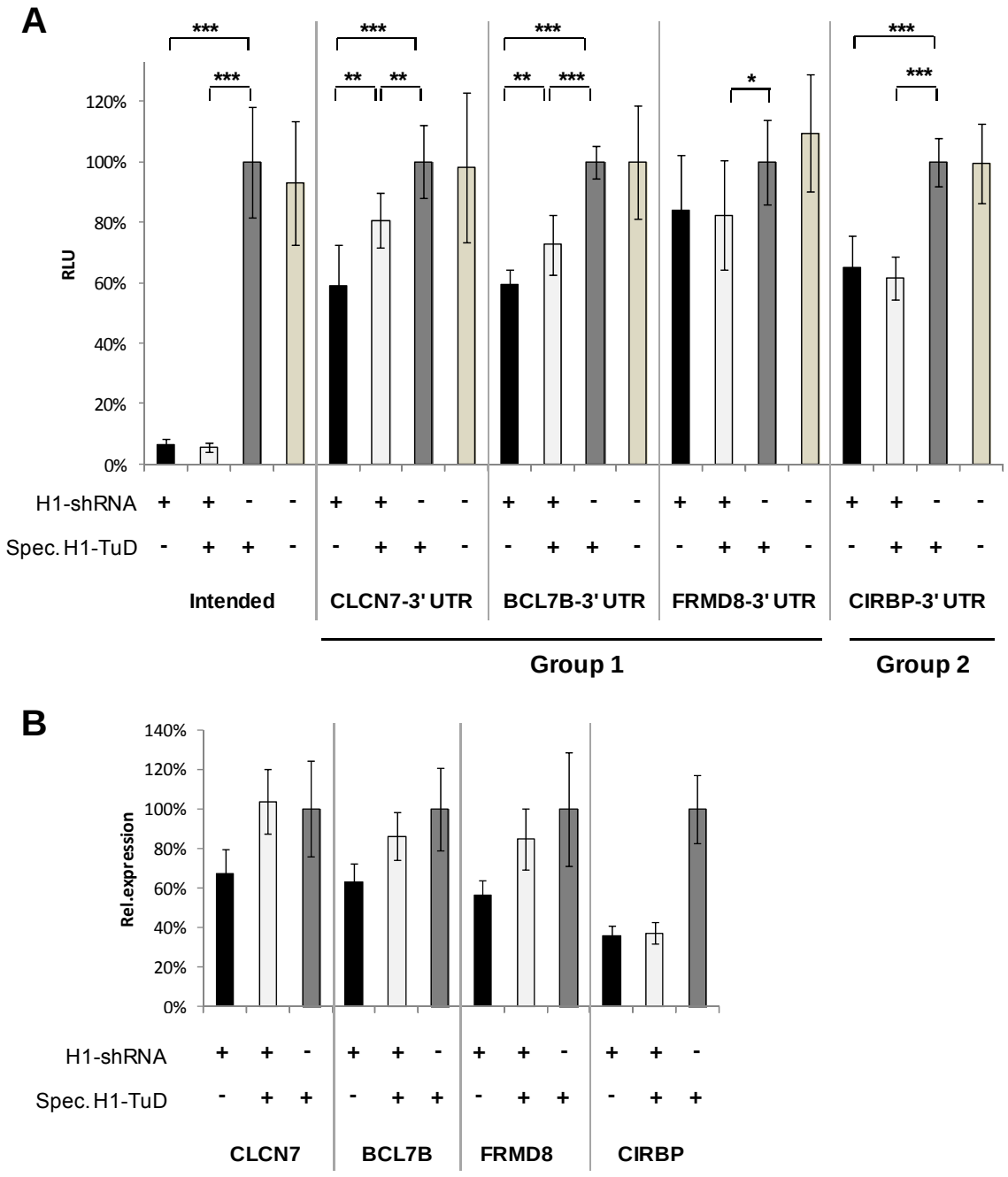

Fig. 17: Validation of shHCV318 off-targets by 3' UTR cloning. A: 3' UTRs of three Group 1 genes (CLCN7, BCL7B, FRMD8) carrying sense strand seed matches and of one Group 2 gene (CIRBP) carrying an antisense seed match were cloned into the 3' UTR of a Rluc reporter. Huh7 cells were transduced with rAAV2 vectors carrying shRNA and TuD as indicated (MOI=10^5) and co-transfected with the off-target reporters or a perfect antisense reporter (Intended) as control. 48h post-transfection reporter silencing was measured by dual luciferase assay. Significance was determined by an unpaired, two-sided T-test (* $p<0.05$; ** $p<0.005$; *** $p<0.0005$). **B:** miArray results for the same genes for comparison.

The Group 2 reporter carrying the CIRBP 3' UTR was silenced in the presence of both control and specific TuD as expected. Likewise, silencing of the perfect match target for the antisense strand that was measured in parallel as control was not affected. Importantly, we did not observe any different behavior between the two NSC for any of the 3' UTR reporters. Taken together, the RT-qPCR and 3' UTR results therefore at least partly confirmed the validity of the results from expression profiling.

3.4 Effect of shRNA and TuD expression on the endogenous miRNA pathway

Previous studies have shown the perturbation of the endogenous miRNA pathway upon shRNA expression both *in vivo* and *in vitro* (Grimm *et al.*, 2006a; Pan *et al.*, 2011). This could be linked to oversaturation of protein factors such as Exportin-5. As TuD molecules are also hairpin structures that are exported from the nucleus by Exportin-5, TuD expression might likewise interfere with miRNA functionality. We therefore examined potential adverse effects of our expression system on the miRNA pathway. To this end, we compared miR-122-5p expression levels in Huh7 cells transduced with shHCV318 and either control or specific TuD to naïve Huh7 cells. We found that miR-122-5p expression was mildly reduced in the cells expressing shHCV318 (Fig. 18A). The two NSC with either control or specific TuD did not produce any noticeable alterations in miR-122-5p expression indicating that TuD co-expression does not derogate miRNA maturation like shRNAs. We next examined whether the mild miR-122-5p reduction in the two shHCV318 samples had any functional consequences on target silencing. We went back to our miArray data and analyzed relative expression levels of a set of 25 experimentally validated miR-122-5p targets (TarBase 6; Vergoulis *et al.*, 2012). In case of reduced miR-122-5p activity in our samples we would expect a general up-regulation of its targets in our dataset. However, in agreement with the only weakly altered intracellular miR-122-5p levels, no such up-regulatory effect was observed for shHCV318 with control or specific TuD (Fig. 18B). In the same manner we also analyzed target genes of other miRNAs expressed in Huh7 cells according to the microRNA.org database. We observed a slight tendency towards up-regulation of target genes of the

analyzed miRNAs (Suppl.Fig. 5). Yet, the degree of this dysregulation was minor. We hence conclude that despite the observed reduction in miR-122-5p levels shHCV318 expression did not generally perturb the miRNA pathway and no signs of adverse effects of TuD expression were detected in our experimental system.

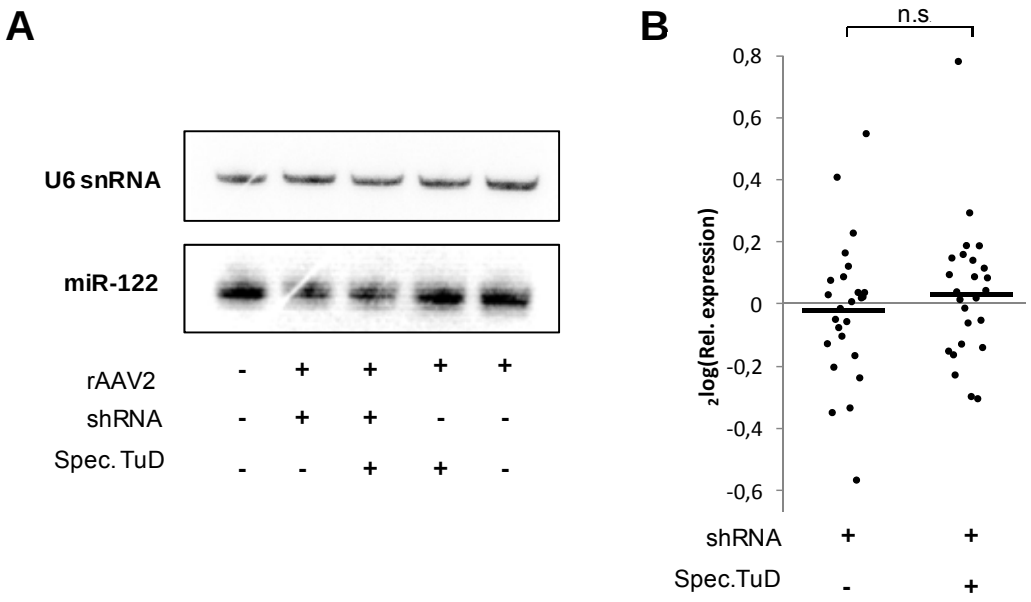

Fig. 18: Effects of shHCV318 expression on miRNA pathway. A: miR-122 expression in naive Huh7 cells or 48h after infection with rAAV2 carrying shRNA and/or TuD as indicated (MOI=10^5). **B:** 25 targets (TarBase 6) of miR-122 were analyzed for dysregulation in the miArray data generated before. The mean relative expression in both data sets does not differ considerably from the NSC and differences between the two set were not significant (T-test, unpaired, two-sided, $p<0.05$).

3.5 Adaptation of TuD strategy to different shRNAs

To adapt the sense strand inhibition strategy to additional unrelated shRNAs we first used hAAT25 as its strand activities had been characterized already. Two target sites with single mismatches that we had found in the random target screen were used for construction of an H1-TuD against the hAAT25 sense strand. By utilizing the same vector backbone as previously for shHCV318 we achieved an over 3-fold improvement of the relative strand activities for hAAT25 after plasmid transfection in HEK293T cells (Suppl. Fig. 6A). We next packaged the vector into rAAV2 and tested strand activities upon Huh7 transduction. In this setting no significant sense strand counteraction by the TuD could be observed (Suppl. Fig. 6B). We argued that this issue could be solved by increasing TuD

expression levels relative to shRNA levels and tested this hypothesis by exchanging the H1-TuD by a U6-TuD of the same sequence. Indeed, we were able to successfully counteract the sense strand both after transfection and transduction (Fig. 19A-B). Vector titration experiments showed that the U6-TuD reduced hAAT sense strand activity at high MOIs with maximal effects of over 2.5-fold (Fig. 19B).

We next also constructed a U6-driven TuD against the sense strand of another shRNA that is directed against the hepatitis B virus sAg termed shHBVS122nt. This shRNA was based on a previously published 20-mer shRNA that had been successfully used for HBV inhibition in mice (Chen *et al*., 2006). As with shHCV318 previously we added 2nt to the shRNA to obtain a stem of 22nt so that the shRNA would fit to the design rules. We constructed a U6-TuD containing two target sites with single mismatches similar to what we had used before. As with hAAT25, we saw an over 3-fold inhibitory effect after transfection of HEK293T cells (Fig. 19C). Upon rAAV2-mediated delivery of shHBVS122 to Huh7 cells, co-expression of the specific TuD achieved a modest but significant sense strand counteraction of 1.5-fold at the highest MOI (Fig. 19D).

To more easily compare the results for the different shRNAs, we calculated and plotted the RSAs for all three shRNAs tested at the different MOIs after Huh7 transduction (Fig. 19E). In the presence of the control TuD, the three shRNAs displayed remarkably different behaviors in terms of strand activities. The strands of shHCV318 have more or less the same activities and the RSA does not change with increasing MOIs. hAAT25 naturally has a good RSA which drops at the highest MOI. shHBVS122 has an intermediate RSA at he lowest MOI which drops already at MOI 10^4 and remains constantly low at MOI 10^5. The shRNAs also differ in their responsiveness to the TuD with shHCV318 allowing the highest degree of counteraction, and with hAAT25 reaching the best RSA values in combination with its specific TuD. All three shRNAs have in common that improvement of RSA via the specific TuD increases with MOI further strongly supporting the model emerging from this work that TuD activity is dose-dependent (see section 4.1).

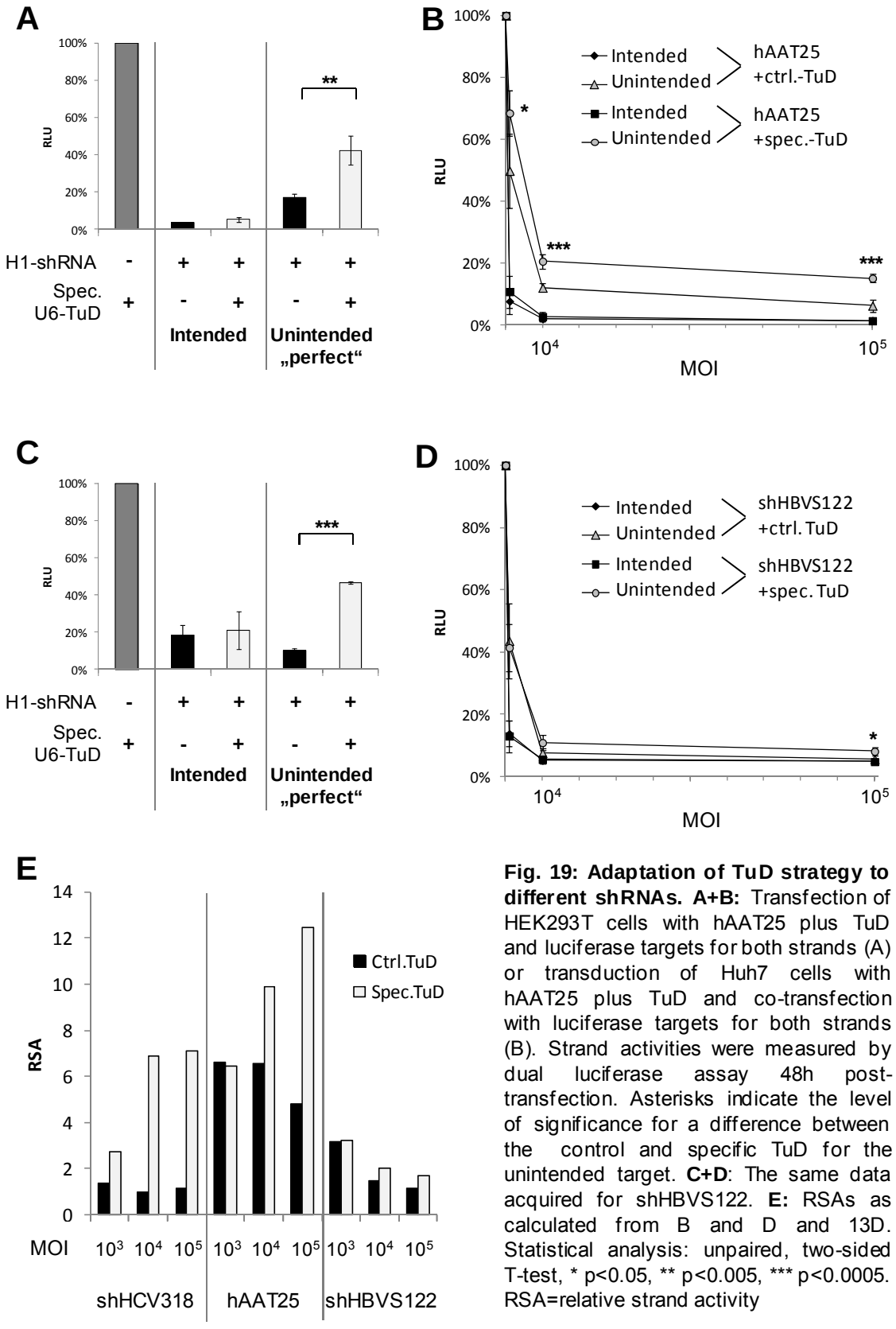

Fig. 19: Adaptation of TuD strategy to different shRNAs. A+B: Transfection of HEK293T cells with hAAT25 plus TuD and luciferase targets for both strands (A) or transduction of Huh7 cells with hAAT25 plus TuD and co-transfection with luciferase targets for both strands (B). Strand activities were measured by dual luciferase assay 48h post-transfection. Asterisks indicate the level of significance for a difference between the control and specific TuD for the unintended target. **C+D**: The same data acquired for shHBVS122. **E:** RSAs as calculated from B and D and 13D. Statistical analysis: unpaired, two-sided T-test, * $p<0.05$, ** $p<0.005$, *** $p<0.0005$. RSA=relative strand activity

3.6 Optimization of TuD-mediated sense strand inhibition

3.6.1 Single perfect match target sites are sufficient for optimal TuD activity

In parallel to proving the functionality and utility of the approach we also determined a set of design parameters for both TuDs and shRNAs. Although our previous TuDs all had imperfect targets our strategy would greatly benefit from the possibility of using perfect binding sites as this would allow easier target site design and selection.

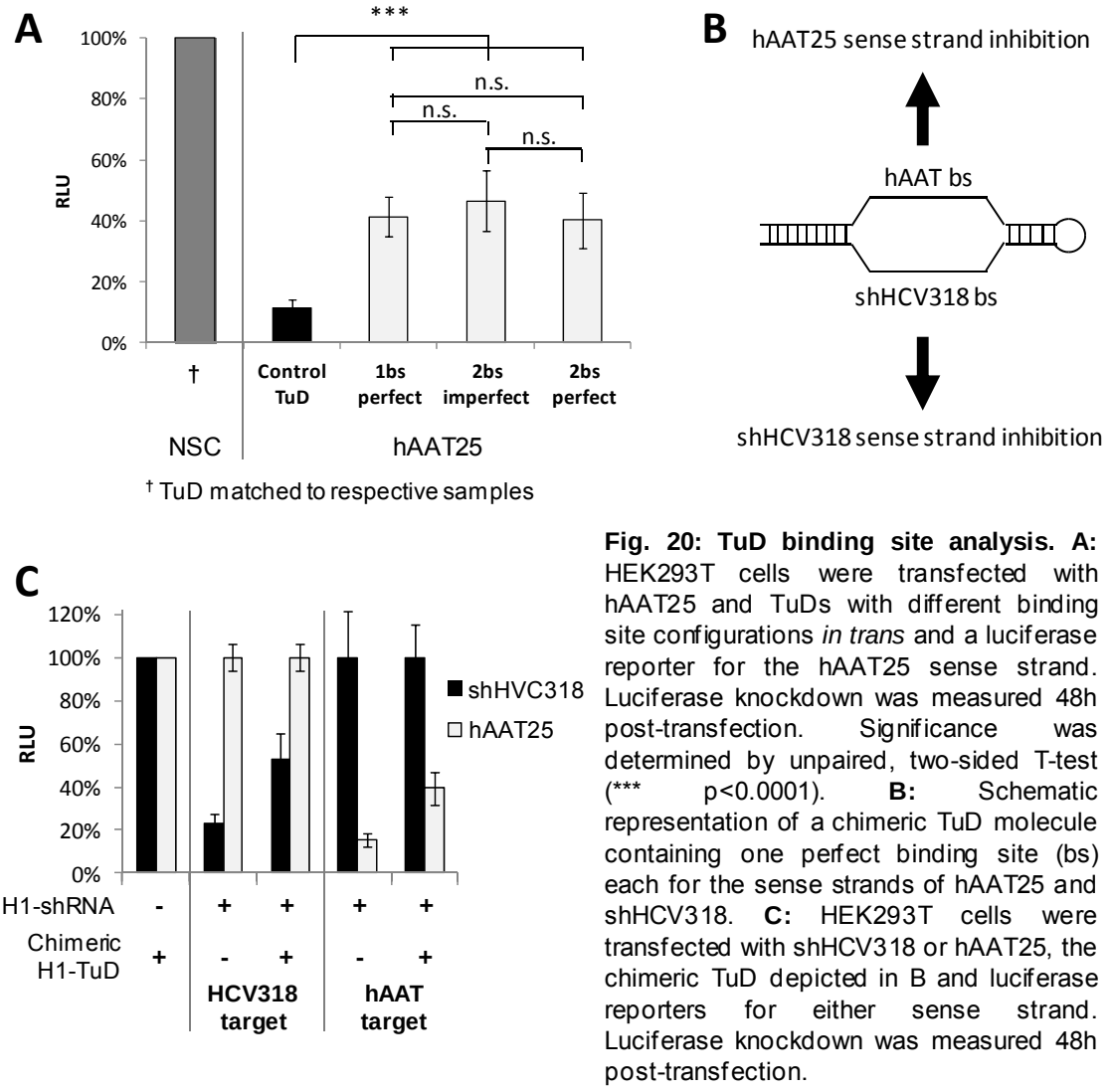

Fig. 20: TuD binding site analysis. A: HEK293T cells were transfected with hAAT25 and TuDs with different binding site configurations *in trans* and a luciferase reporter for the hAAT25 sense strand. Luciferase knockdown was measured 48h post-transfection. Significance was determined by unpaired, two-sided T-test (*** $p<0.0001$). **B:** Schematic representation of a chimeric TuD molecule containing one perfect binding site (bs) each for the sense strands of hAAT25 and shHCV318. **C:** HEK293T cells were transfected with shHCV318 or hAAT25, the chimeric TuD depicted in B and luciferase reporters for either sense strand. Luciferase knockdown was measured 48h post-transfection.

In the original description of TuDs as inhibitors of miRNA activity, the authors suggested imperfect binding sites for TuD construction to achieve maximal effects with miR-21-5p as an example (Haraguchi *et al.*, 2009). Yet, in a follow-up

study with synthetic TuD-based inhibitors they obtained best results with a perfect match target for two other miRNAs (Haraguchi *et al.*, 2012). They also linked the unsatisfactory performance of the miR-21-5p TuD with the perfect target to extensive base pairing between the two TuD target sites which could inhibit miRNA binding. It therefore appears that miR-21-5p is a special case and we consequently tested whether perfect target sites would also work in our approach. In addition, we also examined the importance of the number of target sites within the TuD as it would facilitate the construction of the expression cassette being able to reduce it to only one single binding site.

We hence generated TuDs that had different configurations of perfect or imperfect and one or two binding sites for the hAAT25 sense strand, and then transfected shRNA and TuD in HEK293T cells at equal amounts from separate plasmids. We found that under the conditions tested bulged and perfect target sites in the TuD worked equally well and it also did not make any significant difference whether the TuD contained one or two binding sites for the shRNA sense strand (Fig. 20A). None of the TuDs rescued expression of the sense strand target to 100%, allowing us to conclude that there was no apparent oversaturation which might obscure subtle differences in performance between the configurations. Our findings led us to test the possibility of generating a chimeric TuD that would counteract the sense strands of two shRNAs at the same time. To this end, we constructed a TuD with one perfect binding site for the hAAT25 sense strand and another perfect binding site for the shHCV318 sense strand (Fig. 20B). We transfected HEK293T cells with shHCV318 or hAAT25 and the chimeric TuD and measured luciferase knockdown of sense strand targets for both shRNAs 48h post-transfection. Indeed, our design allowed us to counteract both sense strands with one single construct (Fig. 20C).

3.6.2 5’ but not 3’ strands can be counteracted by TuDs or sponges

We had shown before that 5’ and 3’ strands rely on different principles of maturation (cf. Fig. 5). In an effort to further characterize our system of TuD-mediated sense strand counteraction, we also tested whether it made a difference if the sense strand was located at the 5’ or 3’ end of the shRNA molecule. To this end, we cloned an additional TuD directed against the hAAT antisense strand that in the case of hAAT25 is located at the 3’ end of the

shRNA. We then examined hAAT sense and antisense TuD activities on hAAT25 as well as an additional shRNA with inverted strand order named hAAT25R (Fig. 21A; Grimm *et al.*, 2006a). It has to be noted that even though the sequences of both shRNAs are in principle the same, Dicer processing likely generates sense and antisense strands that are not completely identical. TuDs with mismatch targets that are designed for the hAAT25 sense strand are therefore probably not suitable for hAAT25R. To avoid erroneous results, we hence used perfect match TuDs that should be active regardless of the exact nature of the mature strands (Fig. 21A). We transfected HEK293T cells with shRNA and TuD at equal amounts as well as with perfect Rluc reporters for either shRNA strand. We found that only the 5' strand of hAAT25 and hAAT25R could be counteracted (Fig. 21B).

We knew that for hAAT25 the antisense strand was expressed at much higher levels than the sense strand so that the reason for the observed effect could lie in too high expression of the strand (cf. Fig. 4D). Alternatively, the susceptibilities to counteraction might be inherent features of the respective strands. We argued that in case of a dosage effect limiting the shRNA amounts should enable the TuD to counteract the 3' strands. To address this question, we repeated the same assay as before but this time with a constant high amount of TuD and decreasing amounts of shRNA. hAAT19 was also included in this experiment (cf. Fig. 21A). This shRNA has the same configuration and sequence as hAAT25 but its antisense strand levels are much lower. In case of a dosage effect the 3' antisense strand should therefore be easier to counteract for hAAT19 than for hAAT25. As expected, we found that the 5' sense strand of all three shRNAs could be efficiently counteracted (Fig. 22A). Yet, we were unable to counteract the 3' strand of any of the three shRNAs even at the lowest shRNA dose (Fig. 22A). The antisense TuD worked with hAAT25R, indicating that this TuD was functional even though it had no effect on the hAAT19 and -25 antisense strands. This was observed even though we were not working under saturated conditions anymore so that the 3' strand levels were limited, suggesting that our inability to counteract the 3' strand was not due to too high expression levels of this strand.

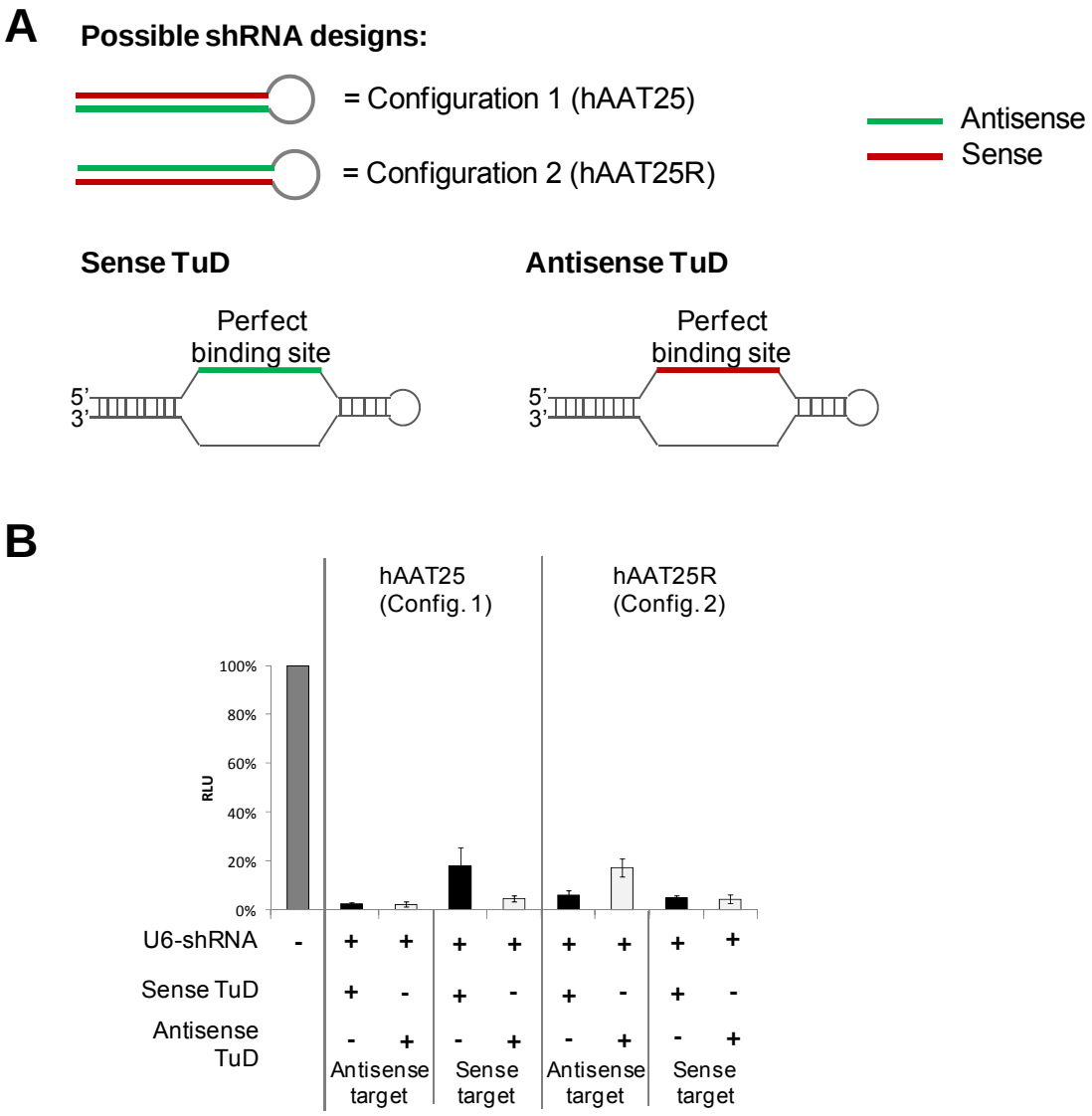

Fig. 21: Efficacy of TuD strategy depends on shRNA strand order. A: Schematic representation of the different shRNA configurations and TuDs used. **B:** HEK293T cells were transfected with equal amounts of shRNA and TuD as well as with luciferase reporters for both strands as indicated. Activity of either strand was measured by dual luciferase assay 48h post-transfection.

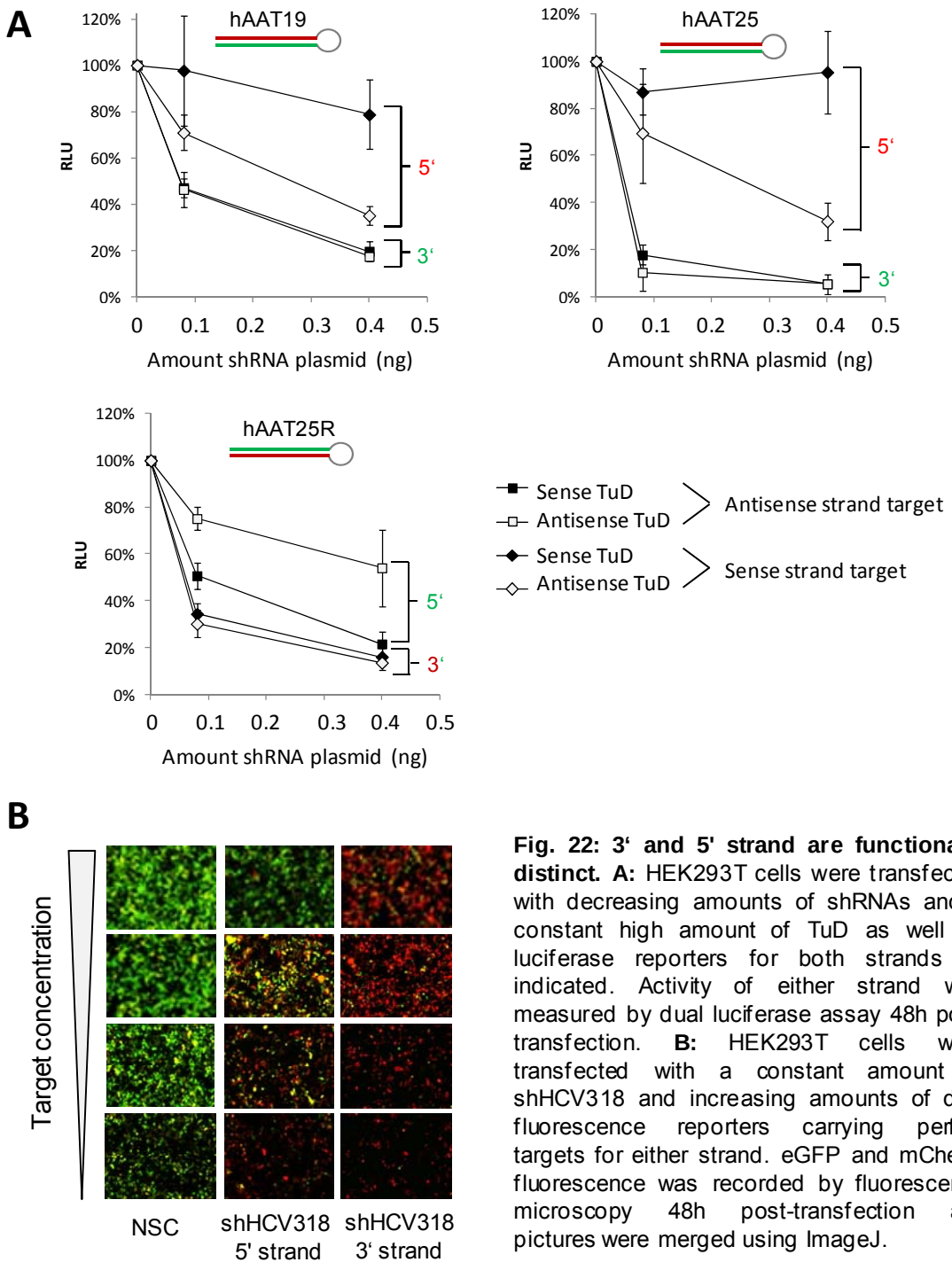

Fig. 22: 3‘ and 5' strand are functionally distinct. A: HEK293T cells were transfected with decreasing amounts of shRNAs and a constant high amount of TuD as well as luciferase reporters for both strands as indicated. Activity of either strand was measured by dual luciferase assay 48h post-transfection. **B:** HEK293T cells were transfected with a constant amount of shHCV318 and increasing amounts of dual fluorescence reporters carrying perfect targets for either strand. eGFP and mCherry fluorescence was recorded by fluorescence microscopy 48h post-transfection and pictures were merged using ImageJ.

To investigate whether this effect was specific to TuD-mediated inhibition, we conducted an analogous experiment with RNA-pol II sponges. To this end, we co-transfected shHCV318 with the dual fluorescence reporter system described earlier (cf.Fig. 12). We transfected a constant amount of the shRNA and increasing amounts of perfect target reporters for the 5’ or the 3’ strand. From a certain concentration, we expected the d2eGFP targets to act as sponges which

would lead to decreased potencies of silencing and hence increased eGFP expression levels. Indeed, we saw that the degree of silencing of the 5' strand target decreased at high reporter levels (Fig. 22B). However, we did not see such an effect for the 3' strand where the degree of silencing remained constantly high over the whole range of tested concentrations.

The fact that both TuD and sponge were unable to counteract shRNA 3' strands thus implies that there is an as of yet unknown functional difference between the two strands of shRNAs with perfect stems.

3.7 Alternative uses of our bi-functional vectors

In certain applications it could be useful to combine RNAi with miRNA inhibition. For this purpose our vector design is ideal as it permits co-expression of an shRNA and an inhibitor RNA from one single rAAV vector. One such application could again be HCV inhibition. The liver-specific miR-122-5p plays a fundamental role for the virus and reduction of miR-122-5p activity drastically decreases HCV replication (see section 1.2). A powerful approach for HCV inhibition might hence be to combine RNAi and miR-122-5p inhibition. To test the general feasibility of this concept, we generated a TuD directed against miR-122-5p using a vector construct derived from this study.

We first tested functionality of the TuD by transfecting HEK293T cells with an shRNA mimicking miR-122 along with control or specific TuD and an imperfect target reporter for miR-122-5p. The TuD efficiently counteracted miR-122-5p target inhibition thereby proving its functionality (Fig. 23A). We next packaged control and specific TuD into rAAV2 vectors and transduced Huh7 cells carrying HCV replicons of genotype 1b. We observed a dose-dependent inhibition of HCV replication of up to 20-fold. These promising results demonstrate that our vectors are easily adaptable for rAAV-mediated miRNA inhibition. We are currently testing the possibility of combining shRNA and miRNA TuD in a single vector.

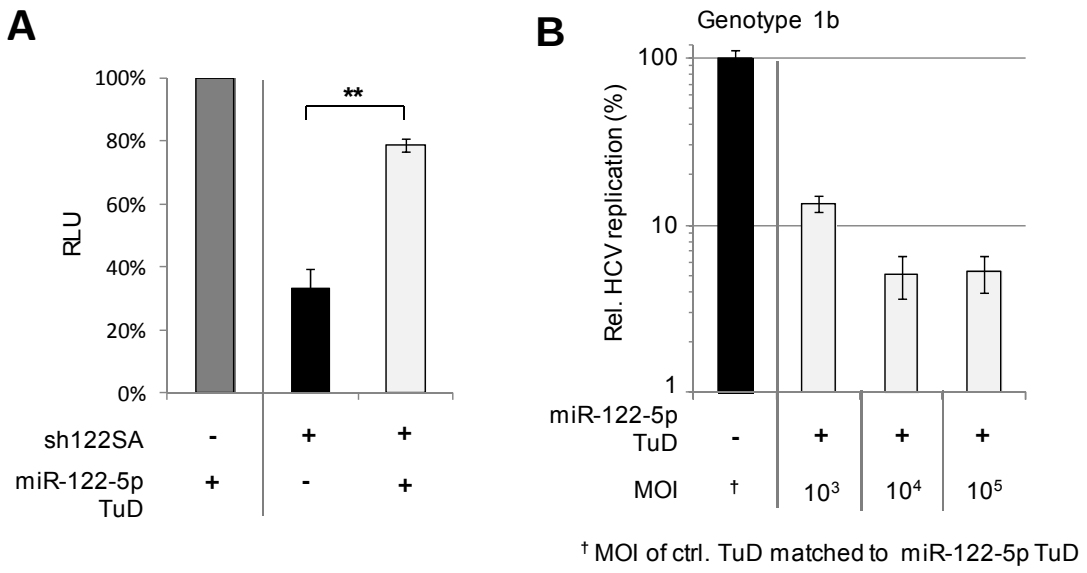

Fig. 23: HCV inhibition by TuD-mediated miR-122-5p inactivation. A: HEK293T cells were transfected with sh122SA (an shRNA mimicking miR-122), a miR-122-5p target reporter and a control or specific TuD against miR-122-5p. Reporter knockdown was measured 48h post-transfection by dual luciferase assay. Statistical analysis: unpaired, two-sided T-test, ** $p<0.005$. **B:** Inhibition of HCV replication by the miR-122-5p TuD after transduction of Huh7 cells carrying subgenomic replicons of HCV genotype 1b at indicated MOIs 48h post-infection. HCV replication was quantified by measurement of Fluc activity encoded by the HCV replicons. MOI=multiplicity of infection.

4 DISCUSSION

In this study, we set up a novel system to improve relative shRNA strand activities in order to increase specificity without compromising the silencing potential of the antisense strand. Our method is based on sequestration and concomitant partial inactivation of shRNA sense strands by inhibitor RNA molecules carrying specific binding sites. In our experiments, we observed strong sense strand activities for all shRNAs tested despite of naturally occurring strand biasing mechanisms that favor activation of the antisense strand. Importantly, we could prove that the sense strand of an exemplary anti-HCV shRNA indeed contributed to off-target silencing of endogenous genes and that this could be counteracted by our inhibition method. The results on functional characterization of shRNAs and inhibitor molecules as well as potential future applications and improvements of our method will be discussed in the following.

4.1 Sense strand activity and its counteraction

4.1.1 Alleviation of off-targeting by sense strand inhibition

In this study, we provide detailed data about the relative strand activities of shRNAs with perfectly matched stems. We could show that these RNAi triggers have a general functional bias towards the 3' strand when the stem of the shRNA accounts for more than 21 nucleotides. The undesired sense strand should therefore be placed at the 5' end of the molecule to reduce its activity. Yet, we found that despite this design rule the sense strands of all tested shRNAs were highly active, albeit to varying degrees. This is in contrast to previous studies that showed an almost complete lack of sense strand activity (Boudreau *et al.*, 2008; Boudreau *et al.*, 2011; Gu *et al.*, 2011). The general design of the shRNAs used in these studies (RNA-pol III-expressed, stem longer than 20nt, sense strand at 5' end, 3' overhangs of 2nt) is similar to ours so that this factor alone cannot explain the discrepancy to our results. The only noticeable difference lies in the loop sequence. However, in the aforementioned studies the applied loops were copied from two endogenous miRNAs -miR-30 and miR-22, respectively- whose natural strand bias according to miRBase 18 is towards the 5‘ strand (see section 6.2 for weblink to database). It therefore seems highly unlikely that these particular sequences increase the activity of the 3' strand in the context of an artificial

shRNA molecule. The variability in strand biasing observed with our own shRNAs rather suggests that strand selection mechanisms are strongly influenced by the nature of the stem sequence which in turn depends on the shRNA target site. It is hence possible that the high degree of strand biasing observed in the aforementioned studies was simply due to the nature of their target sequences. However, in some applications this parameter cannot be freely chosen, *e.g.* in the case of certain viruses the choice of target sites is rather limited.

These considerations imply that the sense strand cannot be readily inactivated for any given shRNA by placing it at the 5' end of the molecule. This is exemplified by our anti-HCV shRNA that exerted high levels of sense strand activity which also contributed to off-target silencing of endogenous genes under the tested experimental conditions. For this shRNA the options for reduction of sense strand activity are limited. Although our data suggest that this is possible by lowering the intracellular shRNA amounts it is at the cost of also losing the optimal potency of the antisense strand which in the case of shHCV318 would be counterproductive. In addition, fine-tuning of the intracellular shRNA levels is not readily achievable in all settings which is true especially in *in vivo* experiments. Upon systemic administration it is difficult to deliver an exact vector dose, *e.g.* to the liver, to precisely tune shRNA expression.

Expression profiling by miArray revealed that global dysregulation of gene expression in transduced Huh7 cells induced by shHCV318 could be reduced by co-expression of a TuD molecule for the shRNA sense strand. This effect could be linked to specific de-repression of off-targets carrying sense strand seed matches. From this we conclude that sense strand sequestration may indeed increase shRNA specificity. We suggest that our method may be especially useful in the case of shRNAs whose strand bias is not well pronounced due to the nature of their target sequence.

4.1.2 Considerations on inhibitor functionality and mode of action

Using RNA-pol III-transcribed TuD molecules we were able to reduce the sense strand activities of three independent shRNAs. An interesting and initially unexpected observation was that the degree of sense strand counteraction differed considerably between these shRNAs. Best results were obtained with shHCV318 followed by hAAT25 and then shHBVS122. All three shRNA have

their sense strand activities in the same range (90-95% silencing upon Huh7 transduction) and yet differ in their responsiveness to the TuD. In a recent study it has been suggested that the extent of base pairing between the two TuD binding sites is indicative of TuD functionality (Haraguchi *et al*., 2012). In case of extensive interaction between the two strands (over nine base pairs as predicted by Centroid fold, see section 6.2 for weblink) the TuD could lose its activity because the binding sites are not accessible. However, for all of our TuDs we only found very little predicted interaction between the two binding sites so that this issue apparently does not play a role here. We therefore propose another theory in which the different efficiencies of our TuDs are linked to the sequence of the shRNA. The thermodynamic stability of the seed-target duplex has been shown to be a determinant of how well a target can be bound (Naito *et al.*, 2009). Due to the nature of its target site shHCV318 has a much higher GC content in its sense strand seed (75%) as compared to hAAT25 or shHBVS122 (50% and 37.5%, respectively) which is a good indicator for the thermodynamic stability of the seed-target duplex. Curiously, the GC contents correlate with the efficiencies of the TuDs. We therefore argue that the inhibitory effect might be more pronounced with shHCV318 than with the other two shRNAs because the binding affinity to the TuD is strongest.

Another essential factor that severely influenced the efficacy of our approach appeared to be the relative expression of shRNA and inhibitor RNA. This is supported by the fact that for hAAT25 we could improve the strategy by replacing the H1 by the stronger U6 promoter. Our rAAV titration experiments in Huh7 cells further demonstrated that the degree of sense strand counteraction by the TuD was dependent on the vector dose. The higher the dose the better the effect (for shHCV318 a plateau was reached already at MOI 10^4). We conclude that the two molecules have different expression kinetics, with shRNAs reaching activities close to the maximum at lower vector doses than the inhibitor molecule. This is not necessarily a drawback of the strategy as sense strand counteraction is especially important at higher MOIs where silencing is most pronounced. TuDs may hence buffer sense strand activity at doses where it is especially needed.

Our system behaved differently in transfection and transduction experiments. This becomes evident when looking at sense strand counteraction for shHCV318

which was over 8-fold upon HEK293T transfection but only ~4.5-fold upon transduction of the same cells even though sense strand activity *per se* was similar in both settings (cf.Fig. 10B and 12A). A comparison between HEK293T transfection and Huh7 transduction for all shRNAs hints into the same direction for all shRNAs. We hence conclude the gene delivery method has a critical influence on the efficiency of our strategy.

It has been shown previously that RNA targets induce miRNA degradation by certain tailing and trimming mechanisms (Ameres *et al.*, 2010). A recent publication on the use of TuDs for miRNA counteraction in mice and cultured human cells showed similar effects (Xie *et al.*, 2012). These authors hence claimed that TuD activity is based on target miRNA degradation. However, neither we nor the original study on TuDs found any changes in shRNA or miRNA levels upon TuD expression, respectively (Haraguchi *et al.*, 2008). In the results of Xie and colleagues the reduction in target miRNA levels is potent (>4-fold) when measured by RT-qPCR but subtle (~1.5-fold) when visualized by Northern blot. The same discrepancy was observed by Haraguchi and colleagues before and they hypothesized that TuD-miRNA interaction might interfere with proper detection by RT-qPCR. Therefore Northern blotting under denaturing conditions - as done in our study- appears to be better suited to gain insights into the intracellular levels of the miRNA or shRNA strand that is to be inhibited. Important to point out again, the present work is the first to employ TuD technology in the context of shRNAs. Therefore, our data not only validate the mechanism of TuD inhibition via target RNA sequestration, but concurrently also extend this finding to an entirely different class of small RNAs.

4.1.3 Parameters for optimal TuD design

Expression of inhibitor molecules like TuDs can lead to sequestration of specific miRNAs due to sequence homologies. It has recently been shown that a seed match alone is not sufficient for miRNA counteraction by TuD-like inhibitors (Haraguchi *et al.*, 2012). Extensive base-pairing at the 3' end of the miRNA was required in addition to the seed match indicating that the target requirements for efficient counteraction are rather stringent. Nevertheless, it is important to exclude sequences with high homologies to cellular miRNAs when designing TuD target sites and to omit seed matches as effectively as possible.

Our data demonstrates that binding sites with perfect complementarity to the shRNA sense strand work as equally well as mismatched targets. This finding indicates that the design rules in the original report might not be optimal for all RNAi triggers (Haraguchi *et al.*, 2008). The initial notion that perfect binding sites worked less efficiently than mismatched counterparts was only based on one single miRNA, *i.e.* miR-21-5p. In a recent follow-up study the same authors tested counteraction of several miRNAs -including miR-21-5p- with synthetic TuD-like inhibitors (Haraguchi *et al.*, 2012). They showed that miR-21-5p is a special case as for two additional miRNAs they found best counteraction via perfect match targets strongly supporting our data on target site requirements. The authors linked poor performance of the miR-21-5p TuD with perfect target to extensive base pairing between the two target sites which could limit accessibility for the miRNA. In combination with our own results we therefore assume that binding site requirements for miRNA and shRNA inhibition are similar and that perfect binding sites for TuD construction are generally at least as potent as mismatched counterparts. The latest results of Haraguchi *et al.* even support the idea that perfect sites could in general be better than imperfect sites since TuD efficiency appears to increase with homology to the target. The fact that perfect and mismatched targets performed equally well in our assays does not contradict this hypothesis. All our imperfect targets had single central mismatches which probably only marginally reduced the stability of the resulting TuD-sense duplex as compared to perfect match targets.

While the possibility to use perfect target sites for TuD construction is important in terms of design rules, it is also interesting from a biological perspective. In the original report on miRNA sponges the authors showed that for both RNA-pol II- and RNA-pol III-transcribed inhibitors perfect target sites were outperformed by imperfect counterparts (Ebert *et al*., 2007). The most likely explanation for this is efficient degradation via hAgo2-mediated slicing and hence reduced activity of perfect match inhibitors as compared to mismatched ones. As this effect -*i.e.* superior performance of imperfect versus perfect targets- is absent in TuDs we suggest that perfect binding sites in TuDs are apparently not readily sliced by hAgo2. This might be because the complex structure of the TuD does not allow

proper positioning of the target site relative to the RNAi trigger so that no slicing reaction can occur.

A particularly novel and important finding during our comprehensive analysis of various TuD designs was that single target binding sites already suffice to yield maximum inhibition. The fact that we did not see any disparity between TuDs with one or two binding sites suggests that the intracellular TuD concentration is more important than the number of targets. In any case, it is questionable whether it would be sterically possible for one single TuD molecule to bind two sense strand loaded RISCs at the same time. Our finding opens up the possibility to generate inhibitors that inhibit two RNAi triggers at the same time as exemplified by our chimeric TuD against hAAT25 and shHCV318. We are convinced that this concept will prove useful in applications where multiple shRNA sense strands and/or miRNAs should be counteracted (see section 4.3.4).

Taken together, our data identified two essential design parameters that determine the efficiency of this inhibitor class: 1) Perfect binding sites work better than imperfect sites, 2) a single perfect binding site suffices to yield maximum inhibition. For future *de novo* construction of TuDs both against shRNA sense strands and miRNAs we therefore recommend to use single perfect binding sites if possible. This allows easy design and cost- and time-effective cloning procedures. If a perfect target happens to insufficiently inhibit sense strand or miRNA activity -as in the case of miR-21-5p- or if the sequence of the binding site exhibits homologies to untargeted miRNAs, high affinity targets with single mismatches at position 10 or 11 can be used instead.

4.1.4 Possible optimizations

Although we were able to achieve an improvement of relative strand activity for all three shRNAs we clearly see room for further optimization of the strategy. Based on our results with our first generation of TuD vectors, we envision the following beneficial modifications in future designs:

Firstly, it will be useful to further improve the ratio between TuD and sense strand expression levels, which can be achieved in numerous ways. For instance, the shRNA could be transcribed from an even weaker promoter which likely would not severely compromise shRNA efficiency but could improve the ratio between TuD and sense strand expression levels. Such a promoter could be an

attenuated version of H1 as described in a report on the functional characterization of this promoter (Hannon *et al*., 1991). Alternatively or in addition, the TuD can be placed under the control of a very potent promoter such as U6 as used in this study. An alternative way of attenuating sense strand levels relative to TuD levels without exchanging promoters could be to embed the shRNA within a miRNA scaffold (Zeng and Cullen, 2003b). This structure requires an additional processing step by Drosha and leads to lower intracellular levels of mature shRNA strands as compared to classical shRNAs of the same sequence (Boudreau *et al*., 2008). Potentially decreased efficiency of intended target silencing could be outweighed by increased specificity via more potent sense strand inactivation. The usefulness of this latter strategy is currently experimentally addressed in our lab on the example of shHBVS122.

Secondly, in potential therapeutic applications inducible expression is absolutely necessary given the potential adverse side effects associated with high shRNA abundance. We therefore envision a future optimized variant of our system to express shRNAs expressed from an H1 and TuD from a U6 promoter that are both doxycycline-responsive as previously described (Aagaard *et al.*, 2007). This would allow tight co-regulation of expression of both molecules. Pilot experiments for inducible TuD expression are currently ongoing in our lab.

4.1.5 HCV inhibition by RNAi

It has been shown that in the case of rapidly evolving viruses it is necessary to take measures to avoid viral mutational escape from therapy. One such measure is to target conserved sequences that are less prone to sequence modifications as done for the shRNA that shHCV318 is based on (Krönke *et al.*, 2004). In addition, it is also helpful to use more than one shRNA which likewise makes viral escape from therapy less likely (Grimm and Kay, 2007b). Alternatively, RNAi can be combined with therapeutic measures that are based on different molecular principles (Anderson *et al.*, 2007). In the case of HCV it has recently been demonstrated that miR-122-5p enhances HCV replication and antiviral treatment based on inhibition of this miRNA has already shown promising results (Jopling, 2008; Lanford *et al.*, 2010). miR-122-5p counteraction could hence be a good complementation to RNAi-mediated HCV inhibition. Our rAAV-based TuD expression strategy could be well suited for this approach especially since our lab

also possesses an AAV capsid variant with improved *in vivo* liver tropism (Grimm *et al*., 2008). Indeed, our preliminary data on inhibition of replication of HCV replicons provide a promising proof-of-concept. Our next step therefore is to combine shRNA and TuD in one single rAAV vector cooperatively expressing shHCV318 and a chimeric TuD that counteracts the shRNA sense strand and miR-122-5p at the same time. This combination of miR-122-5p inhibition and shHCV318 antisense activity should improve the efficiency of HCV treatment and at the same time decrease off-targeting from the shRNA sense strand merely by co-expressing two small RNA molecules (shRNA and TuD).

We also use HCV as a model for this novel concept but it generally demonstrates that the possibilities of our system go beyond shRNA sense strand counteraction although this was the primary goal of our study. Additional applications for single vectors co-expressing an shRNA and a miRNA inhibitor include treatment of cancer and HIV as well as basic research related-questions. In some cancers miRNAs can act as antiapoptotic factors, such as miR-21-5p in glioblastoma (Chan *et al*., 2005). Co-inhibition of miR-21-5p by a TuD and an essential oncogene like *c-myc* by an shRNA might yield an additive effect (Wang *et al*., 2008). During HIV infection, viral latency in resting CD4+ T-lymphocytes was linked to the activity of certain miRNAs, *e.g.* miR-125b-5p (Huang *et al*., 2007). HIV reservoirs might therefore be purged by inhibition of miR-125b-5p and concomitant shRNA-mediated degradation of newly produced HIV mRNAs; this strategy will in fact be tested in our laboratory using the vectors developed in this study.

Successful shHCV318 sense strand counteraction was also interesting from a more biological point of view. HCV is a RNA (+) virus that produces a (-) strand as replication intermediate. While RNAi triggers are usually directed against the (+) strand genome it would be therapeutically useful to also target and destroy the (-) strand (Krönke *et al.*, 2004; Wilson *et al.* 2005). Yet, a previous study in which sequences in the HCV 5' UTR or NS5B were targeted with siRNAs suggested that the (-) strand is potentially immune to RNAi (Smith *et al.*, 2007). This lack of (-) strand targeting could have two reasons: On the one hand, the (-) strand probably folds into a completely different 3D structure than the (+) strand. The target sites of the siRNAs could thus be accessible in the (+) but not the (-) strand. On the other hand, the (-) strand could be completely inaccessible to

RNAi triggers due to its intracellular localization. This hypothesis would be supported by the fact that the HCV (-) strand is associated with a virus-induced membranous microenvironment that could exclude certain cellular factors - including RISC- and thus protect the strand against degradation (Herker and Ott, 2011).

The fact that inhibition of HCV replication was not altered by reducing sense strand activity via TuD co-expression indicated that HCV knockdown was entirely mediated by the shHCV318 antisense strand. We hence conclude that the HCV (-) strand was not targeted by our shRNA despite its high sense strand activity as measured by reporter assays. Our experimental setup thus provided a novel way of addressing the interactions between an RNAi trigger and HCV and confirmed the unique character of the HCV (-) strand.

4.2 Processing and functionality of 5' and 3' strands

While surprising at first, our finding that short shRNAs have the same Dicer requirements as longer versions does not necessarily disagree with previous *in vitro* data showing Dicer cleavage only in the case of a 25-mer shRNA but not a 19-mer shRNA (Siolas *et al.*, 2004). The discrepancy could be the reflection of experimental differences between *in vitro* assays and cell-based assays. Given that Dicer cuts the precursor into 22-mer pieces it seems logical that a 19-mer stem could be a worse substrate than a 25-mer stem. In the *in vitro* assays the shRNA substrates are incubated with purified Dicer for 2h which might then allow visualization of processing products of the 25-mer but not the 19-mer. However, this does not mean that the 19-mer is not processed at all. Instead, it is possible that upon expression in cells a low processing rate still yields functional levels of mature 3' strands in the steady-state. If in our case hAAT19 really was no Dicer substrate at all we would not expect to observe any mature 3' strands. Yet, we do observe a 3' product but in agreement with lower processing rates at much lower levels than observed for the longer hAAT25 shRNA (cf. Fig.1E). 19-mer shRNAs thus seem to be processed by Dicer but are worse substrates than ≥21-mer shRNAs. Our findings demonstrate that while *in vitro* experiments may provide important insights into cellular processes they do not necessarily reflect the exact situation in living cells.

It was briefly discussed in the introduction (section 1.1.7.2) whether Dicer processing *per se* may lead to a strand bias or whether the key determinant is the thermodynamic asymmetry of the duplex. The results presented in this study support both views. We observed a bias towards the 3' strand for all shRNAs that are supposedly good Dicer substrates, *i.e.* those with stem lengths of 21nt or longer. This finding along with the different Dicer dependencies of the two strands strongly implies that Dicer binding and/or processing *per se* indeed leads to preferential incorporation of the 3' strand into RISC. However, we also saw drastic differences between different shRNAs in the degree of that strand bias implying that there are other parameters to take into account that are linked to the sequence of the respective RNAi trigger. In the case of shRNAs with perfect or almost perfect matched stems a combination of Dicer processing and sequence features such as thermodynamic asymmetry therefore seems to drive selection of the strands.

It is noteworthy that the different Dicer dependencies of the two shRNA strands match recent observations by other groups on the Dicer-independent processing of a particular miRNA -*i.e.* miR-451- which upon review we found to have striking similarities to the shRNAs used here (Cheloufi *et al.*, 2010; Cifuentes *et al.*, 2010; Yang *et al.*, 2010a). More precisely, the structure of pre-miR-451 resembles an 18-mer stem shRNA. It expresses its 5' strand by a Dicer-independent but Ago2 slicing-dependent mechanism. This involves binding of Ago2 to the 5' end of the shRNA, subsequent cleavage of the 3' strand and resection to a size of 22-23nt. Our data suggest that this maturation process is not unique to miR-451 but, instead, is natural for all hairpin RNA molecules with perfectly matched stems, at least with stem lengths between 19 and 25nt.

While the 3' strands of all four shRNAs were non-functional in MEF Dicer-/- cells we observed a concomitant highly significant increase of 5' strand activity with hAAT19 and a mildly significant increase with hAAT21. This augmented 5' strand potency was also observed independently by another group that used the structure of miR-451 to design artificial hairpin molecules (Yang *et al.*, 2010a). While in WT cells the 5' strands of most of their constructs only had low silencing potentials the situation was dramatically different in Dicer-/- cells. Based on this and our own data we propose that Dicer binding might inhibit the non-canonical 5' strand activation mechanism possibly by sterically hindering Ago2 binding. This

could even be part of the mechanism by which Dicer introduces the strand bias towards the 3' strand. Interestingly, the enhanced potency of the 5' strand is only observed for the shorter shRNAs but not the 23- and 25-mer versions. Altogether, these findings indicate that Dicer exerts a very complex role in modulating the activity of the 5' strand whose further elucidation will be an important and exciting goal for future studies.

Notably, we were able to associate the difference in Dicer requirement with unique behavior of the two shRNA strands. Our hallmark finding was that the 5' strand could be counteracted by an inhibitor molecule whereas the 3' strand was principally inert. This novel and unanticipated observation suggests that the shRNA maturation processes yield functionally distinct strands. Interestingly, prior biochemical data indicate that RISC is relatively flexible and interacts with many different cellular factors (Meister *et al.*, 2005; Landthaler *et al.*, 2008) in turn implying that RISC composition varies according to *e.g.* cell types, cellular stress states or target mRNAs. A tempting ensuing hypothesis is that the composition of RISC may also differ between the 5' and the 3' strand of an shRNA, which could readily explain the functional peculiarities observed in this study. If true, this exciting new finding would fundamentally modify and expand our current understanding of cellular processes for small RNA maturation and activity, and thus have broad implications for future basic and applied RNAi research. Fortunately, the present work has not only paved the way for this potential important biological discovery, but has concurrently also already provided the experimental tools and strategies for its further dissection as well as, ideally, for its looming biomedical translation.

5 CONCLUSION

In this study, we demonstrate that undesired sense strand activity can have a greater impact on the specificity of an shRNA than generally believed (see Fig. 24 for graphical summary of results). We have generated bi-functional rAAV vectors that express an shRNA along with an inhibitor RNA. Our vector design allows counteraction of undesired sense strand activity upon shRNA expression and thereby reduction of off-target effects. As improving specificity is a major concern in the design of exogenous RNAi triggers, we are convinced that our novel sequestration-based method holds marked potential to be applied in the future design of shRNA-based silencing strategies. In addition, we envision the use of our bi-functional vectors in biomedical applications in which shRNA-mediated silencing should be combined with inhibition of specific miRNAs.

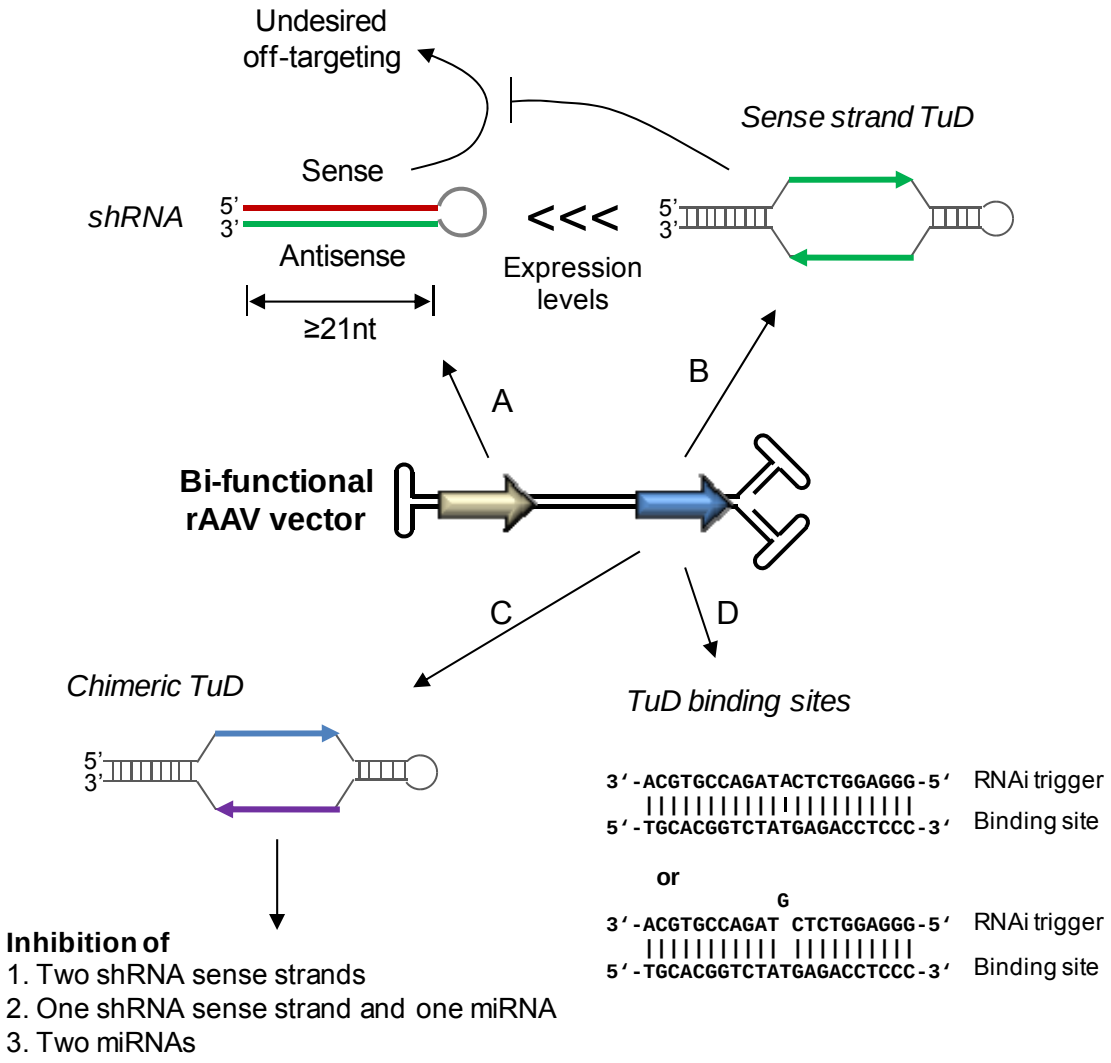

Fig. 24: Summary of results. We have generated bi-functional self-complementary rAAV vectors for the expression of both an shRNA and an inhibitor RNA molecule. **A:** The shRNA should be designed with the antisense strand at the 3‘ end and a stem of 21nt or more. Despite this design, the shRNA sense strand can be highly active and produce off-target effects. **B:** Co-expression of a TuD directed against the shRNA sense strand can counteract its activity and thereby partially relieve off-targeting. This approach requires that TuD expression is considerably more potent than shRNA expression. **C:** One binding site is sufficient for maximal TuD activity. TuDs can thus be generated with bindings sites for two different triggers of RNAi which can be useful in a variety of different applications. **D**: TuD binding sites are best designed with perfect complementarity to the RNAi trigger. Alteratively, high affinity sites with single mismatches at position 10 or 11 can be used.

6 SUPPLEMENTARY MATERIAL

6.1 Supplementary data

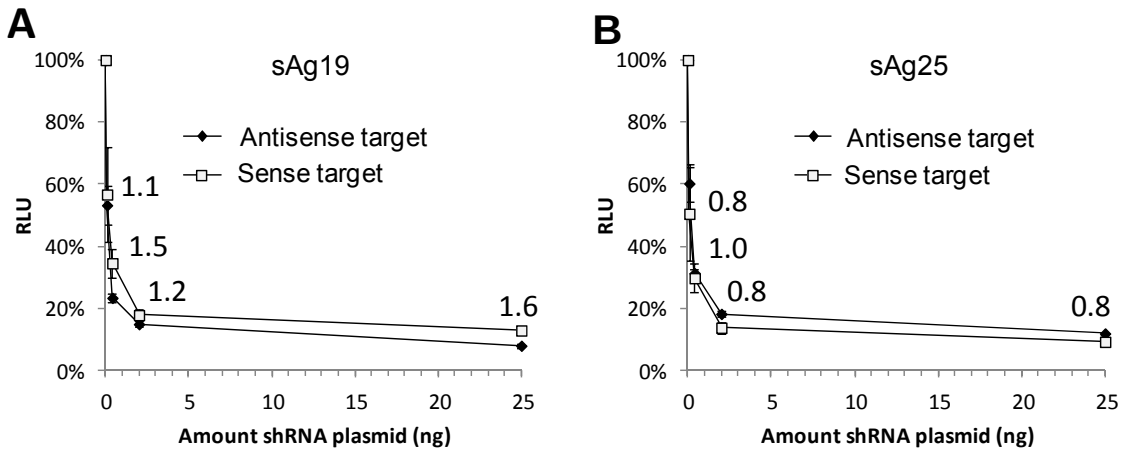

Suppl.Fig. 1: Analysis of 3‘ and 5' strand activities for the shRNAs sAg19 and sAg25. A+B: HEK293T cells were transfected with indicated amounts of U6-sAg19 (A) or sAg25 (B) and strand activities were determined at 48h post-transfection. Numbers indicate the RSAs at the respective concentrations. RSA=relative strand activity.

shRNAs

Name	**Sequence** (5'→3', 5'arm-loop-3' arm, antisense strand underlined, loop in italics)
sAg19	GAACAAATGGCACTAGTAA *TCAAGAG* TTACTAGTGCCATTTGTTC
sAg25	GAACAAATGGCACTAGTAAACTGAG *TCAAGAG* CTCAGTTTACTAGTGCCATTTGTTC
sAg21SA	GTTTACTAGTGCCATTTGTTC *TCAAGAG* GAACAAATGGCACTAGTAAAC
hAAT19	GAAGCGTTTAGGCATGTTT *TCAAGAG* AAACATGCCTAAACGCTTC
hAAT21	GAAGCGTTTAGGCATGTTTAA *TCAAGAG* TTAAACATGCCTAAACGCTTC
hAAT23	GAAGCGTTTAGGCATGTTTAACA *TCAAGAG* TGTTAAACATGCCTAAACGCTTC
hAAT25	GAAGCGTTTAGGCATGTTTAACATC *TCAAGAG* GATGTTAAACATGCCTAAACGCTTC
hAAT25R	GATGTTAAACATGCCTAAACGCTTC *TCAAGAG* GAAGCGTTTAGGCATGTTTAACATC
shHBVS1	GGTATGTTGCCCGTTTGTCT *TCAAGAG* AGACAAACGGGCAACATACC
shHBVS122	GGTATGTTGCCCGTTTGTCTTC *TCAAGAG* GAAGACAAACGGGCAACATACC
shHCV318	GGGAGGTCTCGTAGACCGTGCA *TCAAGAG* TGCACGGTCTACGAGACCTCCC
shP53P7	GGAGCTGAATGAGGCCTTAGA *TCAAGAG* TCTAAGGCCTCATTCAGCTCC
sh122SA	TGGAGTGTGACAATGGTGTTTGT *CCTGACCCA* ACAAACACCATTGTCACACTCCA
sh122AS	ACAAACACCATTGTCACACTCCA *CCTGACCCA* TGGAGTGTGACAATGGTGTTTGT

Binding sites in Rluc or d2eGFP 3' UTRs

Name	**Sequence** (5'→3')
hAAT „Intended" (=3' strand target for hAAT19-25 and 5' strand target for hAAT25R in Fig. 1)	GAAGCGTTTAGGCATGTTTAACATC
hAAT „Unintended perfect" (=5' target strand for hAAT19-25 and 3' strand target for hAAT25R in Fig. 1)	GATGTTAAACATGCCTAAACGCTTC
hAAT „Unintended imperfect"	GATGTTAAACATGC**T**TAAACGCTTC
HCV318 „Intended" (=3' strand target in Fig. 1)	GGGAGGTCTCGTAGACCGTGCA
HCV318 „Unintended perfect" (=5' strand target in Fig. 1)	TGCACGGTCTACGAGACCTCCC
HCV318 „Unintended imperfect"	TGCACGGTCTA**T**GAGACCTCCC
HBVS1 „Intended" (=3' strand target in Fig. 1)	GGTATGTTGCCCGTTTGTCT
HBVS1 „Unintended perfect" (=5' strand target in Fig. 1)	AGACAAACGGGCAACATACC
sAg 3' strand target (Fig.1 and Suppl.Fig. 1)	CTCAGTTTACTAGTGCCATTTGTTC
sAg 5' strand target (Fig.1 and Suppl.Fig. 1)	GAACAAATGGCACTAGTAAACTGAG
P53P7 3' strand target (Fig.1)	GGAGCTGAATGAGGCCTTAGA
P53P7 5' strand target (Fig.1)	TCTAAGGCCTCATTCAGCTCC
sh122SA 3' strand target (Fig.1)	TGGAGTGTGACAATGGTGTTTGT
sh122SA 5' strand target (Fig.1)	ACAAACACCATTGTCACACTCCA
sh122AS 3' strand target (Fig.1)	ACAAACACCATTGTCACACTCCA
sh122AS 5' strand target (Fig.1)	TGGAGTGTGACAATGGTGTTTGT
Random target for hAAT sense strand	GATGTTAAACATG NNN AAACGCTTC
miR-122-5p imperfect site, Fig. 23	ACAAACACCATGCCAACACTCCA

TuD binding sites

Name (bs1/bs2; i=imperfect, p=perfect, u=unspecific)	**Sequence** (5'→3', bs1-stem loop-bs2, stem loop in italics)
TuD-HCV318 for sense strand (u/i)	AGCACGATAAATGAGACCTCCC *CAAGTATTCTGGTCACAGAATACAAC* TGCACGGTCTATGAGACCTCCC
TuD-hAAT for sense strand (i/i)	TTAAACATGCATAAACGCTTC *CAAGTATTCTGGTCACAGAATACAAC* TTAAACATGCCGAAACGCTTC
TuD-HBVS1 for sense strand (i/i)	AGACAAACGTGCAACATACC *CAAGTATTCTGGTCACAGAATACAAC* AGACAAACGAGCAACATACC
TuD-hAAT for sense strand (p/p)	TTAAACATGCCTAAACGCTTC *CAAGTATTCTGGTCACAGAATACAAC* GTTAAACATGCCTAAACGCTTC
TuD-hAAT for antisense strand (p/u)	AGCGTTTAGGCATGTTTAACAT *CAAGTATTCTGGTCACAGAATACAAC* TGCACGGTCTATGAGACCTCCC
Chimeric TuD-hAAT/HCV318 for sense strands (p/p)	TTAAACATGCCTAAACGCTTC *CAAGTATTCTGGTCACAGAATACAAC* TGCACGGTCTACGAGACCTCCC
TuD-miR-122-5p (i/i)	CAAACACCATGCCAACACTCCA *CAAGTATTCTGGTCACAGAATACAAC* CAAACACCATGCCAACACTCCA

Suppl.Tab. 1: Sequences of shRNAs, 3' UTR targets and TuDs used in this study.

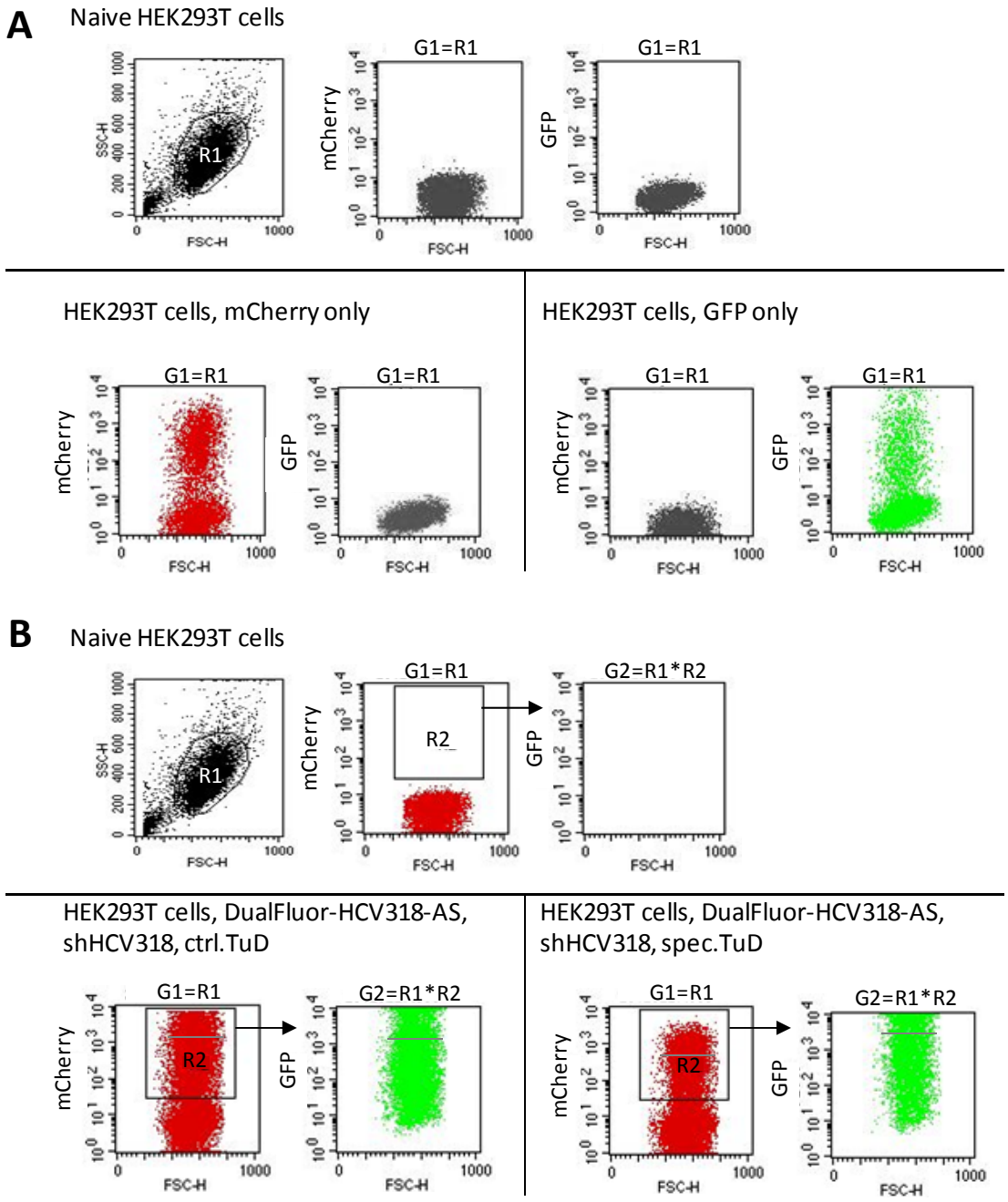

Suppl.Fig. 2: Fluorescence reporter knockdown analysis by FACS. A: For setup of the gating strategy and adjustment of compensation settings, HEK293T cells were either left naïve or transfected with an mCherry or eGFP expression plasmid and analyzed by FACS 48h post-transfection. Detector and compensation settings were adjusted so that naive cells were below 10^1 and no false positive cells appeared in the mCherry channel for eGFP only. **B:** For measurement of mCherry and eGFP expression, HEK293T cells -either naive or transfected with dual fluorescence and shRNA plasmids- were analyzed by FACS 48h post-transfection. Viable cells were gated through R1. mCherry-positive cells were gated through R2. Mean values for mCherry and eGFP expression in R2 were used for calculation of relative eGFP expression. Shown are two exemplary samples of the knockdown analysis. shHCV318 with control or specific TuD was transfected into HEK293T cells along with dual fluorescence reporter plasmids. Grey bars indicate mean expression values.

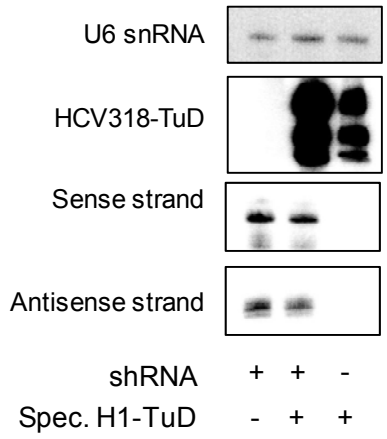

Suppl.Fig. 3: TuD expression by far exceeds shRNA expression. Huh7 cells were transduced (MOI=10^5) with rAAV2 encoding shRNA and TuD as indicated. 48h post-transduction, total RNA was extracted, and shRNA and TuD were detected by Northern blot. Perfectly matched probes were used for each molecule and contrast settings for TuD and shRNA sense or antisense strand are similar. The complex structure of the TuD can lead to the detection of several bands despite denaturing running conditions (Haraguchi *et al.*, 2009)

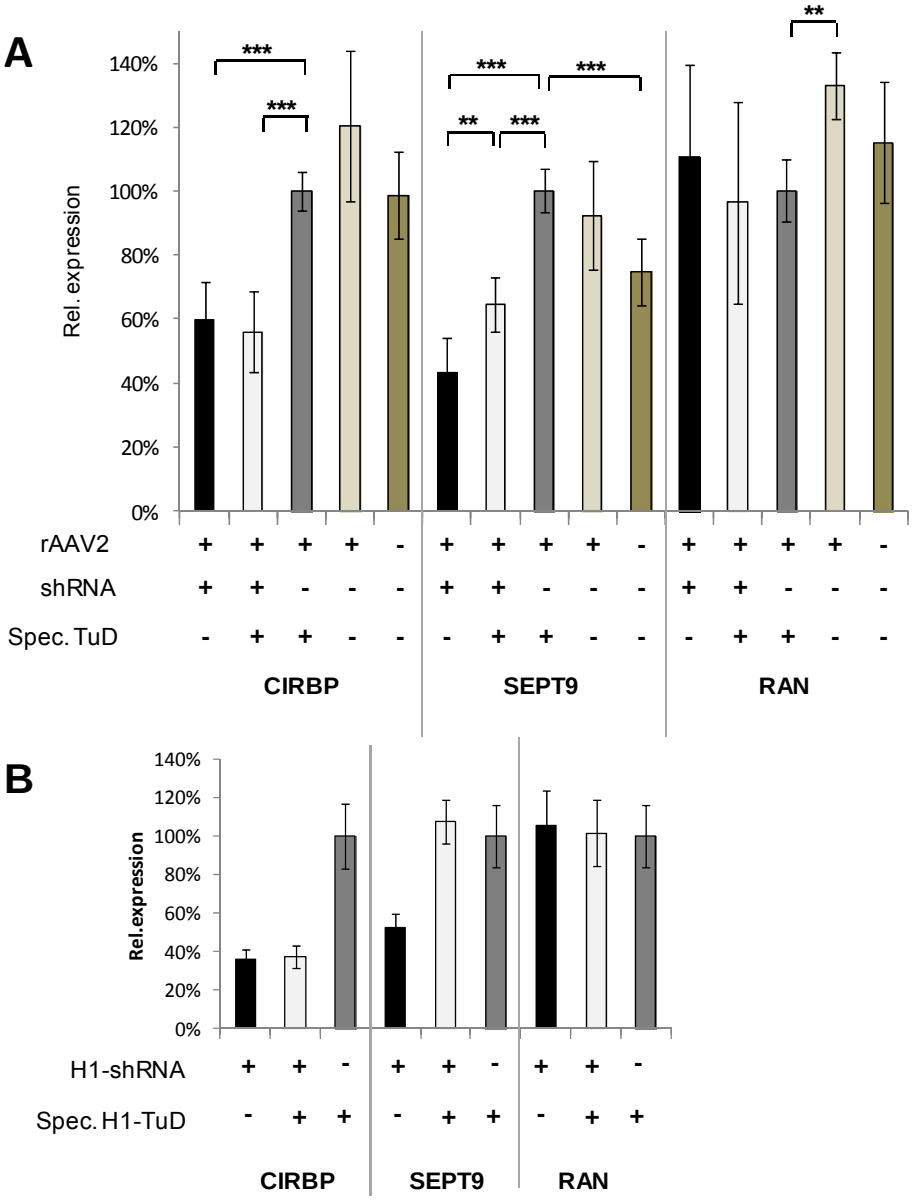

Suppl.Fig. 4: miArray validation by qPCR. A: Total RNA was extracted from naive Huh7 cells or Huh7 cells transduced with rAAV2 (MOI=10^5) encoding shRNA and TuD as indicated. Transcript levels of indicated genes were measured by RT-qPCR. Significance was determined by unpaired, two-sided T-test (* $p<0.05$; ** $p<0.005$; *** $p<0.0005$). **B**: miArray results for the same genes for comparison.

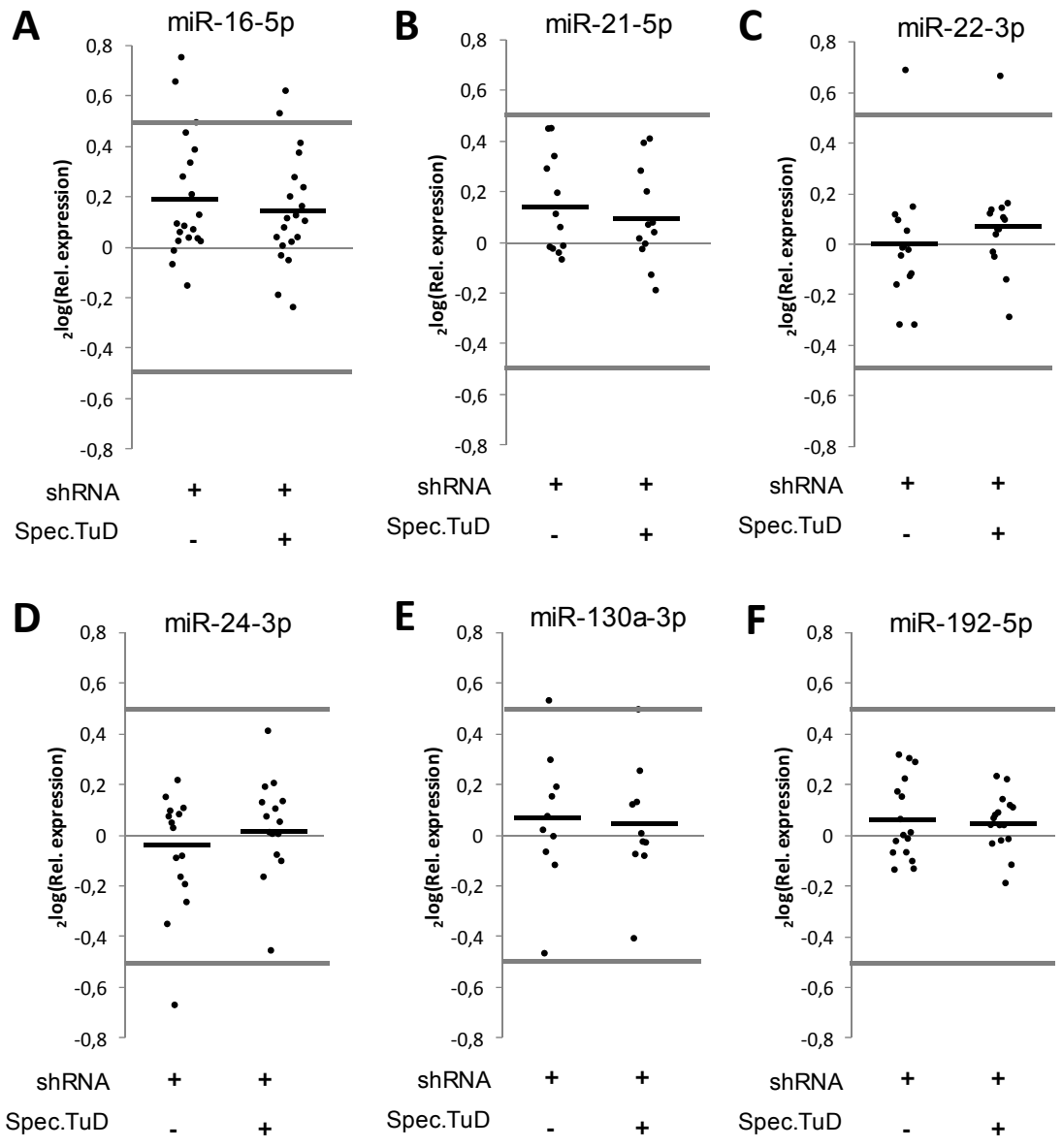

Suppl.Fig. 5: Analysis of target dysregulation for other hepatic miRNAs. A-C: Relative expression of validated target genes of miR-16-5p (A), miR-21-5p (B), miR-22-3p (C), miR-24-3p (D), miR-130a-3p (E), and miR-192-5p (F), as determined by miArray were plotted. For easy comparison to the data to Fig.15 the threshold used for off-target analysis previously is shown as grey line. Black bars represent the mean values of each dataset.

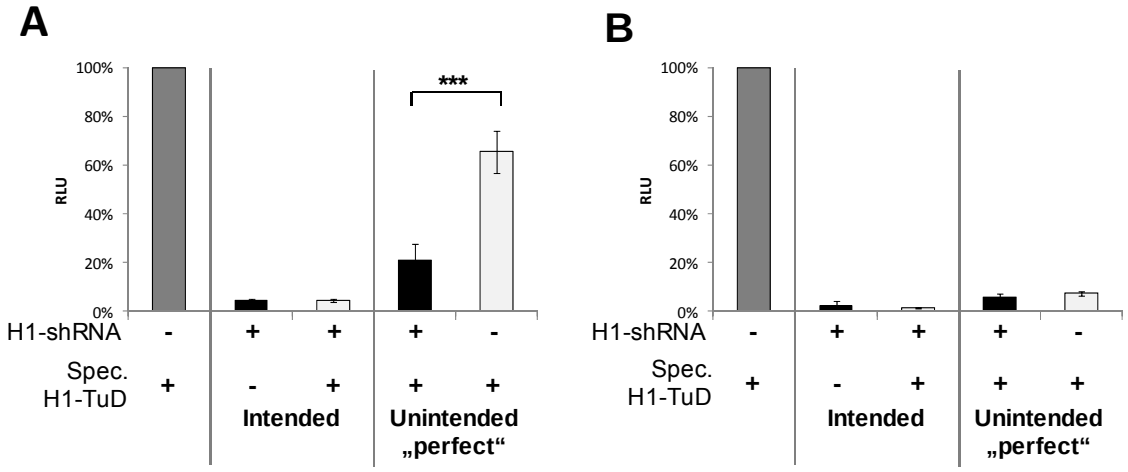

Suppl.Fig. 6: For some shRNAs H1-TuDs do not counteract sense strand upon rAAV2-mediated transduction. A+B: Transfection of HEK293T cells with hAAT25 plus TuD and luciferase targets for both strands (A) or transduction of Huh7 cells (MOI=10^5) with hAAT25 plus TuD and co-transfection with luciferase targets for both strands (B). Strand activities were measured by dual luciferase assay 48h post-transfection. Statistical analysis: unpaired, two-sided T-test, ** $p<0.005$, *** $p<0.0005$.

6.2 Relevant weblinks

microRNA database miRBase: www.mirbase.org

Journal of Gene Medicine, information on gene therapy trials:
http://www.abedia.com/wiley/vectors.php

Biomart tool: www.biomart.org

TarBase : http://diana.cslab.ece.ntua.gr/DianaToolsNew/index.php?r=tarbase/index

Primer bank database: http://pga.mgh.harvard.edu/primerbank/

microRNA.org database: www.microRNA.org

Centroid fold RNA folding prediction: www.ncrna.org/centroidfold

7 REFERENCES

Alvisi, G., Madan, V., and Bartenschlager, R. (2011). Hepatitis c virus and host cell lipids An intimate connection. RNA Biology 8, 258-269.

Ambros, V. (2001). microRNAs: Tiny regulators with great potential. Cell 107, 823-826.

Ameres, S.L., Horwich, M.D., Hung, J.H., Xu, J., Ghildiyal, M., Weng, Z.P., and Zamore, P.D. (2010). Target RNA-Directed Trimming and Tailing of Small Silencing RNAs. Science 328, 1534-1539.

An, D.S., Qin, F.X.F., Auyeung, V.C., Mao, S.H., Kung, S.K.P., Baltimore, D., and Chen, I.S.Y. (2006). Optimization and functional effects of stable short hairpin RNA expression in primary human lymphocytes via lentiviral vectors. Molecular Therapy 14, 494-504.

Anderson, J., Li, M.J., Palmer, B., Remling, L., Li, S., Yam, P., Yee, J.K., Rossi, J., Zaia, J., and Akkina, R. (2007). Safety and efficacy of a lentiviral vector containing three anti-HIV genes - CCR5 ribozyme, tat-rev siRNA, and TAR decoy - in SCID-hu mouse-derived T cells. Molecular Therapy 15, 1182-1188.

Anderson, E.M., Birmingham, A., Baskerville, S., Reynolds, A., Maksimova, E., Leake, D., Fedorov, Y., Karpilow, J., and Khvorova, A. (2008). Experimental validation of the importance of seed complement frequency to siRNA specificity. RNA-a Publication of the RNA Society 14, 853-861.

Bartel, D.P. (2009). MicroRNAs: Target Recognition and Regulatory Functions. Cell 136, 215-233.

Bartenschlager, R., and Lohmann, V. (2000). Replication of hepatitis C virus. Journal of General Virology 81, 1631-1648.

Bartenschlager, R., Penin, F., Lohmann, V., and Andre, P. (2011). Assembly of infectious hepatitis C virus particles. Trends in Microbiology 19, 95-103.

Beer, S., Bellovin, D.I., Lee, J.S., Komatsubara, K., Wang, L.S., Koh, H., Boerner, K., Storm, T.A., Davis, C.R., Kay, M.A., et al. (2010). Low-level shRNA Cytotoxicity Can Contribute to MYC-induced Hepatocellular Carcinoma in Adult Mice. Molecular Therapy 18, 161-170.

Behm-Ansmant, I., Rehwinkel, J., Doerks, T., Stark, A., Bork, P., and Izaurralde, E. (2006). MRNA degradation by miRNAs and GW182 requires both CCR4 : NOT deadenylase and DCP1 : DCP2 decapping complexes. Genes & Development 20, 1885-1898.

Berns, K.I., and Adler, S. (1972). Separation of Two Types of Adeno-Associated Virus Particles Containing Complementary Polynucleotide Chains. Journal of Virology 9, 394-396.

Berns, K.I., and Giraud, C. (1995). Adenovirus and adeno-associated virus as vectors for gene therapy. DNA Vaccines 772, 95-104.

Bernstein, E., Caudy, A.A., Hammond, S.M., and Hannon, G.J. (2001). Role for a bidentate ribonuclease in the initiation step of RNA interference. Nature 409, 363-366.

Betancur, J.G., and Tomari, Y. (2012). Dicer is dispensable for asymmetric RISC loading in mammals. RNA-a Publication of the RNA Society 18, 24-30.

Birmingham, A., Anderson, E.M., Reynolds, A., Ilsley-Tyree, D., Leake, D., Fedorov, Y., Baskerville, S., Maksimova, E., Robinson, K., Karpilow, J., et al. (2006). 3 ' UTR seed matches, but not overall identity, are associated with RNAi off-targets. Nature Methods 3, 199-204.

Bish, L.T., Sleeper, M.M., Reynolds, C., Gazzara, J., Withnall, E., Singletary, G.E., Buchlis, G., Hui, D., High, K.A., Gao, G.P., et al. (2011). Cardiac Gene Transfer of Short Hairpin RNA Directed Against Phospholamban Effectively Knocks Down Gene Expression but Causes Cellular Toxicity in Canines. Human Gene Therapy 22, 969-977.

Blakely, K., Ketela, T., Moffat, J., Cagney, G., and Emili, A. (2011). Pooled Lentiviral shRNA Screening for Functional Genomics in Mammalian Cells Network Biology. In (Humana Press), pp. 161-182.

Boudreau, R.L., Monteys, A.M., and Davidson, B.L. (2008). Minimizing variables among hairpin-based RNAi vectors reveals the potency of shRNAs. RNA-a Publication of the RNA Society 14, 1834-1844.

Boudreau, R.L., Spengler, R.M., and Davidson, B.L. (2011). Rational Design of Therapeutic siRNAs: Minimizing Off-targeting Potential to Improve the Safety of RNAi Therapy for Huntington's Disease. Molecular Therapy 19, 2169-2177.

Bridge, A.J., Pebernard, S., Ducraux, A., Nicoulaz, A.L., and Iggo, R. (2003). Induction of an interferon response by RNAi vectors in mammalian cells. Nature Genetics 34, 263-264.

Buhler, S., and Bartenschlager, R. (2012). New targets for antiviral therapy of chronic hepatitis C. Liver International 32, 9-16.

Burchard, J., Jackson, A.L., Malkov, V., Needham, R.H.V., Tan, Y.J., Bartz, S.R., Dai, H.Y., Sachs, A.B., and Linsley, P.S. (2009). MicroRNA-like off-target transcript regulation by siRNAs is species specific. RNA-a Publication of the RNA Society 15, 308-315.

Caplen, N.J., Parrish, S., Imani, F., Fire, A., and Morgan, R.A. (2001). Specific inhibition of gene expression by small double-stranded RNAs in invertebrate and vertebrate systems. Proceedings of the National Academy of Sciences of the United States of America 98, 9742-9747.

Castanotto, D., Sakurai, K., Lingeman, R., Li, H.T., Shively, L., Aagaard, L., Soifer, H., Gatignol, A., Riggs, A., and Rossi, J.J. (2007). Combinatorial delivery of small interfering RNAs reduces RNAi efficacy by selective incorporation into RISC. Nucleic Acids Research 35, 5154-5164.

Cerutti, H., and Casas-Mollano, J.A. (2006). On the origin and functions of RNA-mediated silencing: from protists to man. Current Genetics 50, 81-99.

Chan, J.A., Krichevsky, A.M., and Kosik, K.S. (2005). MicroRNA-21 is an antiapoptotic factor in human glioblastoma cells. Cancer Research 65, 6029-6033.

Cheloufi, S., Dos Santos, C.O., Chong, M.M.W., and Hannon, G.J. (2010). A Dicer-independent miRNA biogenesis pathway that requires Ago catalysis. Nature 465, 584-U576.

Chen, C., Ko, T., Ma, H., Wu, H., Xiao, X., Li, J., Chang, C., Wu, P., Chen, C., Han, J., et al. (2006). Long-term inhibition of hepatitis B virus in transgenic mice by pseudotyped

adeno-associated virus-mediated RNA interference. Journal of Clinical Virology 36, S86-S86.

Chen, P.Y., Weinmann, L., Gaidatzis, D., Pei, Y., Zavolan, M., Tuschl, T., and Meister, G. (2008). Strand-specific 5'-O-methylation of siRNA duplexes controls guide strand selection and targeting specificity. RNA-a Publication of the RNA Society 14, 263-274.

Chendrimada, T.P., Gregory, R.I., Kumaraswamy, E., Norman, J., Cooch, N., Nishikura, K., and Shiekhattar, R. (2005). TRBP recruits the Dicer complex to Ago2 for microRNA processing and gene silencing. Nature 436, 740-744.

Chi, S.W., Hannon, G.J., and Darnell, R.B. (2012). An alternative mode of microRNA target recognition. Nature Structural and Molecular Biology 19, 321-327.

Cifuentes, D., Xue, H.L., Taylor, D.W., Patnode, H., Mishima, Y., Cheloufi, S., Ma, E.B., Mane, S., Hannon, G.J., Lawson, N.D., et al. (2010). A Novel miRNA Processing Pathway Independent of Dicer Requires Argonaute2 Catalytic Activity. Science 328, 1694-1698.

Contreras, A.M., Hiasa, Y., He, W.P., Terella, A., Schmidt, E.V., and Chung, R.T. (2002). Viral RNA mutations are region specific and increased by ribavirin in a full-length hepatitis C virus replication system. Journal of Virology 76, 8505-8517.

Cummins, J.M., He, Y.P., Leary, R.J., Pagliarini, R., Diaz, L.A., Sjoblom, T., Barad, O., Bentwich, Z., Szafranska, A.E., Labourier, E., et al. (2006). The colorectal microRNAome. Proceedings of the National Academy of Sciences of the United States of America 103, 3687-3692.

Czauderna, F., Fechtner, M., Dames, S., Aygun, H., Klippel, A., Pronk, G.J., Giese, K., and Kaufmann, J. (2003). Structural variations and stabilising modifications of synthetic siRNAs in mammalian cells. Nucleic Acids Research 31, 2705-2716.

Danos, O. (2008). AAV vectors for RNA-based modulation of gene expression. Gene Therapy 15, 864-869.

Didiano, D., and Hobert, O. (2006). Perfect seed pairing is not a generally reliable predictor for miRNA-target interactions. Nature Structural & Molecular Biology 13, 849-851.

Diederichs, S., and Haber, D.A. (2007). Dual role for argonautes in MicroRNA processing and Posttranscriptional regulation of MicroRNA expression. Cell 131, 1097-1108.

Doench, J.G., Petersen, C.P., and Sharp, P.A. (2003). siRNAs can function as miRNAs. Genes & Development 17, 438-442.

Doench, J.G., and Sharp, P.A. (2004). Specificity of microRNA target selection in translational repression. Genes & Development 18, 504-511.

Dong, J.Y., Fan, P.D., and Frizzell, R.A. (1996). Quantitative analysis of the packaging capacity of recombinant adeno-associated virus. Human Gene Therapy 7, 2101-2112.

Ebert, M.S., Neilson, J.R., and Sharp, P.A. (2007). MicroRNA sponges: competitive inhibitors of small RNAs in mammalian cells. Nature Methods 4, 721-726.

Ebert, M.S., and Sharp, P.A. (2010). MicroRNA sponges: Progress and possibilities. RNA-a Publication of the RNA Society 16, 2043-2050.

Elbashir, S.M., Harborth, J., Lendeckel, W., Yalcin, A., Weber, K., and Tuschl, T. (2001a). Duplexes of 21-nucleotide RNAs mediate RNA interference in cultured mammalian cells. Nature 411, 494-498.

Elbashir, S.M., Lendeckel, W., and Tuschl, T. (2001b). RNA interference is mediated by 21-and 22-nucleotide RNAs. Genes & Development 15, 188-200.

Elmen, J., Thonberg, H., Ljungberg, K., Frieden, M., Westergaard, M., Xu, Y.H., Wahren, B., Liang, Z.C., Urum, H., Koch, T., et al. (2005). Locked nucleic acid (LNA) mediated improvements in siRNA stability and functionality. Nucleic Acids Research 33, 439-447.

Fabian, M.R., Sonenberg, N., and Filipowicz, W. (2010). Regulation of mRNA Translation and Stability by microRNAs. Annual Review of Biochemistry 79, 351-379.

Fedorov, Y., Anderson, E.M., Birmingham, A., Reynolds, A., Karpilow, J., Robinson, K., Leake, D., Marshall, W.S., and Khvorova, A. (2006). Off-target effects by siRNA can induce toxic phenotype. RNA-a Publication of the RNA Society 12, 1188-1196.

Ferrari, F.K., Samulski, T., Shenk, T., and Samulski, R.J. (1996). Second-strand synthesis is a rate-limiting step for efficient transduction by recombinant adeno-associated virus vectors. Journal of Virology 70, 3227-3234.

Fire, A., Xu, S.Q., Montgomery, M.K., Kostas, S.A., Driver, S.E., and Mello, C.C. (1998). Potent and specific genetic interference by double-stranded RNA in Caenorhabditis elegans. Nature 391, 806-811.

Fisher, K.J., Gao, G.P., Weitzman, M.D., DeMatteo, R., Burda, J.F., and Wilson, J.M. (1996). Transduction with recombinant adeno-associated virus for gene therapy is limited by leading-strand synthesis. Journal of Virology 70, 520-532.

Flotte, T.R., Afione, S.A., and Zeitlin, P.L. (1994). Adenoassociated Virus Vector Gene-Expression Occurs in Nondividing Cells in the Absence of Vector DNA Integration. American Journal of Respiratory Cell and Molecular Biology 11, 517-521.

Frank, F., Sonenberg, N., and Nagar, B. (2010). Structural basis for 5 '-nucleotide base-specific recognition of guide RNA by human AGO2. Nature 465, 818-822.

Friebe, P., and Bartenschlager, R. (2009). Role of RNA Structures in Genome Terminal Sequences of the Hepatitis C Virus for Replication and Assembly. Journal of Virology 83, 11989-11995.

Gao, G.P., Alvira, M.R., Wang, L.L., Calcedo, R., Johnston, J., and Wilson, J.M. (2002). Novel adeno-associated viruses from rhesus monkeys as vectors for human gene therapy. Proceedings of the National Academy of Sciences of the United States of America 99, 11854-11859.

Giering, J.C., Grimm, D., Storm, T.A., and Kay, M.A. (2008). Expression of shRNA from a tissue-specific pol II promoter is an effective and safe RNAi therapeutic. Molecular Therapy 16, 1630-1636.

Gonzalez-Gonzalez, E., Lopez-Casas, P.P., and del Mazo, J. (2008). The expression patterns of genes involved in the RNAi pathways are tissue-dependent and differ in the

germ and somatic cells of mouse testis. Biochimica Et Biophysica Acta-Gene Regulatory Mechanisms 1779, 306-311.

Grimm, D., and Kay, M.A. (2003). From Virus Evolution to Vector Revolution: Use of Naturally Occurring Serotypes of Adeno-associated Virus (AAV) as Novel Vectors for Human Gene Therapy. Current Gene Therapy 3, 281-304.

Grimm, D., and Kay, M.A. (2006). Therapeutic short hairpin RNA expression in the liver: viral targets and vectors. Gene Therapy 13, 563-575.

Grimm, D., Streetz, K.L., Jopling, C.L., Storm, T.A., Pandey, K., Davis, C.R., Marion, P., Salazar, F., and Kay, M.A. (2006a). Fatality in mice due to oversaturation of cellular microRNA/short hairpin RNA pathways. Nature 441, 537-541.

Grimm, D., Pandey, K., Nakai, H., Storm, T.A., and Kay, M.A. (2006b). Liver transduction with recombinant adeno-associated virus is primarily restricted by capsid serotype not vector genotype. Journal of Virology 80, 426-439.

Grimm, D., and Kay, M.A. (2007a). Therapeutic application of RNAi: is mRNA targeting finally ready for prime time? Journal of Clinical Investigation 117, 3633-3641.

Grimm, D., and Kay, M.A. (2007b). Combinatorial RNAi: A winning strategy for the race against evolving targets? Molecular Therapy 15, 878-888.

Grimm, D., Lee, J.S., Wang, L., Desai, T., Akache, B., Storm, T.A., and Kay, M.A. (2008). In vitro and in vivo gene therapy vector evolution via multispecies interbreeding and retargeting of adeno-associated viruses. Journal of Virology 82, 5887-5911.

Grimm, D., Wang, L., Lee, J.S., Schurmann, N., Gu, S., Borner, K., Storm, T.A., and Kay, M.A. (2010). Argonaute proteins are key determinants of RNAi efficacy, toxicity, and persistence in the adult mouse liver. Journal of Clinical Investigation 120, 3106-3119.

Grimm, D. (2011). The dose can make the poison: lessons learned from adverse in vivo toxicities caused by RNAi overexpression. Silence 2, 8.

Gu, S., Jin, L., Zhang, F.J., Sarnow, P., and Kay, M.A. (2009). Biological basis for restriction of microRNA targets to the 3 ' untranslated region in mammalian mRNAs. Nature Structural & Molecular Biology 16, 144-150.

Gu, S., Jin, L., Zhang, F.J., Huang, Y., Grimm, D., Rossi, J.J., and Kay, M.A. (2011). Thermodynamic stability of small hairpin RNAs highly influences the loading process of different mammalian Argonautes. Proceedings of the National Academy of Sciences of the United States of America 108, 9208-9213.

Gupta, S., Schoer, R.A., Egan, J.E., Hannon, G.J., and Mittal, V. (2004). Inducible, reversible, and stable RNA interference in mammalian cells. Proceedings of the National Academy of Sciences of the United States of America 101, 1927-1932.

Hafner, M., Landthaler, M., Burger, L., Khorshid, M., Hausser, J., Berninger, P., Rothballer, A., Ascano, M., Jungkamp, A.C., Munschauer, M., et al. (2010). Transcriptome-wide Identification of RNA-Binding Protein and MicroRNA Target Sites by PAR-CLIP. Cell 141, 129-141.

Han, J.J., Lee, Y., Yeom, K.H., Kim, Y.K., Jin, H., and Kim, V.N. (2004). The Drosha-DGCR8 complex in primary microRNA processing. Genes & Development 18, 3016-3027.

Hannon, G.J., Chubb, A., Maroney, P.A., Hannon, G., Altman, S., and Nilsen, T.W. (1991). Multiple Cis-Acting Elements Are Required for RNA Polymerase-Iii Transcription of the Gene Encoding H1 RNA, the RNA Component of Human RNAse-P. Journal of Biological Chemistry 266, 22796-22799.

Haraguchi, T., Nakano, H., Tagawa, T., Ohki, T., Ueno, Y., Yoshida, T., and Iba, H. (2012). A potent 2'-O-methylated RNA-based microRNA inhibitor with unique secondary structures. Nucleic Acids Research, advanced online publication.

Haraguchi, T., Ozaki, Y., and Iba, H. (2009). Vectors expressing efficient RNA decoys achieve the long-term suppression of specific microRNA activity in mammalian cells. Nucleic Acids Research 37(6), 43-56.

Herker, E., and Ott, M. (2011). Unique ties between hepatitis C virus replication and intracellular lipids. Trends in Endocrinology and Metabolism 22, 241-248.

Hu, Z.H. (2009). Insight into microRNA regulation by analyzing the characteristics of their targets in humans. BMC Genomics 10, 594.

Huang, J.L., Wang, F.X., Argyris, E., Chen, K.Y., Liang, Z.H., Tian, H., Huang, W.L., Squires, K., Verlinghieri, G., and Zhang, H. (2007). Cellular microRNAs contribute to HIV-1 latency in resting primary CD4(+) T lymphocytes. Nature Medicine 13, 1241-1247.

Inagaki, K., Fuess, S., Storm, T.A., Gibson, G.A., Mctiernan, C.F., Kay, M.A., and Nakai, H. (2006). Robust systemic transduction with AAV9 vectors in mice: Efficient global cardiac gene transfer superior to that of AAV8. Molecular Therapy 14, 45.

Jackson, A.L., Bartz, S.R., Schelter, J., Kobayashi, S.V., Burchard, J., Mao, M., Li, B., Cavet, G., and Linsley, P.S. (2003). Expression profiling reveals off-target gene regulation by RNAi. Nature Biotechnology 21, 635-637.

Jackson, A.L., Burchard, J., Schelter, J., Chau, B.N., Cleary, M., Lim, L., and Linsley, P.S. (2006a). Widespread siRNA "off-target" transcript silencing mediated by seed region sequence complementarity. RNA-a Publication of the RNA Society 12, 1179-1187.

Jackson, A.L., Burchard, J., Leake, D., Reynolds, A., Schelter, J., Guo, J., Johnson, J.M., Lim, L., Karpilow, J., Nichols, K., et al. (2006b). Position-specific chemical modification of siRNAs reduces "off-target" transcript silencing. RNA-a Publication of the RNA Society 12, 1197-1205.

Jackson, A.L., and Linsley, P.S. (2010). Recognizing and avoiding siRNA off-target effects for target identification and therapeutic application. Nature Reviews Drug Discovery 9, 57-67.

Jin, X., Sun, T., Zhao, C., Zheng, Y., Zhang, Y., Cai, W., He, Q., Taira, K., Zhang, L., and Zhou, D. (2011). Strand antagonism in RNAi: an explanation of differences in potency between intracellularly expressed siRNA and shRNA. Nucleic Acids Research.

Jopling, C.L., Yi, M.K., Lancaster, A.M., Lemon, S.M., and Sarnow, P. (2005). Modulation of hepatitis C virus RNA abundance by a liver-specific microRNA. Science 309, 1577-1581.

Jopling, C.L. (2008). Regulation of hepatitis C virus by microRNA-122. Biochemical Society Transactions 36, 1220-1223.

Judge, A., and Maclachlan, I. (2008). Overcoming the innate immune response to small interfering RNA. Human Gene Therapy 19, 111-124.

Judge, A.D., Sood, V., Shaw, J.R., Fang, D., McClintock, K., and MacLachlan, I. (2005). Sequence-dependent stimulation of the mammalian innate immune response by synthetic siRNA. Nature Biotechnology 23, 457-462.

Kapadia, S.B., Brideau-Andersen, A., and Chisari, F.V. (2003). Interference of hepatitis C virus RNA replication by short interfering RNAs. Proceedings of the National Academy of Sciences of the United States of America 100, 2014-2018.

Kaplitt, M.G., Leone, P., Samulski, R.J., Xiao, X., Pfaff, D.W., Omalley, K.L., and During, M.J. (1994). Long-Term Gene-Expression and Phenotypic Correction Using Adenoassociated Virus Vectors in the Mammalian Brain. Nature Genetics 8, 148-154.

Kariko, K., Bhuyan, P., Capodici, J., and Weissman, D. (2004). Small interfering RNAs mediate sequence-independent gene suppression and induce immune activation by signaling through toll-like receptor 3. Journal of Immunology 172, 6545-6549.

Kennerdell, J.R., and Carthew, R.W. (1998). Use of dsRNA-mediated genetic interference to demonstrate that frizzled and frizzled 2 act in the wingless pathway. Cell 95, 1017-1026.

Keravala, A., Portlock, J.L., Nash, J.A., Vitrant, D.G., Robbins, P.D., and Calos, M.P. (2006). PhiC31 integrase mediates integration in cultured synovial cells and enhances gene expression in rabbit joints. Journal of Gene Medicine 8, 1008-1017.

Kertesz, M., Iovino, N., Unnerstall, U., Gaul, U., and Segal, E. (2007). The role of site accessibility in microRNA target recognition. Nature Genetics 39, 1278-1284.

Khan, A.A., Betel, D., Miller, M.L., Sander, C., Leslie, C.S., and Marks, D.S. (2009). Transfection of small RNAs globally perturbs gene regulation by endogenous microRNAs. Nature Biotechnology 27, 671-671.

Khvorova, A., Reynolds, A., and Jayasena, S.D. (2003). Functional siRNAs and rniRNAs exhibit strand bias. Cell 115, 209-216.

Kim, D.H., Behlke, M.A., Rose, S.D., Chang, M.S., Choi, S., and Rossi, J.J. (2005). Synthetic dsRNA Dicer substrates enhance RNAi potency and efficacy. Nature Biotechnology 23, 222-226.

Klinghoffer, R.A., Magnus, J., Schelter, J., Mehaffey, M., Coleman, C., and Cleary, M.A. (2010). Reduced seed region-based off-target activity with lentivirus-mediated RNAi. RNA-a Publication of the RNA Society 16, 879-884.

Kotin, R.M., Siniscalco, M., Samulski, R.J., Zhu, X.D., Hunter, L., Laughlin, C.A., Mclaughlin, S., Muzyczka, N., Rocchi, M., and Berns, K.I. (1990). Site-Specific Integration by Adenoassociated Virus. Proceedings of the National Academy of Sciences of the United States of America 87, 2211-2215.

Kronke, J., Kittler, R., Buchholz, F., Windisch, M.P., Pietschmann, T., Bartenschlager, R., and Frese, M. (2004). Alternative approaches for efficient inhibition of hepatitis C virus RNA replication by small interfering RNAs. Journal of Virology 78, 3436-3446.

Kuchenbauer, F., Mah, S.M., Heuser, M., McPherson, A., Ruschmann, J., Rouhi, A., Berg, T., Bullinger, L., Argiropoulos, B., Morin, R.D., et al. (2011). Comprehensive analysis of mammalian miRNA* species and their role in myeloid cells. Blood 118, 3350-3358.

Kuiken, C., Simmonds, P., and Tang, H. (2009). Nomenclature and Numbering of the Hepatitis C Virus Hepatitis C. Humana Press, pp. 33-53.

Lai, E.C. (2002). Micro RNAs are complementary to 3 ' UTR sequence motifs that mediate negative post-transcriptional regulation. Nature Genetics 30, 363-364.

Landthaler, M., Gaidatzis, D., Rothballer, A., Chen, P.Y., Soll, S.J., Dinic, L., Ojo, T., Hafner, M., Zavolan, M., and Tuschl, T. (2008). Molecular characterization of human Argonaute-containing ribonucleoprotein complexes and their bound target mRNAs. RNA-a Publication of the RNA Society 14, 2580-2596.

Lanford, R.E., Hildebrandt-Eriksen, E.S., Petri, A., Persson, R., Lindow, M., Munk, M.E., Kauppinen, S., and Orum, H. (2010). Therapeutic Silencing of MicroRNA-122 in Primates with Chronic Hepatitis C Virus Infection. Science 327, 198-201.

Lazzaretti, D., Tournier, I., and Izaurralde, E. (2009). The C-terminal domains of human TNRC6A, TNRC6B, and TNRC6C silence bound transcripts independently of Argonaute proteins. RNA-a Publication of the RNA Society 15, 1059-1066.

Lee, R.C., and Ambros, V. (2001). An extensive class of small RNAs in Caenorhabditis elegans. Science 294, 862-864.

Lee, R.C., Feinbaum, R.L., and Ambros, V. (1993). The C-Elegans Heterochronic Gene Lin-4 Encodes Small RNAs with Antisense Complementarity to Lin-14. Cell 75, 843-854.

Lee, Y., Ahn, C., Han, J.J., Choi, H., Kim, J., Yim, J., Lee, J., Provost, P., Radmark, O., Kim, S., et al. (2003). The nuclear RNase III Drosha initiates microRNA processing. Nature 425, 415-419.

Lee, Y., Jeon, K., Lee, J.T., Kim, S., and Kim, V.N. (2002). MicroRNA maturation: stepwise processing and subcellular localization. EMBO Journal 21, 4663-4670.

Lee, Y., Kim, M., Han, J.J., Yeom, K.H., Lee, S., Baek, S.H., and Kim, V.N. (2004). MicroRNA genes are transcribed by RNA polymerase II. EMBO Journal 23, 4051-4060.

Lewis, B.P., Burge, C.B., and Bartel, D.P. (2005). Conserved seed pairing, often flanked by adenosines, indicates that thousands of human genes are microRNA targets. Cell 120, 15-20.

Li, F., and Mahato, R.I. (2009). Bipartite vectors for co-expression of a growth factor cDNA and short hairpin RNA against an apoptotic gene. Journal of Gene Medicine 11, 764-771.

Li, K., Chen, Z.H., Kato, N., Gale, M., and Lemon, S.M. (2005). Distinct poly(I-C) and virus-activated signaling pathways leading to interferon-beta production in hepatocytes. Journal of Biological Chemistry 280, 16739-16747.

Liu, J.D., Carmell, M.A., Rivas, F.V., Marsden, C.G., Thomson, J.M., Song, J.J., Hammond, S.M., Joshua-Tor, L., and Hannon, G.J. (2004). Argonaute2 is the catalytic engine of mammalian RNAi. Science 305, 1437-1441.

Lohmann, V., Korner, F., Koch, J.O., Herian, U., Theilmann, L., and Bartenschlager, R. (1999). Replication of subgenomic hepatitis C virus RNAs in a hepatoma cell line. Science 285, 110-113.

Lytle, J.R., Yario, T.A., and Steitz, J.A. (2007). Target mRNAs are repressed as efficiently by microRNA-binding sites in the 5 ' UTR as in the 3 ' UTR. Proceedings of the National Academy of Sciences of the United States of America 104, 9667-9672.

Marques, J.T., Devosse, T., Wang, D., Zamanian-Daryoush, M., Serbinowski, P., Hartmann, R., Fujita, T., Behlke, M.A., and Williams, B.R.G. (2006). A structural basis for discriminating between self and nonself double-stranded RNAs in mammalian cells. Nature Biotechnology 24, 559-565.

Martinez, J., Patkaniowska, A., Urlaub, H., Luhrmann, R., and Tuschl, T. (2002). Single-stranded antisense siRNAs guide target RNA cleavage in RNAi. Cell 110, 563-574.

Matranga, C., Tomari, Y., Shin, C., Bartel, D.P., and Zamore, P.D. (2005). Passenger-strand cleavage facilitates assembly of siRNA into Ago2-containing RNAi enzyme complexes. Cell 123, 607-620.

Matsushita, T., Elliger, S., Elliger, C., Podsakoff, G., Villarreal, L., Kurtzman, G.J., Iwaki, Y., and Colosi, P. (1998). Adeno-associated virus vectors can be efficiently produced without helper virus. Gene Therapy 5, 938-945.

Mazumder, B., Seshadri, V., and Fox, P.L. (2003). Translational control by the 3 '-UTR: the ends specify the means. Trends in Biochemical Sciences 28, 91-98.

McBride, J.L., Boudreau, R.L., Harper, S.Q., Staber, P.D., Monteys, A.M., Martins, I., Gilmore, B.L., Burstein, H., Peluso, R.W., Polisky, B., et al. (2008). Artificial miRNAs mitigate shRNA-mediated toxicity in the brain: Implications for the therapeutic development of RNAi. Proceedings of the National Academy of Sciences of the United States of America 105, 5868-5873.

McCarty, D.M., Fu, H., Monahan, P.E., Toulson, C.E., Naik, P., and Samulski, R.J. (2003). Adeno-associated virus terminal repeat (TR) mutant generates self-complementary vectors to overcome the rate-limiting step to transduction in vivo. Gene Therapy 10, 2112-2118.

McIntyre, G.J., and Fanning, G.C. (2006). Design and cloning strategies for constructing shRNA expression vectors. Bmc Biotechnology 6.

Mcintyre, G.J., Yu, Y.H., Lomas, M., and Fanning, G.C. (2011). The effects of stem length and core placement on shRNA activity. Bmc Molecular Biology 12.

McManus, M.T., Petersen, C.P., Haines, B.B., Chen, J.Z., and Sharp, P.A. (2002). Gene silencing using micro-RNA designed hairpins. RNA-a Publication of the RNA Society 8, 842-850.

Meister, G., Landthaler, M., Patkaniowska, A., Dorsett, Y., Teng, G., and Tuschl, T. (2004). Human Argonaute2 mediates RNA cleavage targeted by miRNAs and siRNAs. Molecular Cell 15, 185-197.

Miyagishi, M., and Taira, K. (2002). U6 promoter-driven siRNAs with four uridine 3 ' overhangs efficiently suppress targeted gene expression in mammalian cells. Nature Biotechnology 20, 497-500.

Mockenhaupt, S., Grimm, D. (2011). Adeno-assoziierte Viren für effizientes Gene Targeting in humanen Zellen. In Biospektrum 5/11, pp. 533-536.

Naito, Y., Nishi, K., Juni, A., and Ui-Tei, K. (2009). Functional shRNA expression system with reduced off-target effects. Paper presented at: Micro-NanoMechatronics and Human Science, 2009 MHS 2009 International Symposium on.

Nakai, H., Storm, T.A., and Kay, M.A. (2000). Recruitment of single-stranded recombinant adeno-associated virus vector genomes and intermolecular recombination are responsible for stable transduction of liver in vivo. Journal of Virology 74, 9451-9463.

Noland, C.L., Ma, E.B., and Doudna, J.A. (2011). siRNA Repositioning for Guide Strand Selection by Human Dicer Complexes. Molecular Cell 43, 110-121.

Paddison, P.J., Caudy, A.A., Bernstein, E., Hannon, G.J., and Conklin, D.S. (2002). Short hairpin RNAs (shRNAs) induce sequence-specific silencing in mammalian cells. Genes & Development 16, 948-958.

Pan, Q.W., de Ruiter, P.E., von Eije, K.J., Smits, R., Kwekkeboom, J., Tilanus, H.W., Berkhout, B., Janssen, H.L.A., and van der Laan, L.J.W. (2011). Disturbance of the microRNA pathway by commonly used lentiviral shRNA libraries limits the application for screening host factors involved in hepatitis C virus infection. FEBS Letters 585, 1025-1030.

Parker, R., and Sheth, U. (2007). P bodies and the control of mRNA translation and degradation. Molecular Cell 25, 635-646.

Pasquinelli, A.E., Reinhart, B.J., Slack, F., Martindale, M.Q., Kuroda, M.I., Maller, B., Hayward, D.C., Ball, E.E., Degnan, B., Muller, P., et al. (2000). Conservation of the sequence and temporal expression of let-7 heterochronic regulatory RNA. Nature 408, 86-89.

Petri, S., Dueck, A., Lehmann, G., Putz, N., Rudel, S., Kremmer, E., and Meister, G. (2011). Increased siRNA duplex stability correlates with reduced off-target and elevated on-target effects. RNA-a Publication of the RNA Society 17, 737-749.

Podsakoff, G., Wong, K.K., and Chatterjee, S. (1994). Efficient Gene-Transfer into Nondividing Cells by Adenoassociated Virus-Based Vectors. Journal of Virology 68, 5656-5666.

Provost, P., Dishart, D., Doucet, J., Frendewey, D., Samuelsson, B., and Radmark, O. (2002). Ribonuclease activity and RNA binding of recombinant human Dicer. EMBO Journal 21, 5864-5874.

Rabinowitz, J.E., Rolling, F., Li, C.W., Conrath, H., Xiao, W.D., Xiao, X., and Samulski, R.J. (2002). Cross-packaging of a single adeno-associated virus (AAV) type 2 vector genome into multiple AAV serotypes enables transduction with broad specificity. Journal of Virology 76, 791-801.

Rand, T.A., Petersen, S., Du, F.H., and Wang, X.D. (2005). Argonaute2 cleaves the anti-guide strand of siRNA during RISC activation. Cell 123, 621-629.

Randall, G., Grakoui, A., and Rice, C.M. (2003). Clearance of replicating hepatitis C virus replicon RNAs in cell culture by small interfering RNAs. Proceedings of the National Academy of Sciences of the United States of America 100, 235-240.

Reczko, M., Maragkakis, M., Alexiou, P., Grosse, I., and Hatzigeorgiou, A.G. (2012). Functional microRNA targets in protein coding sequences. Bioinformatics. doi: 10.1093/bioinformatics/bts043

Reinhart, B.J., Slack, F.J., Basson, M., Pasquinelli, A.E., Bettinger, J.C., Rougvie, A.E., Horvitz, H.R., and Ruvkun, G. (2000). The 21-nucleotide let-7 RNA regulates developmental timing in Caenorhabditis elegans. Nature 403, 901-906.

Reynolds, A., Anderson, E.M., Vermeulen, A., Fedorov, Y., Robinson, K., Leake, D., Karpilow, J., Marshall, W.S., and Khvorova, A. (2006). Induction of the interferon response by siRNA is cell type- and duplex length-dependent. RNA-a Publication of the RNA Society 12, 988-993.

Ro, S., Park, C., Young, D., Sanders, K.M., and Yan, W. (2007). Tissue-dependent paired expression of miRNAs. Nucleic Acids Research 35, 5944-5953.

Rose, J.A., Maizel, J.V., Inman, J.K., and Shatkin, A.J. (1971). Structural Proteins of Adenovirus-Associated Viruses. Journal of Virology 8, 766-770.

Rose, S.D., Kim, D.H., Amarzguioui, M., Heidel, J.D., Collingwood, M.A., Davis, M.E., Rossi, J.J., and Behlke, M.A. (2005). Functional polarity is introduced by Dicer processing of short substrate RNAs. Nucleic Acids Research 33, 4140-4156.

Rosen, H.R. (2011). Chronic Hepatitis C Infection. New England Journal of Medicine 364, 2429-2438.

Schultz, N., Marenstein, D., De Angelis, D., Wang, W., Nelander, S., Jacobsen, A., Marks, D., Massague, J., and Sander, C. (2011). Off-target effects dominate a large-scale RNAi screen for modulators of the TGF-beta pathway and reveal microRNA regulation of TGFBR2. Silence 2, 3.

Schwarz, D.S., Hutvagner, G., Du, T., Xu, Z.S., Aronin, N., and Zamore, P.D. (2003). Asymmetry in the assembly of the RNAi enzyme complex. Cell 115, 199-208.

Shimakami, T., Jangra, R.K., Welsch, C., Yamane, D., Hensley, L., Honda, M., Kaneko, S., and Lemon, S. (2011). 3 ' Supplementary Base-Pair Interactions of Mir-122 with Hepatitis C Virus RNA Contribute to Stabilization of the HCV RNA Genome. Hepatology 54, 405-405.

Shin, C., Nam, J.W., Farh, K.K.H., Chiang, H.R., Shkumatava, A., and Bartel, D.P. (2010). Expanding the MicroRNA Targeting Code: Functional Sites with Centered Pairing. Molecular Cell 38, 789-802.

Smith, R.M., Smolic, R., Volarevic, M., and Wu, G.Y. (2007). Positional effects and strand preference of RNA interference against hepatitis C virus target sequences. Journal of Viral Hepatitis 14, 194-212.

Snyder, R.O., Im, D.S., Ni, T.H., Xiao, X., Samulski, R.J., and Muzyczka, N. (1993). Features of the Adenoassociated Virus Origin Involved in Substrate Recognition by the Viral Rep Protein. Journal of Virology 67, 6096-6104.

Soifer, H.S., Sano, M., Sakurai, K., Chomchan, P., Saetrom, P., Sherman, M.A., Collingwood, M.A., Behlke, M.A., and Rossi, J.J. (2008). A role for the Dicer helicase domain in the processing of thermodynamically unstable hairpin RNAs. Nucleic Acids Research 36, 6511-6522.

Sonntag, F., Schmidt, K., and Kleinschmidt, J.A. (2010). A viral assembly factor promotes AAV2 capsid formation in the nucleolus. Proceedings of the National Academy of Sciences of the United States of America 107, 10220-10225.

Su, H., Trombly, M.I., Chen, J., and Wang, X.Z. (2009). Essential and overlapping functions for mammalian Argonautes in microRNA silencing. Genes & Development 23, 304-317.

Surosky, R.T., Urabe, M., Godwin, S.G., McQuiston, S.A., Kurtzman, G.J., Ozawa, K., and Natsoulis, G. (1997). Adeno-associated virus Rep proteins target DNA sequences to a unique locus in the human genome. Journal of Virology 71, 7951-7959.

Tiemann, K., and Rossi, J.J. (2009). RNAi-based therapeutics-current status, challenges and prospects. Embo Molecular Medicine 1, 142-151.

Tomari, Y., and Zamore, P.D. (2005). Perspective: machines for RNAi. Genes & Development 19, 517-529.

Ui-Tei, K., Naito, Y., Zenno, S., Nishi, K., Yamato, K., Takahashi, F., Juni, A., and Saigo, K. (2008). Functional dissection of siRNA sequence by systematic DNA substitution: modified siRNA with a DNA seed arm is a powerful tool for mammalian gene silencing with significantly reduced off-target effect. Nucleic Acids Research 36, 2136-2151.

Valencia-Sanchez, M.A., Liu, J.D., Hannon, G.J., and Parker, R. (2006). Control of translation and mRNA degradation by miRNAs and siRNAs. Genes & Development 20, 515-524.

Verdel, A., Jia, S.T., Gerber, S., Sugiyama, T., Gygi, S., Grewal, S.I.S., and Moazed, D. (2004). RNAi-mediated targeting of heterochromatin by the RITS complex. Science 303, 672-676.

Vergoulis, T., Vlachos, I.S., Alexiou, P., Georgakilas, G., Maragkakis, M., Reczko, M., Gerangelos, S., Koziris, N., Dalamagas, T., and Hatzigeorgiou, A.G. (2012). TarBase 6.0: capturing the exponential growth of miRNA targets with experimental support. Nucleic Acids Research 40, D222-D229.

Vickers, T.A., Lima, W.F., Wu, H.J., Nichols, J.G., Linsley, P.S., and Crooke, S.T. (2009). Off-target and a portion of target-specific siRNA mediated mRNA degradation is Ago2 'Slicer' independent and can be mediated by Ago1. Nucleic Acids Research 37, 6927-6941.

von Eije, K.J., ter Brake, O., and Berkhout, B. (2008). Human immunodeficiency virus type I escape is restricted when conserved genome sequences are targeted by RNA interference. Journal of Virology 82, 2895-2903.

Wang, J.L., Wang, H., Li, Z.Z., Wu, Q.L., Lathia, J.D., McLendon, R.E., Hjelmeland, A.B., and Rich, J.N. (2008). c-Myc Is Required for Maintenance of Glioma Cancer Stem Cells. Plos One 3(11). e3769. doi:10.1371/journal.pone.0003769

Wei, J.X., Yang, J., Sun, J.F., Jia, L.T., Zhang, Y., Zhang, H.Z., Li, X., Meng, Y.L., Yao, L.B., and Yang, A.G. (2009). Both Strands of siRNA Have Potential to Guide Posttranscriptional Gene Silencing in Mammalian Cells. Plos One 4(4). doi:10.1371/journal.pone.0005382

Wilson, J.A., Jayasena, S., Khvorova, A., Sabatinos, S., Rodrigue-Gervais, I.G., Arya, S., Sarangi, F., Harris-Brandts, M., Beaulieu, S., and Richardson, C.D. (2003). RNA interference blocks gene expression and RNA synthesis from hepatitis C replicons propagated in human liver cells. Proceedings of the National Academy of Sciences of the United States of America 100, 2783-2788.

Wilson, J.A., and Richardson, C.D. (2005). Hepatitis C virus replicons escape RNA interference induced by a short interfering RNA directed against the NS5b coding region. Journal of Virology 79, 7050-7058.

Xiao, X., Xiao, W.D., Li, J., and Samulski, R.J. (1997). A novel 165-base-pair terminal repeat sequence is the sole cis requirement for the adeno-associated virus life cycle. Journal of Virology 71, 941-948.

Xie, J., Ameres, S.L., Friedline, R., Hung, J.-H., Zhang, Y., Xie, Q., Zhong, L., Su, Q., He, R., Li, M., et al. (2012). Long-term, efficient inhibition of microRNA function in mice using rAAV vectors. Nat Meth advance online publication. doi:10.1038/nmeth.1903

Yan, Z.Y., Zak, R., Zhang, Y.L., and Engelhardt, J.F. (2005). Inverted terminal repeat sequences are important for intermolecular recombination and circularization of adeno-associated virus genomes. Journal of Virology 79, 364-379.

Yang, J.S., Maurin, T., Robine, N., Rasmussen, K.D., Jeffrey, K.L., Chandwani, R., Papapetrou, E.P., Sadelain, M., O'Carroll, D., and Lai, E.C. (2010a). Conserved vertebrate mir-451 provides a platform for Dicer-independent, Ago2-mediated microRNA biogenesis. Proceedings of the National Academy of Sciences of the United States of America 107, 15163-15168.

Yang, J.S., Phillips, M.D., Betel, D., Mu, P., Ventura, A., Siepel, A.C., Chen, K.C., and Lai, E.C. (2011). Widespread regulatory activity of vertebrate microRNA* species. RNA-a Publication of the RNA Society 17, 312-326.

Yang, X.A., Haungot, V., Zhou, S.Z., Luo, G.X., and Couto, L.B. (2010b). Inhibition of Hepatitis C Virus Replication Using Adeno-Associated Virus Vector Delivery of an Exogenous Anti-Hepatitis C Virus MicroRNA Cluster. Hepatology 52, 1877-1887.

Yi, R., Qin, Y., Macara, I.G., and Cullen, B.R. (2003). Exportin-5 mediates the nuclear export of pre-microRNAs and short hairpin RNAs. Genes & Development 17, 3011-3016.

Yu, J.Y., DeRuiter, S.L., and Turner, D.L. (2002). RNA interference by expression of short-interfering RNAs and hairpin RNAs in mammalian cells. Proceedings of the National Academy of Sciences of the United States of America 99, 6047-6052.

Zaiss, A.K., Liu, Q., Bowen, G.P., Wong, N.C.W., Bartlett, J.S., and Muruve, D.A. (2002). Differential activation of innate immune responses by adenovirus and adeno-associated virus vectors. Journal of Virology 76, 4580-4590.

Zeng, Y., and Cullen, B.R. (2003a). Sequence requirements for micro RNA processing and function in human cells. RNA-a Publication of the RNA Society 9, 112-123.

Zeng, Y., and Cullen, B.R. (2004). Structural requirements for pre-microRNA binding and nuclear export by Exportin 5. Nucleic Acids Research 32, 4776-4785.

Zeng, Y., Wagner, E.J., and Cullen, B.R. (2002). Both natural and designed micro RNAs technique can inhibit the expression of cognate mRNAs when expressed in human cells. Molecular Cell 9, 1327-1333.

Zeng, Y., Yi, R., and Cullen, B.R. (2003). MicroRNAs and small interfering RNAs can inhibit mRNA expression by similar mechanisms. Proceedings of the National Academy of Sciences of the United States of America 100, 9779-9784.

Zeuzem, S., Asselah, T., Angus, P., Zarski, J.P., Larrey, D., Mullhaupt, B., Gane, E., Schuchmann, M., Lohse, A., Pol, S., et al. (2011). Efficacy of the Protease Inhibitor BI 201335, Polymerase Inhibitor BI 207127, and Ribavirin in Patients With Chronic HCV Infection. Gastroenterology 141, 2047-2055.

Zhang, H.D., Kolb, F.A., Brondani, V., Billy, E., and Filipowicz, W. (2002). Human Dicer preferentially cleaves dsRNAs at their termini without a requirement for ATP. EMBO Journal 21, 5875-5885.

Zhou, H.B., Huang, X.F., Cui, H.J., Luo, X.B., Tang, Y.J., Chen, S.L., Wu, L., and Shen, N. (2010). miR-155 and its star-form partner miR-155* cooperatively regulate type I interferon production by human plasmacytoid dendritic cells. Blood 116, 5885-5894.

Zignego, A.L., Macchia, D., Monti, M., Thiers, V., Mazzetti, M., Foschi, M., Maggi, E., Romagnani, S., Gentilini, P., and Brechot, C. (1992). Infection of Peripheral Mononuclear Blood-Cells by Hepatitis-C Virus. Journal of Hepatology 15, 382-386.

Zipprich, J.T., Bhattacharyya, S., Mathys, H., and Filipowicz, W. (2009). Importance of the C-terminal domain of the human GW182 protein TNRC6C for translational repression. RNA-a Publication of the RNA Society 15, 781-793.

REMARKS

I hereby declare that I have written the submitted dissertation myself and in this process have used no other sources or materials than those expressly indicated. Moreover I hereby declare that I have not applied to be examined at any other institution, nor have I used the dissertation in this or any other form at any other institution as an examination paper, nor submitted it to any other faculty as a dissertation.

Date:_____ Signature:_____

ACKNOWLEDGEMENTS

I would like to thank my supervisor Dr. Dirk Grimm for giving me the opportunity to complete my PhD in the very stimulating field of applied RNAi. I truly appreciate his supervision that provided me with both support and a lot of scientific freedom to pursue my own interests. I am also very grateful for his helpful suggestions and support for the preparation of this manuscript.

I would like to express my gratitude to Prof. Dr. Ralf Bartenschlager for agreeing to be the first referee of my thesis.

I thank the members of my examination committee, Prof. Dr. Ralf Bartenschlager, Dr. Dirk Grimm, Dr. Friedrich Frischknecht and PD Dr. Karsten Rippe for their time and efforts.

I would like to thank all members of my HBIGS thesis advisory committee, Prof. Dr. Ralf Bartenschlager, Dr. Dirk Grimm, Prof. Dr. Hans-Georg Kräusslich, Dr. Georg Stöcklin, and Prof. Dr. Gerhard Schratt for their time, discussions, and helpful suggestions.

I thank the Hartmut Hoffmann-Berling International Graduate School of Molecular and Cellular Biology (HBIGS) for offering excellent training opportunities. I want to thank the Cluster of Excellence CellNetworks for the financial support of my work.

I would also like to thank Dr. Andrea Bauer and Dr. Christian Bender for their helpful advice and assistance.

Furthermore, I am grateful to Elena Senis Herrero, Eike Kienle, Stefanie Große, Ellen Wiedtke, and especially Nina Schürmann for their help and technical assistance, kindness, support, helpful discussions and everything else. I would like to thank the whole lab for the great atmosphere that we had.

I am particularly thankful to Daniela Cerny for her great support and patience, keeping me motivated, encouraged, and inspired. Dana, thank you for all the nice things that you have brought into my life.

I would like to express my deepest appreciation and gratitude to my parents for their support, encouragement, inspiration, and for always believing in me.